JOURNAL OF THE AMERICAN

ROCKET

SOCIETY

A journal devoted to rocket technology and the jet propulsion sciences

STACKS

VOLUME 23 MARCH-APRIL 1953 NUMBER 2

Servo-Stabilization of Low-Frequency Oscillations in a Liquid Bipropellant Rocket Motor . . . . . *Frank E. Marble and Dale W. Cox, Jr.* 63

Stability and Control of Liquid Propellant Rocket Systems . . . . . *Y. C. Lee, M. R. Gore, and C. C. Ross* 75

The Velocity of Sound in Some Rocket Propellant Liquids . . . . . *George G. Kretschmar* 82

On Maximum Evaporation Rates of Liquid Droplets in Rocket Motors . . . . . *S. S. Penner* 85

Combustion Studies in Rocket Motors . . *Kurt Berman and Samuel H. Cheney, Jr.* 89

Technical Notes 97
Abramson, on Porous, Sweat, or Film Cooling

Jet Propulsion News 99

American Rocket Society News 103

Technical Literature Digest 106

ARS SUMMER MEETING LOS ANGELES, CALIF. JULY 2, 1953

ROCKET POWER

FOR FAST INTERCEPTION

RMI ROCKET POWERED AIR FORCE XF-91 INTERCEPTOR TYPE AIRCRAFT.

First combat-ready interceptor aircraft
to fly at supersonic speeds in level flight.
RMI 6000 pound thrust rocket engine propels
turbojet-powered Republic XF-91 at Mach 1 plus.

RMI FOREMOST IN ROCKET POWER

REACTION MOTORS, INC., ROCKAWAY, NEW JERSEY

EDITORIAL BOARD

D. ALTMAN
California Institute of Technology

L. CROCCO
Princeton University

P. DUWEZ
California Institute of Technology

R. D. GECKLER
Aerojet Engineering Corporation

C. A. GONGWER
Aerojet Engineering Corporation

C. A. MEYER
Westinghouse Electric Corporation

P. F. WINTERNITZ
Reaction Motors, Inc.

K. WOHL
University of Delaware

M. J. ZUCROW
Purdue University

JOURNAL OF THE AMERICAN

ROCKET

SOCIETY

PUBLICATION OFFICE:
20th and Northampton Sts., Easton, Pa.

EXECUTIVE OFFICES:
Engineering Societies Building
29 West 39th Street, New York 18, N. Y.

EDITOR-IN-CHIEF
MARTIN SUMMERFIELD
Princeton University

ASSOCIATE EDITORS
C. F. WARNER—*Jet Propulsion News*
Purdue University

H. K. WILGUS—*ARS News*
New York, N. Y.

H. S. SEIFERT—*Literature Digest*
California Institute of Technology

ASSISTANT EDITOR
IRVIN GLASSMAN
Princeton University

MANAGING EDITOR
H. K. WILGUS
New York, N. Y.

ADVISORS ON PUBLICATION POLICY

L. G. DUNN
Director, Jet Propulsion Laboratory
California Institute of Technology

T. C. FETHERSTON
General Publicity Department
Union Carbide and Carbon Corporation

R. E. GIBSON
Director, Applied Physics Laboratory
Johns Hopkins University

H. F. GUGGENHEIM
President, The Daniel and Florence
Guggenheim Foundation

LOVELL LAWRENCE, JR.
Engineering Consultant

D. L. PUTT
Major General, U.S. Air Force
Vice Commander, Air Research
and Development Command

T. VON KÁRMÁN
Chairman, Scientific Advisory Board
U.S. Air Force

W. E. ZISCH
General Manager
Aerojet Engineering Corporation

Scope of the Journal

The Journal of the American Rocket Society is devoted to the advancement of the field of jet propulsion through the publication of original papers disclosing new knowledge and new developments. The term "jet propulsion" as used herein is understood to embrace all engines that develop thrust by rearward discharge of a jet through a nozzle or duct, and thus includes systems utilizing atmospheric air and underwater systems, as well as rocket engines. The Journal is open to contributions, either fundamental or applied, dealing with specialized aspects of jet and rocket propulsion, such as fuels and propellants, combustion, heat transfer, high temperature materials, mechanical design analyses, flight mechanics of jet-propelled vehicles, astronautics, and so forth. The Journal endeavors, also, to keep its subscribers informed of the affairs of the Society and of outstanding events in the rocket and jet propulsion field.

Submission of Manuscripts

Manuscripts should be submitted in duplicate to the Editor-in-Chief, Martin Summerfield, Professor of Aeronautical Engineering, Princeton University, Princeton, N. J. See instructions on the inside back cover.

Security Clearance

Manuscripts must be accompanied by written assurance as to security clearance in the event the subject matter of the manuscript is considered to lie in a classified area. Alternatively, written assurance that clearance is unnecessary should be submitted. Full responsibility for obtaining authoritative clearance rests with the author.

Advertisements

Information on advertising rates is obtainable from the Secretary of the Society.

Limitation of Responsibility

Statements and opinions expressed in the Journal are to be understood as the individual expressions of the authors and do not necessarily reflect the views of the Editors or the Society.

Copyright

Copyright, 1953, by the American Rocket Society, Inc. Permission for reprinting material in the Journal will be granted only upon application to the Secretary of the Society.

Subscription Rates

One year (six bimonthly issues)	$7.50
Foreign countries, including Canada	add .50
Single copies	1.25
Back numbers	1.50

Subscriptions and orders for single copies should be addressed to the Secretary of the Society.

Change of Address

Notices of change of address should be sent to the Secretary of the Society at least 30 days prior to the date of publication.

Explanation of Numbering of Issues

The September 1951 issue was the first of a new series of expanded scope and contents. This series is numbered on an annual volume basis, beginning each year with the January issue as Number 1. Correspondingly, the September issue was Number 5, and since 1951 was the 21st year of publication the new series started with Volume 21 Number 5. This replaced Number 86 of the previous series.

Published Bimonthly by the American Rocket Society, Inc.

Journal of the American Rocket Society, published bimonthly by the American Rocket Society at 20th and Northampton Streets, Easton, Pa., U.S.A. The Editorial Office is located at the Engineering Societies Building, 29 West 39th Street, New York 18, N. Y. Price $1.25 per copy, $7.50 per year. Entered as second-class matter at the Post Office at Easton, Pa., under the Act of March 3, 1879.

As an Oxidant in Liquid Propellants

NITROGEN TETROXIDE

offers outstanding advantages to designers of rocket motors

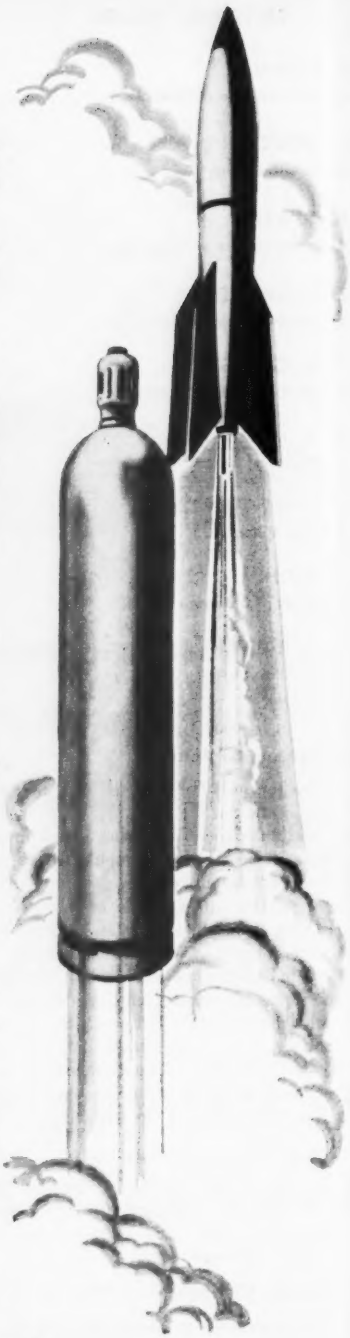

HIGH SPECIFIC IMPULSE: Nitrogen Tetroxide exceeds many other well-known oxidizers in pounds of thrust developed per pound of fuel consumed per second.

EASY TO HANDLE: Nitrogen Tetroxide may be shipped, piped and stored in ordinary carbon steel equipment. It possesses high chemical stability, high density, low freezing point, and a reasonably low vapor pressure.

Nitrogen Tetroxide is available at low cost in 125-pound I.C.C. approved steel cylinders and 1-ton containers.

Address your inquiry to the Product Development Department

NITROGEN DIVISION ALLIED CHEMICAL

Nitrogen Division

ALLIED CHEMICAL & DYE CORPORATION

40 RECTOR STREET, NEW YORK 6, N. Y.

Technical service and development on Nitrogen Tetroxide—formerly handled by the Product Development Department, Solvay Process Division—are now handled by Nitrogen Division, Allied Chemical & Dye Corporation.

CONCEPTION TO COMPLETION

In the field of Guided Missiles an engineering team which can carry a program forward from the very conception of the idea to the completion of a missiles weapon system is essential. Such a team is at work in Fairchild's Guided Missiles Division. Supporting this experienced engineering team is a production organization which has produced complete missile weapon systems for all three branches of the Armed Services. Recently Fairchild completed this country's first privately built plant devoted exclusively to missile design, development and production.

ENGINE AND AIRPLANE CORPORATION

FAIRCHILD

Guided Missiles Division

Wyandanch, L. I., N. Y.

Other Divisions: Aircraft Division, Hagerstown, Md.
Engine Division, Farmingdale, N. Y.

SCINTILLA MAGNETO DIVISION

BENDIX AVIATION CORPORATION

Sidney, New York

Manufacturers of Ignition Systems for Jet, Turbine, Piston Power Plants, and Rocket Motors; Electrical Connectors; Ignition Analyzers, Moldings and other Components and Accessories.

FREE design information

on Miniature Ball Bearings

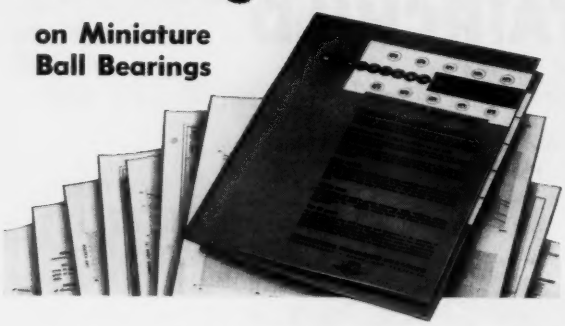

Ultra small precision ball bearings supply accurate alignment, long life and attention-free operation to aviation instruments, railway and marine indicating and recording devices, medical appliances, and similar fine mechanisms.

Complete specifications are given in new Catalog 52B. Engineering data sheets, speed load charts, and measuring unit conversion tables are available. For these and for further information write or phone H. D. Gilbert at the plant.

Miniature *Precision* Bearings

Incorporated MPB Keene, New Hampshire

Pioneer Precisionists to the World's Foremost Instrument Manufacturers — ***SAVE SPACE, WEIGHT, FRICTION***

Get the Facts about your Future with *Martin!*

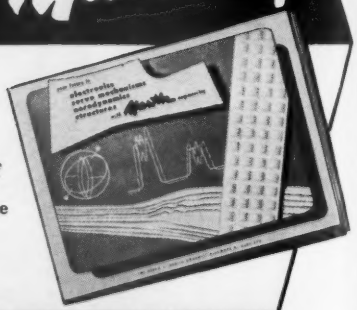

Discover the greater opportunities offered engineers by the greatest diversity of projects of any aircraft company in the East! Write today for fact-packed brochure.

SEND FOR ENGINEERING BROCHURE

THE GLENN L. MARTIN COMPANY
Personnel Dept. • Section A • Baltimore 3, Md.
Please send me your brochure describing engineering opportunities at Martin.

Name .....

Address .....

City and state .....

Engineering field .....

Where Systems Engineering lives

Martin systems engineering is the advanced concept of designing aircraft as integrated airborne systems . . . from the little black boxes that tell them *where to go* to the thundering jet aircraft that get *them there!*

Hundreds of Martin scientists in the Engineering Building above, work with our Armed Services to overcome man's physical limitations in a supersonic age.

Their field of endeavor is the unknown. Their tools are revolutionary developments in airframe, power plants, armament, electronic guidance, instrumentation and navigation. Their object is air supremacy for our United States.

THE GLENN L. MARTIN COMPANY
BALTIMORE 3, MARYLAND

Martin
AIRCRAFT

"Straight up" bat-wing interceptor
lands with ease on aircraft carriers

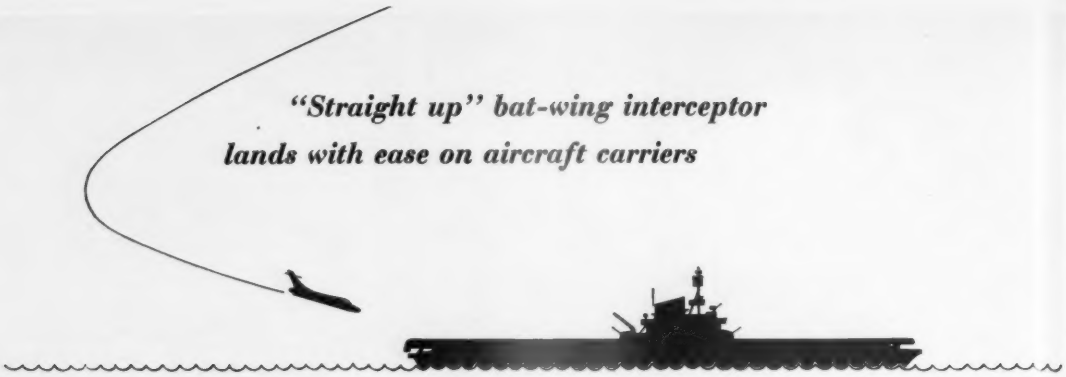

___the Douglas F4D Skyray

Problem: to find a Navy interceptor to operate from aircraft carriers and meet the threat of today's fast jet bombers. Answer: the Douglas F4D Skyray.

With its mighty power plant and radical swept-back wings, Skyray zooms into action at blazing speed. Minutes after radar warning, it's off the deck and on station—ready to intercept approaching aircraft with a lethal load of bullets and rockets. Yet for all its power and speed, this agile interceptor lands at low speeds—is perfectly adapted to requirements of present carriers.

Performance of the U. S. Navy's F4D Skyray is another example of Douglas leadership in aviation. Developing both military and civilian planes that can be produced in quantity—to *fly faster and farther with a bigger payload*—is the basic rule of Douglas design.

Depend on *DOUGLAS* **First in Aviation**

MARCH-APRIL 1953
VOLUME 23 NUMBER 2

JOURNAL OF THE AMERICAN ROCKET SOCIETY

Editor-in-Chief
MARTIN SUMMERFIELD

Servo-Stabilization of Low-Frequency Oscillations in a Liquid Bipropellant Rocket Motor

FRANK E. MARBLE[1] and DALE W. COX, JR.[2]

Daniel and Florence Guggenheim Jet Propulsion Center, California Institute of Technology, Pasadena, Calif.

The recent work of H. S. Tsien concerning the servo-stabilization of rocket motors is extended to the liquid bipropellant rocket motor. It is shown that by use of a feedback system containing a device to sense the combustion chamber pressure, a suitably designed amplifier, and a servomechanism which governs the propellant flow, the low-frequency oscillations which occur in the rocket configuration may be stabilized for any value of combustion time lag. A method is given for determining a transfer function of the feedback loop which will assure stable operation. The technique of the Satche diagram is employed in stability analysis.

Introduction

THE low-frequency instability of liquid propellant rocket motors has been attributed by Gunder and Friant (1),[3] Yachter (2), Summerfield (3), and Crocco (4) to the coupled oscillations of rocket chamber pressure and of flow rates of propellant in the feed lines. The instability arises from the fact that propellant combustion lags injection, due to the heat transfer required for propellant evaporation, time required for chemical reaction, etc., thereby introducing a phase difference between the oscillations of the two systems. The most general of these analyses is that of Crocco which treats both monopropellant and bipropellant systems and gives some physical basis for the introduction of a time lag. This latter aspect has since been generalized by Tsien (5).

Various possibilities have been discussed for removing the low-frequency instability through suitable choice of rocket configuration parameters, such as the propellant pressure drop across the injector nozzle. In some cases these changes may be undesirable or impossible; for example, in a rocket required to have a variable thrust, it may prove difficult to stabilize for all conditions of operation. Tsien (5) has investigated the more general concept of removing combustion chamber instability by use of a feedback servo control which senses the oscillating pressure in the combustion chamber and changes the propellant flow by the proper amount and in the proper phase to damp the oscillation. In the same paper the feasibility of such a system is demonstrated for the monopropellant rocket. For the purpose of this demonstration, Tsien introduced a graphical method of stability analysis, based on a suggestion by Satche (6), which is the appropriate technique for analyzing systems with time lag in the same sense that the familiar Nyquist diagram is appropriate for systems without time lag. Using the Satche diagram, Tsien was able to place quite general restrictions on the feedback loop which would assure stable rocket operation.

The present paper aims to extend these considerations to the bipropellant rocket and to find criteria on the feedback loop to provide stable operation. The authors are deeply grateful to Professor H. S. Tsien for initiating this problem and for his active interest during its progress.

Dynamics of the Bipropellant Rocket

The dynamics of the bipropellant rocket chamber, Fig. 1, are more complicated than those of the monopropellant rocket, due to the additional degree of freedom associated with the second propellant line and to the periodic changes of combustion gas temperature caused by variations in mixture ratio. Because only low-frequency oscillations are under consideration, the pressure at any time will be assumed uniform over the combustion chamber.

If the dependent variables of the system are taken to be the chamber pressure, the oxidizer flow rate, and the fuel flow rate, three equations may be written relating these quantities to each other and to the physical configuration. They are the continuity relation for the combustion chamber, and two conditions of dynamic equilibrium for the fluid in the oxidizer and fuel lines.

Following Crocco's notation (4), let M_g be the mass of burned gas in the combustion chamber, $\dot{m}_b$ the mass rate of burning, and $\dot{m}_e$ the mass rate of ejection from the discharge nozzle. Then the relation $d/dt(M_g) = \dot{m}_b - \dot{m}_e$ expresses

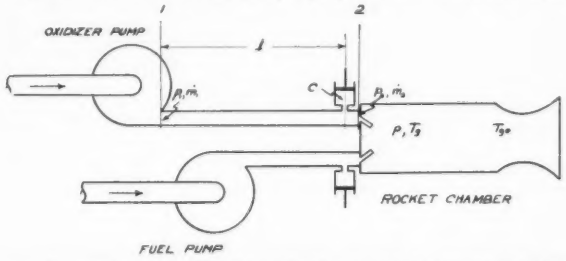

FIG. 1 SCHEMATIC DIAGRAM OF BIPROPELLANT ROCKET AND PROPELLANT FEED SYSTEM

Received October 1, 1952.
[1] Assistant Professor.
[2] Graduate Student; LCDR, U. S. Navy.
[3] Numbers in parentheses refer to the References on page 81.

the conservation of mass. Suppose the state of the dynamic system is always close to an equilibrium value defined by $\bar{M}_g$, $\bar{m}_b = \bar{m}_e = \bar{m}$, then the residence time which, on the average, the burned gas spends in the chamber, is $\vartheta_g = \bar{M}_g/\bar{m}$. Anticipating the use of perturbation analysis, the fractional variation of burning rate and discharge rate may be introduced, $\mu_b = \dfrac{\dot{m}_b - \bar{m}}{\bar{m}}$ and $\mu_e = \dfrac{\dot{m}_e - \bar{m}}{\bar{m}}$ together with a dimensionless time $z = t/\vartheta_g$ to write the mass conservation as

$$\frac{d}{dz}\left(\frac{M_g}{\bar{M}_g}\right) = \mu_b - \mu_e \quad \ldots\ldots\ldots\ldots\ldots [1]$$

The propellant burning rate $\dot{m}_b$ differs from the total propellant injection rate $\dot{m}_i$ because of the combustion time lag. The time τ required for the transformation of propellant into products of combustion may be represented by means of the integral

$$\int_{t-\tau}^{t} f(p, T_g)\, dt' = C = \text{const} \quad \ldots\ldots\ldots\ldots [2]$$

where $f(p, T_g)$ is a function depending upon the mechanics of the process. The chief quantities upon which this function depends are p, the uniform chamber pressure, and T_g, the ambient gas temperature in the neighborhood of the injector. The meaning of this integral may be clarified somewhat by thinking of f to be, for example, the rate of heat transfer to the liquid propellant, a certain total quantity C of heat being required before the transformation is complete. The principal quantities associated with the heat transfer process are the ambient temperature and pressure so that the time τ required for transformation will be large or small depending upon whether the heat transfer rate is small or large.

Now if the time lag were independent of time, the fractional variation of burning rate μ_b would be identical with the fractional variation of injection rate measured at the time τ earlier. Denoting the dimensionless time lag $\tau/\vartheta_g = \delta$, constant time lag would imply $\mu_b(z) = \mu_i(z - \delta)$. However, if the time lag is increasing during the process, the burning rate is depressed below the injection rate in proportion to the product of the propellant flow rate and the rate of change of time lag. Therefore, using dimensionless quantities and neglecting a term of second order in the small variations

$$\mu_b(z) \approx \mu_i(z - \delta) - \frac{d\delta}{dz} = 0 \quad \ldots\ldots\ldots\ldots [3]$$

The dependence of the time lag upon time is, in reality, governed by the integral, Equation [2], and differentiating this with respect to time gives

$$f[p(t), T_g(t)] - f[p(t-\tau), T_g(t-\tau)]\left(1 - \frac{d\tau}{dt}\right) \ldots [4]$$

Since it is assumed that the chamber pressure and ambient temperature vary only slightly from their steady-state values $\bar{p}$ and $\bar{T}_g$, the values of f may be approximated, following Tsien (5), through a Taylor expansion about $p = \bar{p}$, $T_g = \bar{T}_g$

$$f[p(t), T_g(t)] \approx f(\bar{p}, \bar{T}_g) + \frac{\partial f(\bar{p}, \bar{T}_g)}{\partial p}[p(t) - \bar{p}] + \frac{\partial f(\bar{p}, \bar{T}_g)}{\partial \bar{T}_g}[T_g(t) - \bar{T}_g]$$

$$f[p(t-\tau), T_g(t-\tau)] \approx f(\bar{p}, \bar{T}_g) + \frac{\partial f(\bar{p}, \bar{T}_g)}{\partial p}[p(t-\tau) - \bar{p}] + \frac{\partial f(\bar{p}, \bar{T}_g)}{\partial \bar{T}_g}[T_g(t-\tau) - \bar{T}_g]$$

Upon substituting these relations into Equation [4] and deleting second-order differences, the variation of time lag may be expressed

$$\frac{d\tau}{dt} = \frac{\partial \log f(\bar{p}, \bar{T}_g)}{\partial \log \bar{p}}\left[\frac{p(t-\tau) - p(t)}{\bar{p}}\right] + \frac{\partial \log f(\bar{p}, \bar{T}_g)}{\partial \log \bar{T}_g}\left[\frac{T_g(t-\tau) - T_g(t)}{\bar{T}_g}\right] \quad \ldots\ldots\ldots\ldots [5]$$

For a monopropellant rocket the combustion gas temperature is nearly constant so that the second term on the right side of Equation [5] vanishes. Calling $\partial \log f(\bar{p}, \bar{T}_g)/\partial \log \bar{p} \equiv n$, Tsien's generalization of Crocco's treatment is obtained. For the bipropellant rocket the combustion gas temperature may experience considerable variation, resulting from the variation of propellant mixture ratio, and consequently another parameter $\partial \log f(\bar{p}, \bar{T}_g)/\partial \log \bar{T}_g \equiv m$ enters the problem. Knowledge of combustion lag mechanics is so meager, however, that rational estimate of its importance is difficult. Consequently, as in previous investigations, the dependence of combustion time lag upon gas temperature will be neglected. Then, denoting the fractional variation in chamber pressure as $\varphi \equiv (p - \bar{p})/\bar{p}$, the expression for dimensionless time lag variation is

$$\frac{d\delta}{dz} \approx n\,[\varphi(z - \delta) - \varphi(z)] \quad \ldots\ldots\ldots\ldots [6]$$

The fractional variation in total propellant injection rate μ_i, which occurs in Equation [3], is most conveniently expressed in terms of the individual fractional variations of oxidizer flow, $\mu_o \equiv (\dot{m}_o - \bar{m}_o)/\bar{m}_o$, and of fuel flow, $\mu_f \equiv (\dot{m}_f - \bar{m}_f)/\bar{m}_f$, and the steady-state mixture ratio $\bar{r} \equiv \bar{m}_o/\bar{m}_f$. Again following Crocco in defining $H \equiv \bar{r} - 1/2(\bar{R} + 1)$, depending on the steady-state mixture ratio, it is an elementary calculation to show that, to the first order,

$$\mu_i = (1/2 + H)\,\mu_o + (1/2 - H)\,\mu_f$$

Consequently, the propellant burning rate is just

$$\mu_b(z) = \left(\frac{1}{2} + H\right)\mu_o(z - \delta) + \left(\frac{1}{2} - H\right)\mu_f(z - \delta) - n[\varphi(z - \delta) - \varphi(z)] \quad \ldots [7]$$

In calculating the variation of exit nozzle flow, $\dot{m}_e$, it is convenient to consider the nozzle flow as quasi-steady, that is, the flow corresponds to a time sequence of steady equilibrium flow patterns. Then the ratio of instantaneous to steady mass discharge rate is

$$\frac{\dot{m}_e}{\bar{m}} = \frac{p}{\bar{p}}\left(\frac{\bar{T}_g}{T_{ge}}\right)^{1/2} \quad \ldots\ldots\ldots\ldots [8]$$

where T_{ge} is the gas temperature at the exhaust end of the combustion chamber. Tsien has shown (7) that the quasi-steady approximation is adequate for low-frequency instability under discussion here.

For the monopropellant rocket, where T_{ge} is invariable, the mass discharge rate depends directly upon the combustion chamber pressure p, and the fractional variation of mass discharge rate is simply $\mu_e = \varphi$. Where the variation of mixture in a bipropellant rocket causes appreciable variation of temperature, this too must, according to Equation [8], be accounted for in computing the rate of gas discharge. Suppose the gas temperature at the exhaust end is T_{ge} at the time t. Recalling that the gas temperature depends upon only the propellant mixture ratio, the temperature T_{ge} can be related to the injection rates of propellant which formed the gas volume. The generation of gas took place at a time ϑ_g earlier than the gas appeared at the nozzle end of the chamber, that is, at a time $t - \vartheta_g$. Furthermore, the time required between injection of the propellants and generation of the gas is the time lag τ. Therefore the gas temperature at the exhaust end of the chamber is that corresponding to the mixture ratio at the time $t - \vartheta_g - \tau$, or at the dimensionless time $z - 1 - \delta$.

Now if r is the instantaneous mixture ratio, the change of gas temperature from its equilibrium value is, approximately, $(dT_g/dr)_{\bar{r}} \cdot (r - \bar{r})$. Furthermore, the variation of mixture ratio from its equilibrium value follows directly from the definition $r = \dot{m}_o/\dot{m}_f \approx \bar{r}(1 + \mu_o - \mu_f)$. Denoting the di-

mensionless slope of the gas temperature curve, $(\bar{r}/\bar{T}_g)(dT_g/dr)_r$, by $2K$, the effect of combustion gas temperature upon fractional variation of mass discharge is $K[\mu_0(z-\delta-1)-\mu_f(z-\delta-1)]$. Thus the complete expression is

$$\mu_e(z) = \varphi(z) - K[\mu_0(z-\delta-1) - \mu_f(z-\delta-1)] \quad \ldots [9]$$

Finally, the time variation of gas storage within the combustion chamber is shown by Crocco to be

$$\frac{d}{dz}\left(\frac{M_g}{\bar{M}_g}\right) \approx \frac{d\varphi}{dz} + 2K\{[\mu_0(z-\delta-1)-\mu_f(z-\delta-1)] - [\mu_0(z-\delta)-\mu_f(z-\delta)]\} \quad \ldots [10]$$

It is easy to trace the origin of the terms entering the right side of this expression. When the temperature is constant, the variation of mass in the chamber is directly proportional to the fractional variation of the uniform pressure, that is, to $d\varphi/dz$. When the temperature is not constant, a term must appear to account for the fact that the gas leaving the discharge, generated at $z-\delta-1$, is of different temperature and density from that generated at the injector, at $z-\delta$. Conversion of these temperature differences to the corresponding differences in oxidizer and fuel rates leads to the second term on the right side of Equation [10].

Introducing Equations [7], [9], and [10] in the original expression for the mass conservation in the combustion chamber, Equation [1], gives this relation in terms of the desired dependent variables

$$\frac{d\varphi}{dz} + (1-n)\varphi + n\varphi(z-\delta) + \left[K\mu_0(z-\delta-1) - 2K\mu_0(z-\delta) - \left(\frac{1}{2}+H\right)\mu_0(z-\delta)\right] - \left[K\mu_f(z-\delta-1) - 2K\mu_f(z-\delta) + \left(\frac{1}{2}-H\right)\mu_f(z-\delta)\right] = 0 \quad \ldots [11]$$

Description of the system may be completed by relating the individual propellant flow rates to the mechanical properties of the feed system. Consider each propellant feed system to consist, Fig. 1, of a feeding mechanism (e.g., turbopump), a propellant supply line, an injector nozzle, and a variable capacity situated in the line so close to the injector nozzle that the inertia of fluid between the capacity and the injector nozzle may be neglected. Since the process is the same in oxidizer and fuel lines, notation differentiating the two lines will be postponed.

Denote by subscript 1 the conditions in the propellant line just downstream of the pump, and by 2 the conditions just ahead of the injector. Following Tsien (5), the variation of $\dot{m}_1$, the pump discharge rate, from its equilibrium value may be written

$$\frac{\dot{m}_1 - \bar{\dot{m}}_1}{\bar{\dot{m}}_1} = -\alpha\frac{p_1 - \bar{p}_1}{\bar{p}_1} \quad \ldots [12]$$

When $\alpha = 0$, this relation indicates no response of mass flow to a change of line pressure, that is, a positive displacement system. Conversely, when $\alpha = \infty$, no change of line pressure may be effected by changing the flow rate, which is characteristic of the constant pressure feed or pressurized tank. Intermediate values of α correspond to particular types of pump, and if the response time of the turbopump system is very long with respect to the period of chamber pressure oscillation, the pump will operate at constant speed and $-\alpha$ corresponds to the slope of the pump characteristic (Fig. 2).

The pressure difference $p_1 - p$ along the propellant lines is due primarily to the liquid acceleration through the injector nozzle and the inertial reaction of the fluid column in the propellant line. The frictional loss will be neglected. If S is the area of the propellant jet issuing from the injector, and ρ the propellant density, the pressure difference $p_2 - p$ across the injector is $\dot{m}^2/2\rho S^2$. Furthermore, if l and A are the length and cross-sectional area of the connecting line, the inertial pressure difference follows from the momentum equation $(p_1 - p)A = d/dt(l\dot{m}_1)$. The mass flow $\dot{m}$ through the injector may differ from the mass flow $\dot{m}_1$ in the connecting line because of the variable capacitance situated between the two. Since the propellant is considered incompressible, the difference of the two values of mass flow may be expressed $\dot{m} - \dot{m}_1 = dC/dt$, where C is proportional to the instantaneous volume of the capacitance. This capacitance has the dimension of mass per unit time $\times$ time and is conveniently represented in the dimensionless form $k \equiv C/\bar{m}\vartheta_g$. Then if the pressure drop across the propellant injector under steady operation, $\bar{m}^2/2\rho S^2$, is denoted $\Delta\bar{p}$, two dimensionless parameters may be introduced: the inertia of the connecting line $J \equiv l\bar{m}/2\Delta\bar{p}A\vartheta_g$, and the injector pressure ratio $P \equiv \bar{p}/2\Delta\bar{p}$. Finally eliminating variable conditions at the pump and at the capacitance, the dynamic equilibrium of a propellant line may be written

$$J\frac{d\mu}{dz} + \left[\frac{1}{\alpha}\left(P+\frac{1}{2}\right)+1\right]\mu + P\varphi + J\frac{d^2k}{dz^2} + \frac{1}{\alpha}\frac{dk}{dz} = 0 \quad \ldots [13]$$

An equation of this type holds independently for the oxidizer and fuel lines.

Stability of the Bipropellant Rocket

When the propellant lines are of fixed capacity, the system is described by three independent variables, $\varphi(z)$, $\mu_0(z)$, and $\mu_f(z)$ representing the fractional variations in chamber pressure, oxidizer, and fuel flow. The three differential equations are, for the combustion chamber

$$\frac{d\varphi}{dz} + (1-n)\varphi + n\varphi(z-\delta) + \left[K\mu_0(z-\delta-1) - 2K\mu_0(z-\delta) - \left(\frac{1}{2}+H\right)\mu_0(z-\delta)\right] - \left[K\mu_f(z-\delta-1) - 2K\mu_f(z-\delta) + \left(\frac{1}{2}-H\right)\mu_f(z-\delta)\right] = 0 \quad \ldots [14]$$

and for the oxidizer and fuel lines

$$J_0\frac{d\mu_0}{dz} + \left[\frac{1}{\alpha_0}\left(P_0+\frac{1}{2}\right)+1\right]\mu_0 + P_0\varphi = 0$$

$$J_f\frac{d\mu_f}{dz} + \left[\frac{1}{\alpha_f}\left(P_f+\frac{1}{2}\right)+1\right]\mu_f + P_f\varphi = 0 \quad \ldots [15]$$

The stability or instability of the system, that is, whether the amplitude of particular oscillatory solutions will diminish or

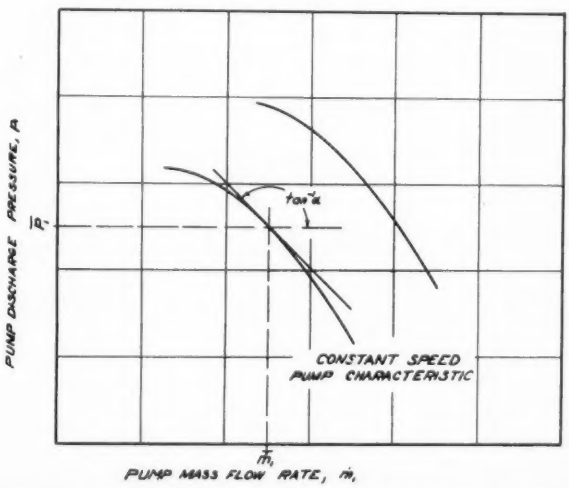

FIG. 2 APPROXIMATION TO CONSTANT SPEED PUMP CHARACTERISTIC

grow, is most easily discussed through introducing the Laplace transform, defined as

$$\Phi(s) = \int_0^\infty \varphi(z)e^{-sz}\,dz \quad \ldots\ldots\ldots\ldots\ldots\ldots [16]$$

for the variable $\varphi(z)$. Similarly defining $M_0(s)$ and $M_f(s)$ as the Laplace transforms of $\mu_0(z)$ and $\mu_f(z)$, each of the differential equations may be transformed, as shown in Appendix 1, into inhomogeneous algebraic equations in the complex variable s. The inhomogeneous portion depends upon the initial conditions of the problem and hence is associated with the solution of transient problems. The corresponding homogeneous equations

$$\begin{aligned}
&[s + 1 - n + ne^{-s\delta}]\Phi(s) + \\
&\quad e^{-s\delta}\left[Ke^{-s} - \left(2K + H + \frac{1}{2}\right)\right]M_0(s) - \\
&\quad e^{-s\delta}\left[Ke^{-s} - \left(2K + H - \frac{1}{2}\right)\right]M_f(s) = 0 \\
&P_0\Phi(s) + \left[J_0 s + \frac{1}{\alpha_0}\left(P_0 + \frac{1}{2}\right) + 1\right]M_0(s) = 0 \\
&P_f\Phi(s) + \left[J_f s + \frac{1}{\alpha_f}\left(P_f + \frac{1}{2}\right) + 1\right]M_f(s) = 0 \quad \ldots [17]
\end{aligned}$$

describe the free oscillations which are of interest in the stability problem. For nontrivial solutions the determinant of the coefficients of Equations [17] must vanish, that is

$$\begin{vmatrix}
s + (1 - n) + ne^{-s\delta} & \left[Ke^{-s} - \left(2K + H + \frac{1}{2}\right)\right]e^{-s\delta} & -\left[Ke^{-s} - \left(2K + H - \frac{1}{2}\right)\right]e^{-s\delta} \\
P_0 & J_0 s + 1 + \frac{1}{\alpha_0}\left(P_0 + \frac{1}{2}\right) & 0 \\
P_f & 0 & J_f s + 1 + \frac{1}{\alpha_f}\left(P_f + \frac{1}{2}\right)
\end{vmatrix} \equiv G'(s) = 0 \quad \ldots [18]$$

Equation [18] is a transcendental equation in the complex variable s, the roots of which determine the stability of rocket chamber pressure oscillations: If any root of $G'(s) = 0$ posseses a positive real part, the system is unstable. To check on the existence of such roots, it is possible to apply the familiar Nyquist criterion which traces the course of the complex function $G'(s)$ as s describes a counterclockwise contour in the right half of the s-plane consisting of the imaginary axis and a large semicircle in the right half plane. Then the negative change in argument of $G'(s)$ is the difference in number of zeros and poles of $G'(s)$ in the right half s-plane. Graphically this number appears as the number of complete revolutions made about the origin by the trace of $G'(s)$. If the number of poles is known independently, the number of zeros in the right half s-plane is known and the stability of the system is determined.

The present problem is complicated by the time lag δ, which not only makes calculation of $G'(s)$ laborious but accentuates the fact that the value of δ is usually not known accurately. To improve this situation, Tsien (5) has introduced another technique based upon a suggestion of Satche (6), which separates the function $G'(s)$ into two parts, the first containing $e^{-s\delta}$ as a factor, the second independent of the time lag. In the present example the separation may be affected by noting that the Equation [18] may be expressed as the combination of two determinants

$$\mathfrak{D}_1(s) = \begin{vmatrix}
s + 1 - n & 0 & 0 \\
P_0 & J_0 s + 1 + \frac{1}{\alpha_0}\left(P_0 + \frac{1}{2}\right) & 0 \\
P_f & 0 & J_f s + 1 + \frac{1}{\alpha_f}\left(P_f + \frac{1}{2}\right)
\end{vmatrix} \quad \ldots [19]$$

$$\mathfrak{D}_2(s) = \begin{vmatrix}
n & Ke^{-s} - \left(2K + H + \frac{1}{2}\right) & -\left[Ke^{-s} - \left(2K + H - \frac{1}{2}\right)\right] \\
P_0 & J_0 s + 1 + \frac{1}{\alpha_0}\left(P_0 + \frac{1}{2}\right) & 0 \\
P_f & 0 & J_f s + 1 + \frac{1}{\alpha_f}\left(P_f + \frac{1}{2}\right)
\end{vmatrix} \quad \ldots [20]$$

such that Equation [18] may be written

$$\mathfrak{D}_1(s) + e^{-s\delta}\mathfrak{D}_2(s) = 0 \quad \ldots\ldots\ldots\ldots [21]$$

Following Tsien in calling $g_1(s) \equiv e^{-s\delta}$ and defining $g_2(s) \equiv -(\mathfrak{D}_1(s)/\mathfrak{D}_2(s))$, the characteristic equation becomes

$$g_1(s) - g_2(s) \equiv G(s) = 0 \quad \ldots\ldots\ldots\ldots [22]$$

where the complex function $G(s)$ is represented as the difference of the two vectors $g_1(s)$ and $g_2(s)$.

Assume for the moment that $G(s)$ has no poles in the right half plane. Then if s describes its previous contour, the number of zeros which $G(s)$ has in the right half plane is equal to the number of complete clockwise rotations made by a vector having its head on the trace of $g_1(s)$ and its tail on the trace of $g_2(s)$. Since all values of $g_1(s)$ lie on or within the unit circle, the vector $G(s)$ can make a complete rotation if the trace of $g_2(s)$ either passes through the unit circle or encircles the origin. Conversely, if the trace of $g_2(s)$ lies outside the unit circle and does not encircle the origin, the system is definitely stable.

Actually, the function $G(s)$ may possess poles in the right half plane, due to zeros of the determinant $\mathfrak{D}_2(s)$ which constitutes the denominator of $g_2(s)$. Thus the number of clockwise turns which $g_2(s)$ makes about the origin must be modified by adding the number of poles induced through the roots of $\mathfrak{D}_2(s)$. This number of poles is found by applying the Nyquist criterion to $\mathfrak{D}_2(s)$ directly.

A few examples will serve to illustrate this technique. To discuss the stability of any bipropellant rocket, two sets of parameters must be known; H, K, and n which depend upon the propellants and their mixture ratio; and P_0, P_f, J_0, J_f, α_0, α_f which are associated with the propellant pumps, feed lines, and injector. In particular, the parameters H, K, and probably n are not independent of each other; H depends upon the propellant mixture ratio, and K upon the slope of the combustion temperature vs. mixture ratio curve at the steady mixture ratio under consideration. For the examples to follow, these values will be taken as given in Table 1 for various mixture ratios.

TABLE 1

$\bar{r}$	$\bar{T}_g$(° F)	$\frac{d\bar{T}_g}{d\bar{r}}$	H	K
2.75	5065	0	0.2335	0
2.50	5010	360	0.2125	0.09
2.25	4880	640	0.1925	0.1475
2.00	4706	850	0.167	0.189

For the first examples, choose the mechanical properties of the system such that

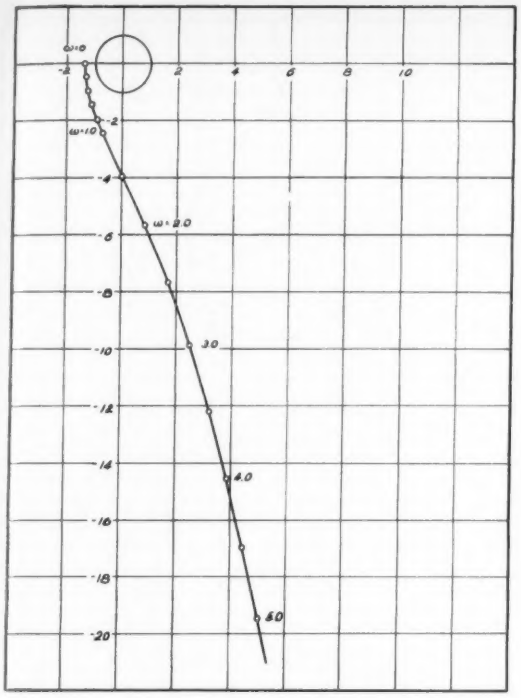

FIG. 3 SATCHE DIAGRAM FOR BIPROPELLANT ROCKET, $\bar{r} = 2.5$, $n = 0.2$; $\alpha_0 = \alpha_f = 1.0$, $P_0 = P_f = 1.0$, $J_0 = 2.0$, $J_f = 1.5$

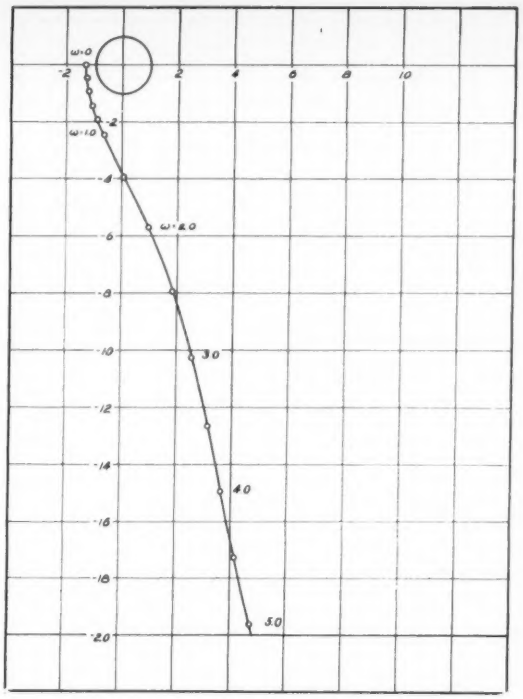

FIG. 4 SATCHE DIAGRAM FOR BIPROPELLANT ROCKET, $\bar{r} = 2.0$, $n = 0.2$; $\alpha_0 = \alpha_f = 1.0$, $P_0 = P_f = 1.0$, $J_0 = 2.0$, $J_f = 1.5$

$$\alpha_0 = \alpha_f = 1.0$$
$$P_0 = P_f = 1.0$$
$$J_0 = 2.0;\ J_f = 1.5$$

and consider four cases corresponding to two values of the steady-state mixture ratio and two values of the coefficient $n = d \log f / d \log \bar{p}$.

	n	$\bar{r}$
1	0.2	2.5
2	0.2	2.0
3	0.6	2.5
4	0.6	2.0

Then for calculating the functions $\mathfrak{D}_1(s)$ and $\mathfrak{D}_2(s)$ for values of s on the imaginary axis, that is, for $s = i\omega$

$$\mathfrak{D}_1(i\omega) = \left\{\frac{25}{4}(1-n) - \left[\frac{35}{4} + 3(1-n)\right]\omega^2\right\} + i\left\{\left[\frac{25}{4} + \frac{35}{4}(1-n)\right]\omega - 3\omega^3\right\}$$

$$\mathfrak{D}_2(i\omega) = \left\{\frac{25}{4}n + \frac{5}{2} - 3n\omega^2\right\} + i\omega\left\{\frac{35}{4}n - \frac{1}{2}(2K+H) + \frac{7}{4}\right\} + \frac{1}{2}K\{i\omega\cos\omega + \omega\sin\omega\}$$

The curves of $g_2(i\omega)$ for $n = 0.2$, calculated using these relations, are shown in Fig. 3 for $\bar{r} = 2.5$, and in Fig. 4 for $\bar{r} = 2.0$. They are nearly identical despite the considerable difference in mixture ratio; neither of them intersect the unit circle. To close the diagram, take $s = Re^{i\vartheta}$ where ϑ decreases from $\pi/2$ to $-(\pi/2)$. For large values of R, $g_2(s)$ behaves as $-J_0J_fR^3e^{3i\vartheta}/nJ_0J_fR^2e^{2i\vartheta} = -(R/n)e^{i\vartheta}$. Thus the $g_2(s)$ curve closes by a large arc in the left half of the Satche diagram, progressing clockwise. Since $g_2(s)$ neither crosses the unit circle nor encircles the origin outside the unit circle, instability can occur only if a zero of $\mathfrak{D}_2(s)$ exists which cancels a root of $g_2(s)$ in the right half s-plane. The presence of such a zero may be detected by applying the Nyquist criterion to $\mathfrak{D}_2(s)$. The Nyquist diagram is shown in Fig. 5 for $n = 0.2$ and $\bar{r} = 2.5$. For large values of R, $\mathfrak{D}_2(Re^{i\vartheta})$ behaves as $nJ_0J_fR^2e^{2i\vartheta}$, and therefore the Nyquist diagram closes with a large arc of 2π radians starting from the upper branch in Fig. 5 and progressing clockwise to the corresponding lower branch (not shown). Since the origin is not enclosed, the system is certainly stable. The same conclusion may easily be reached for the lower mixture ratio, $\bar{r} = 2.0$, $n = 0.2$.

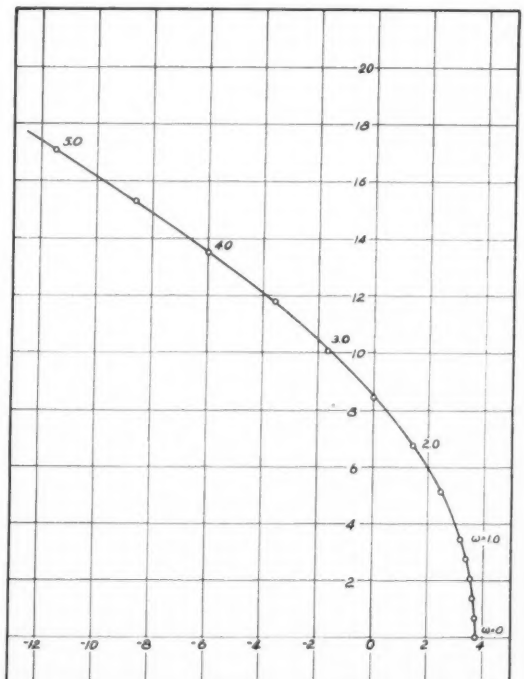

FIG. 5 NYQUIST DIAGRAM FOR $\mathfrak{D}_2(s)$, $\bar{r} = 2.5$, $n = 0.2$; $\alpha_0 = \alpha_f = 1.0$, $P_0 = P_f = 1.0$, $J_0 = 2.0$, $J_f = 1.5$

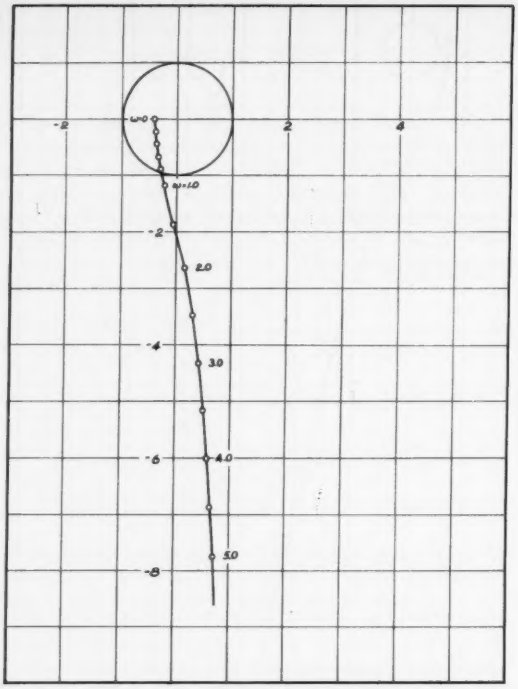

FIG. 6 SATCHE DIAGRAM FOR UNSTABLE BIPROPELLANT ROCKET, $\bar{r} = 2.5$, $n = 0.6$; $\alpha_0 = \alpha_f = 1.0$, $P_0 = P_f = 1.0$, $J_0 = 2.0$, $J_f = 1.5$

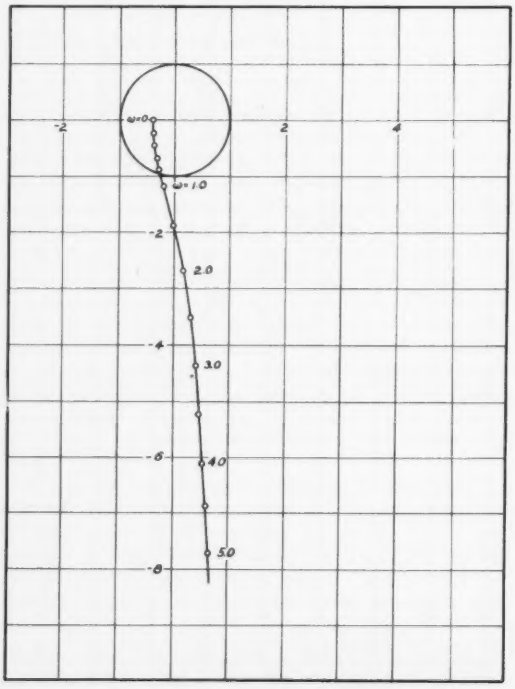

FIG. 7 SATCHE DIAGRAM FOR UNSTABLE BIPROPELLANT ROCKET, $\bar{r} = 2.0$, $n = 0.6$; $\alpha_0 = \alpha_f = 1.0$, $P_0 = P_f = 1.0$, $J_0 = 2.0$, $J_f = 1.5$

The stability curves for the two corresponding examples with $n = 0.6$, shown in Fig. 6 for $\bar{r} = 2.5$, and in Fig. 7 for $\bar{r} = 2.0$, both intersect the unit circle. Therefore a rocket propellant combination having parameters of these values will exhibit a low-frequency instability for some range of time lag δ. The method for determining the critical time lag has been shown by Tsien (5) in his original discussion of this method of analysis. Again the curves for the two values of mixture ratio are very similar. As in the first two examples, the closing arcs in the Satche diagram indicate no further instability of the system.

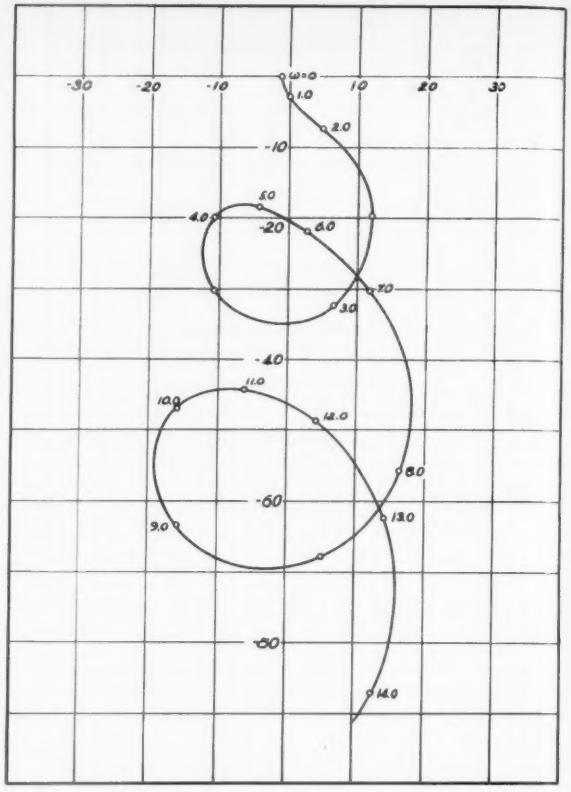

FIG. 8 SATCHE DIAGRAM FOR BIPROPELLANT ROCKET, $\bar{r} = 2.0$, $n = 0.2$; $\alpha_0 = \alpha_f = 1.0$, $P_0 = 1.0$, $P_f = 4.0$, $J_0 = 4.0$, $J_f = 1.0$

Because the mechanical properties of the two propellant systems are nearly identical in the foregoing examples, the change in mixture ratio associated with an oscillation in chamber pressure is very small and the behavior is much like that of a monopropellant rocket without line elasticity. Consequently the Satche diagrams are particularly simple. The influence of mixture ratio oscillation becomes important when the two lines have different inertial constants and injection pressures. As an example, consider a rocket for which

$$\alpha_0 = \alpha_f = 1.0$$
$$J_0 = 4.0 \qquad J_f = 1.0$$
$$P_0 = 1.0 \qquad P_f = 4.0$$
$$\bar{r} = 2.0 \qquad n = 0.2$$

The equations for $\mathfrak{D}_1(i\omega)$ and $\mathfrak{D}_2(i\omega)$ may be written

$$\mathfrak{D}_1(i\omega) = \left\{\frac{55}{4}(1-n) - \left[\frac{49}{2} + 4(1-n)\right]\omega^2\right\} + i\left\{\left[\frac{55}{4} + \frac{49}{2}(1-n)\right]\omega - 4\omega^2\right\}$$

$$\mathfrak{D}_2(i\omega) = \left\{\frac{55}{4}n + \frac{31}{4} - \frac{9}{2}(2K-H) - 4n\omega^2\right\} + i\omega\left\{\frac{49}{2}n + \frac{17}{2} - 15(2K+H)\right\} + \frac{9}{2}K(\cos\omega - i\sin\omega) + 15K(i\omega\cos\omega + \omega\sin\omega)$$

The Satche diagram for this example, Fig. 8, exhibits large loops. These loops originate in the trigonometric terms of $\mathfrak{D}_2(i\omega)$ which, in turn, arise because the change in combustion

temperature associated with a change in mixture ratio does not affect the chamber discharge rate until the residence time ϑ_e later. Consequently these terms are associated with a reduced time lag of unity.

Physically the influence of these terms is easy to see. When a gas mass of low temperature, caused by a fluctuation in mixture ratio, flows to the chamber discharge nozzle, the mass flow rate increases (cf. Equation [8]), causing the chamber pressure to drop. This reduction of chamber pressure causes a variation of mixture ratio which may lead to another negative fluctuation in gas temperature. Clearly, at certain frequencies, these oscillations will reinforce each other so that they will, as in the case of the present calculation, be slowly damped. (As pointed out by Tsien, the Satche diagram indicates possible slowly damped oscillations when the $g_2(i\omega)$ curve passes close to the unit circle.) Furthermore, it is clear that there will be an infinite number of frequencies at which such a reinforcement will take place. In the present example only two show up to any extent. The amplitude of an oscillation which originates in this manner depends to a considerable extent upon the response of the propellant feed system. If the change in pressure produces a large change in propellant flow, the oscillations may be severe; if the response is poor, the oscillation will disappear quickly. Now at high frequencies the inertia of the propellant supply causes the amplitude of its response to decrease, and consequently this particular resonance disappears. Mathematically this may be seen in the fact that for large values of ω the term $nJ_0J_f\omega^2$ governs the behavior of $\mathfrak{D}_2(i\omega)$, whereas the trigonometric terms are at most proportional to ω.

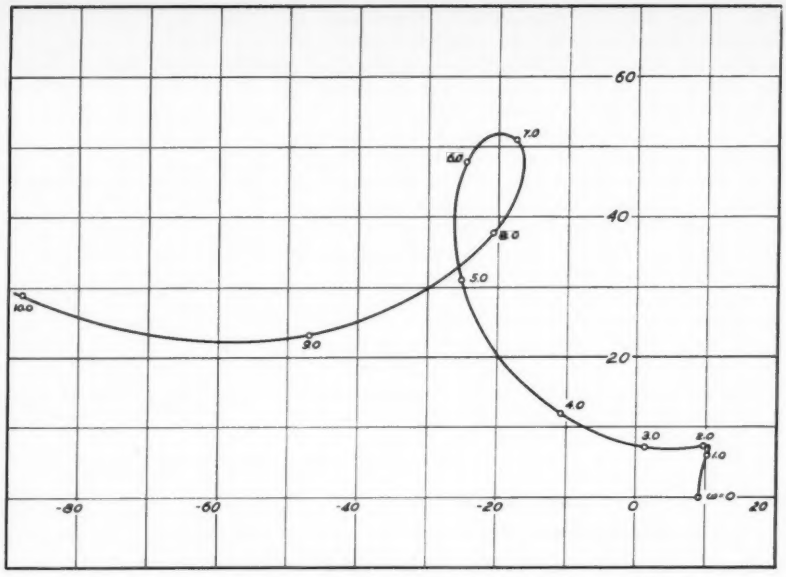

FIG. 9 NYQUIST DIAGRAM ASSOCIATED WITH SATCHE DIAGRAM OF FIG. 8

The closing arc of the $g_2(s)$ curve is the same as those discussed in previous examples. The Nyquist diagram of the denominator $\mathfrak{D}_2(s)$ is shown in Fig. 9, indicating no zeros of this determinant in the right half of the s-plane. The details of the Satche diagram near the unit circle, Fig. 10, show that the curve lies outside the unit circle and, as a consequence of this and the above considerations, the system is conclusively stable for all values of the combustion time lag.

The influence of mixture ratio variation may be further increased by considering a propellant combination for which the curve of combustion temperature vs. mixture ratio has a

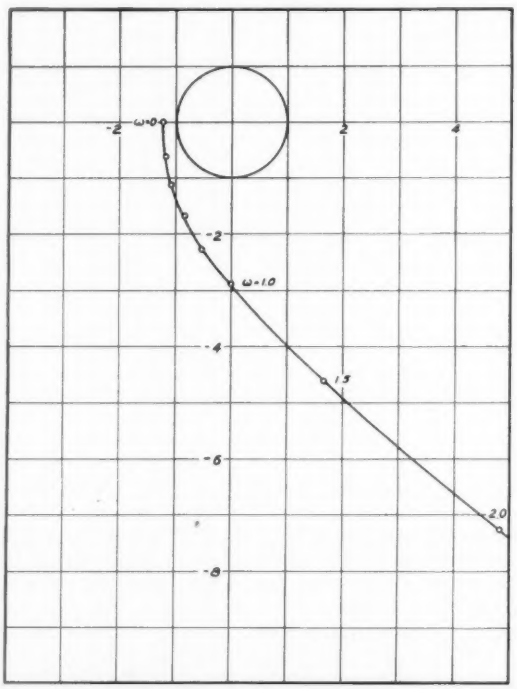

FIG. 10 DETAILS OF SATCHE DIAGRAM NEAR UNIT CIRCLE, $\bar{r} = 2.0$, $n = 0.2$; $\alpha_0 = \alpha_f = 1.0$, $P_0 = 1.0$, $P_f = 4.0$, $J_0 = 4.0$, $J_f = 1.0$

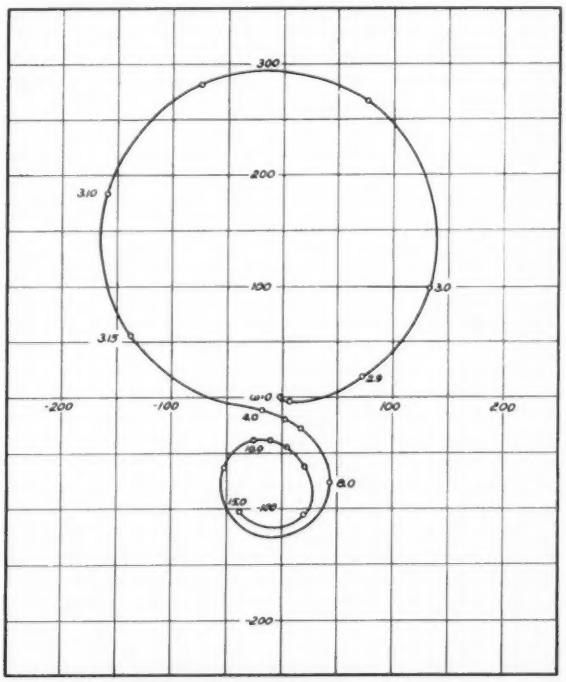

FIG. 11 SATCHE DIAGRAM FOR BIPROPELLANT ROCKET, $K = 0.3$, $\bar{r} = 2.0$, $n = 0.2$; $\alpha_0 = \alpha_f = 1.0$, $P_0 = 1.0$, $P_f = 4.0$, $J_0 = 4.0$, $J_f = 1.0$

slope greater than that considered in the previous example. Let all values of the previous example be retained with the exception that K is arbitrarily increased from 0.189 to 0.30. The resulting Satche diagram, Fig. 11, shows that the loops have now grown so large as to encircle the origin. By drawing the closing arc and checking the course of the complete curve, it is simply found that the $g_2(s)$ curve encircles the origin twice in a counterclockwise direction. The Nyquist diagram of $\mathfrak{D}_2(s)$, Fig. 12, shows a corresponding double encirclement but in the clockwise direction. Consequently, this cancellation indicates that no instability can arise from encirclement of the origin in the Satche diagram. Furthermore, the details of the Satche diagram in the neighborhood of the unit circle, Fig. 13, show no intersection and, thus, the system is definitely stable against all values of the combustion time lag.

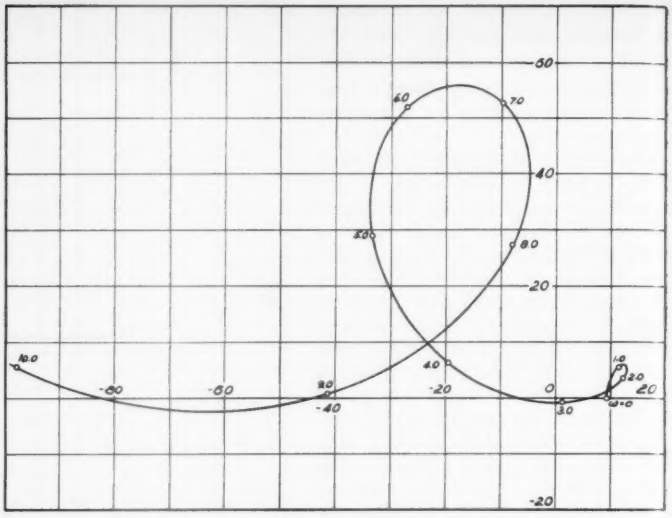

FIG. 12 NYQUIST DIAGRAM ASSOCIATED WITH SATCHE DIAGRAM OF FIG. 11

Servo-Stabilization of the Bipropellant Rocket

Where possible unstable operation of a rocket is indicated, stability may often be assured by modifying the mechanical design of the propellant supply system or injector, or in the extreme, by change in the chemical propellants. Alternatively the stability may be assured by introducing a feedback loop connecting the combustion chamber and the variable capacitances in each propellant line. In the simplest case the loop will consist of a pressure measuring device attached to the rocket chamber, an amplifier, and an appropriate servomechanism to actuate the capacitances in the propellant lines. For the bipropellant rocket, Fig. 14, two separate circuits may be employed, one for each propellant line. However, in the interest of simplicity it may be preferable (Fig. 15) to control only a single propellant line, or to control both through a single amplifier, building any required differences into the servomechanisms or into the capacitances.[4]

In general, then, the capacitances κ_0 and κ_f will be made to vary with time in a manner prescribed according to the variation in chamber pressure. Employing dimensionless forms, the correspondences between the capacitances and the chamber pressure may be written symbolically

$$\kappa_0(z) = F_0\left(\frac{d}{dz}\right)\varphi(z) \quad \text{[23]}$$

$$\kappa_f(z) = F_f\left(\frac{d}{dz}\right)\varphi(z) \quad \text{[24]}$$

where $F_0(d/dz)$ and $F_f(d/dz)$ are linear differential-integral operators. These relations simply indicate that the two capacitances are related to the chamber pressure through linear differential equations with constant coefficients, the forms of which depend upon the pressure pickup, the amplifiers, and the servomechanisms.

The problem is then to design the feedback circuits, that is, to determine the forms of $F_0(d/dz)$ and $F_f(d/dz)$ such that stable rocket operation is achieved. This resolves, practically, to the design of amplifiers to work with given servomechanisms and with a given pressure pickup so as to produce the required forms of F_0 and F_f. The proper forms of these functions can be determined only through stability analysis of the complete set of five differential equations, the original set consisting of Equation [11], and two of the type of Equation [13] augmented by the two equations arising from

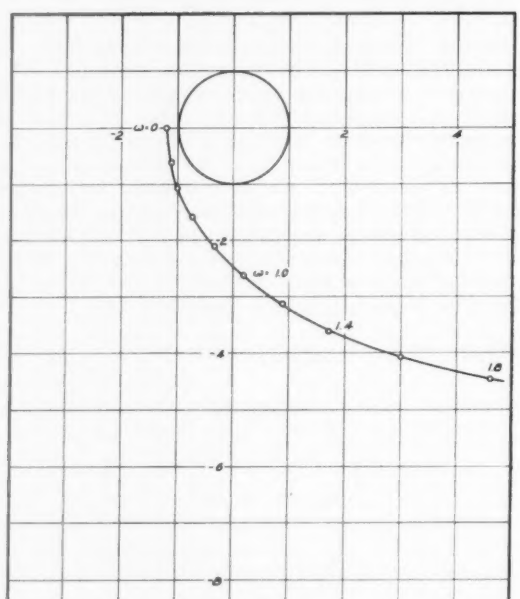

FIG. 13 DETAILS OF SATCHE DIAGRAM NEAR UNIT CIRCLE, $K = 0.3$, $\bar{r} = 2.0$, $n = 0.2$; $\alpha_0 = \alpha_f = 1.0$, $P_0 = 1.0$, $P_f = 4.0$, $J_0 = 4.0$, $J_f = 1.0$

the feedback loops, Equations [23] and [24]. Two additional dependent variables $\kappa_0(z)$ and $\kappa_f(z)$ have been introduced by allowing the capacitances to vary. The Laplace transforms of these equations are given in Appendix 1, and retaining only the homogeneous portion for stability analysis, the set of algebraic equations is

$$[s + 1 - n + ne^{-s\delta}]\Phi(s) + e^{-s\delta}\left[Ke^{-s} - \left(2K + H + \frac{1}{2}\right)\right] M_0(s) - e^{-s\delta}\left[Ke^{-s} - \left(2K + H - \frac{1}{2}\right)\right] M_f(s) = 0$$

[4] It has come to the attention of the authors that Y. C. Lee, M. R. Gore, and C. C. Ross, of the Aerojet Engineering Corporation, have considered a somewhat different arrangement in their paper, "Stability and Control of Liquid Propellant Rocket Systems" (see pp. 75–81 in this issue of the JOURNAL).

$$P_0\Phi(s) + \left[J_0 s + 1 + \frac{1}{\alpha_0}\left(P_0 + \frac{1}{2}\right)\right] M_0(s) + \left[J_0 s^2 + \frac{1}{\alpha_0}\left(P_0 + \frac{1}{2}\right) s\right] K_0(s) = 0$$

$$P_f\Phi(s) + \left[J_f s + 1 + \frac{1}{\alpha_f}\left(P_f + \frac{1}{2}\right)\right] M_f(s) + \left[J_f s^2 + \frac{1}{\alpha_f}\left(P_f + \frac{1}{2}\right) s\right] K_f(s) = 0$$

$$F_0(s)\Phi(s) - K_0(s) = 0$$

$$F_f(s)\Phi(s) - K_f(s) = 0 \quad \ldots\ldots\ldots\ldots\ldots [25]$$

where $K_0(s)$ and $K_f(s)$ are the Laplace transforms of the variable capacitances; $F_0(s)$ and $F_f(s)$ are the transfer functions of the feedback loops. The stability of the system is now dependent upon the roots of the fifth-order determinant constructed from the coefficients of Equations [25]

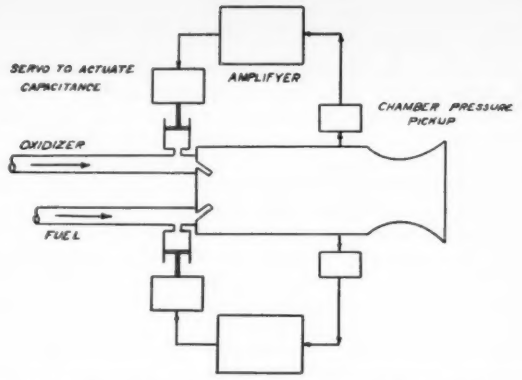

FIG. 14 SCHEMATIC DIAGRAM OF BIPROPELLANT ROCKET INCORPORATING FEEDBACK SYSTEM

$$\begin{vmatrix} s + 1 - n + ne^{-s\delta} & e^{-s\delta}\left[Ke^{-s} - \left(2K + H + \frac{1}{2}\right)\right] & -e^{-s\delta}\left[Ke^{-s} - \left(2K + H - \frac{1}{2}\right)\right] & 0 & 0 \\ P_0 & J_0 s + 1 + \frac{1}{\alpha_0}\left(P_0 + \frac{1}{2}\right) & 0 & J_0 s^2 + \frac{1}{\alpha_0}\left(P_0 + \frac{1}{2}\right) s & 0 \\ P_f & 0 & J_f s + 1 + \frac{1}{\alpha_f}\left(P_f + \frac{1}{2}\right) & 0 & J_f s^2 + \frac{1}{\alpha_f}\left(P_f + \frac{1}{2}\right) s \\ F_0(s) & 0 & 0 & -1 & 0 \\ F_f(s) & 0 & 0 & 0 & -1 \end{vmatrix} \quad \ldots\ldots [26]$$

This determinant is most conveniently expressed through expansion by second-order minors, employing the last two rows for the expansion. Defining two new third-order determinants

$\mathfrak{D}_0(s) =$

$$\begin{vmatrix} Ke^{-s} - \left(2K + H + \frac{1}{2}\right) & -\left[Ke^{-s} - \left(2K + H - \frac{1}{2}\right)\right] & 0 \\ J_0 s + 1 + \frac{1}{\alpha_0}\left(P_0 + \frac{1}{2}\right) & 0 & J_0 s^2 + \frac{1}{\alpha_0}\left(P_0 + \frac{1}{2}\right) s \\ 0 & J_f s + 1 + \frac{1}{\alpha_f}\left(P_f + \frac{1}{2}\right) & 0 \end{vmatrix}$$

$\mathfrak{D}_f(s) =$ $\ldots\ldots [27]$

$$\begin{vmatrix} Ke^{-s} - \left(2K + H - \frac{1}{2}\right) & -\left[Ke^{-s} - \left(2K + H + \frac{1}{2}\right)\right] & 0 \\ J_f s + 1 + \frac{1}{\alpha_f}\left(P_f + \frac{1}{2}\right) & 0 & J_f s^2 + \frac{1}{\alpha_f}\left(P_f + \frac{1}{2}\right) s \\ 0 & J_0 s + 1 + \frac{1}{\alpha_0}\left(P_0 + \frac{1}{2}\right) & 0 \end{vmatrix}$$

$\ldots\ldots [28]$

The characteristic equation obtained by setting the stability determinant (Equation [26]) to zero is

$$\mathfrak{D}_1(s) + e^{-s\delta}[\mathfrak{D}_2(s) + F_0(s)\mathfrak{D}_0(s) + F_f(s)\mathfrak{D}_f(s)] = 0 \ldots [29]$$

The two transfer functions of the feedback loops, $F_0(s)$ and $F_f(s)$, appear as multiplicative factors; each of the determinants depends upon only the original rocket configuration and is independent of the feedback circuit.

The new form of the function $g_2(s)$ is

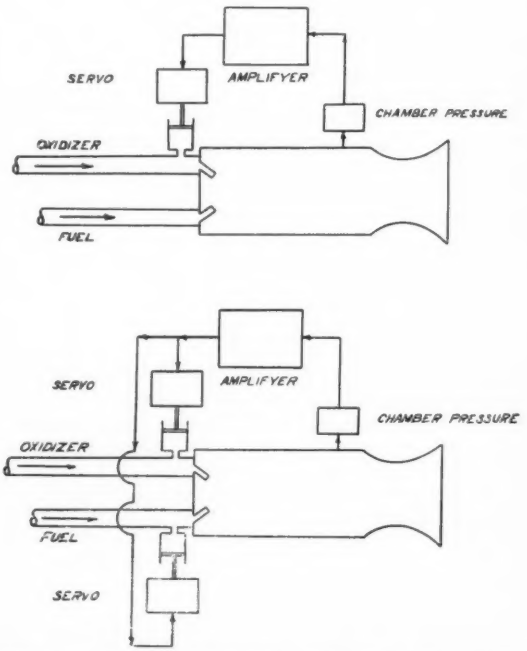

FIG. 15 TWO FEEDBACK CIRCUITS EMPLOYING ONLY A SINGLE AMPLIFIER AND PICKUP

$$g_2 s = \frac{\mathfrak{D}_1(s)}{\mathfrak{D}_2(s) + F_0(s)\,\mathfrak{D}_0(s) + F_f(s)\,\mathfrak{D}_f(s)} \quad \ldots\ldots [30]$$

Stable rocket operation is to be assured by choosing realizable forms of the feedback transfer functions $F_0(s)$ and $F_f(s)$ so that the Satche diagram satisfies the criteria previously discussed. One convenient procedure is to choose an appropriate Satche diagram and solve for the feedback transfer functions. For the present system the result is usually not a realizable or convenient feedback circuit.

When the instability arises from intersection of the $g_2(i\omega)$ curve with the unit circle, as it appears to do in practical cases of low-frequency oscillation, a proper choice of $F_0(s)$ and $F_f(s)$ may be effected quite simply. The intersection, when it exists, occurs for value of ω considerably less than unity; if this were not true, the oscillations would be of rather high frequency considering residence times of the usual magnitude. Hence the modification of the $g_2(i\omega)$ function may be restricted to low values of ω, this is to say, the gain of the amplifier in the feedback system should drop to a low value as the frequency ω increases. The appropriate analytic procedure is then (a) to find the approximate behavior of $F_0(s)$ and $F_f(s)$ for $s = i\omega << i$ such that $g_2(i\omega)$ does not intersect the unit circle, and (b) to determine the functions $F_0(s)$ and $F_f(s)$ so that they have the prescribed behavior for small values of ω and vanish for large ω, thus preserving the original Satche diagram in this range.

This program may be carried out in the following manner. Each of the third-order determinants involved in Equation [30] is regular at $s = 0$, and hence may be approximated by a power series

$$\begin{aligned}
\mathfrak{D}_1(s) &= d_1^{(0)} + d_1^{(1)}s + d_1^{(2)}s^2 + d_1^{(3)}s^3 \\
\mathfrak{D}_2(s) &= d_2^{(0)} + d_2^{(1)}s + d_2^{(2)}s^2 + d_2^{(3)}s^3 + \ldots \\
\mathfrak{D}_0(s) &= d_0^{(0)} + d_0^{(1)}s + d_0^{(2)}s^2 + d_0^{(3)}s^3 + d_0^{(4)}s^4 + \ldots \\
\mathfrak{D}_f(s) &= d_f^{(0)} + d_f^{(1)}s + d_f^{(2)}s^2 + d_f^{(3)}s^3 + d_f^{(4)}s^4 + \ldots
\end{aligned} \quad [31]$$

The coefficients $d_i^{(j)}$ depend only upon the parameters of the original (unstabilized) rocket and hence are known numerical values for any particular case. The expressions for these coefficients are given in Appendix 2. In particular, it appears that $d_0^{(0)} = d_f^{(0)} = 0$, a result which is clear from inspection of $\mathfrak{D}_0(s)$ and $\mathfrak{D}_f(s)$ as given by Equations [27] and [28]. The transfer functions for the feedback loops likewise possess power-series expansions about $s = 0$, although they need not be regular at that point. From the fact that the determinants $\mathfrak{D}_0(s)$ and $\mathfrak{D}_f(s)$ behave as s for small values of s, the expansions of the feedback transfer functions must behave as $1/s$ in order that the value of $g_2(0)$ be changed from that of the original system. That is, the transfer function must correspond to a simple integrating circuit. Thus it is appropriate to choose

$$\begin{aligned}
F_0(s) &= f_0^{(-1)}\frac{1}{s} + f_0^{(0)} + f_0^{(1)}s + f_0^{(2)}s^2 + \ldots \\
F_f(s) &= f_f^{(-1)}\frac{1}{s} + f_f^{(0)} + f_f^{(1)}s + f_f^{(2)}s^2 + \ldots
\end{aligned} \quad \ldots [32]$$

where the $f_0^{(j)}$ and the $f_f^{(j)}$ are unknown constants. Clearly, upon substituting the approximations of Equations [31] and [32] into Equation [30], a power-series representation for $g_2(s)$ is obtained where the unknown coefficients $f_0^{(j)}$, $f_f^{(j)}$ appear in the coefficients of the expansion.

From the viewpoint of insuring against low-frequency instability, the Satche diagram must be such that the $g_2(i\omega)$ curve lies outside the unit circle. For small ω, which are involved near the unit circle, $g_2(i\omega)$ may be approximated by the polynomial

$$g_2(i\omega) = \gamma_0 + \gamma_1(i\omega) + \gamma_2(i\omega)^2 + \gamma_3(i\omega)^3$$

where the γ_i are constants chosen so that this condition is satisfied. Then there are two expressions for $g_2(s)$, valid for small s

$$g_2(s) = \gamma_0 + \gamma_1 s + \gamma_2 s^2 + \gamma_3 s^3 \ldots\ldots [33]$$

and that which followed from expansion of Equation [30]. Since they are both valid power-series expansions, they are equal term by term. The result is four algebraic equations relating the constants $f_0^{(j)}$ and $f_f^{(j)}$ to the rocket parameters and to the chosen form of the Satche diagram near the unit circle. After some simplification these relations are

$$d_0^{(1)}f_0^{(-1)} + d_f^{(1)}f_f^{(-1)} + d_2^{(0)} = -\frac{d_1^{(0)}}{\gamma_0} \quad \ldots\ldots [34]$$

$$d_0^{(2)}f_0^{(-1)} + d_0^{(1)}f_0^{(0)} + d_f^{(2)}f_f^{(-1)} + d_f^{(1)}f_f^{(0)} + d_2^{(1)} = \frac{d_1^{(0)}}{\gamma_0}\left(\frac{\gamma_1}{\gamma_0} - \frac{d_1^{(1)}}{d_1^{(0)}}\right) \quad \ldots [35]$$

$$d_0^{(3)}f_0^{(-1)} + d_0^{(2)}f_0^{(0)} + d_0^{(1)}f_0^{(1)} + d_f^{(3)}f_f^{(-1)} + d_f^{(2)}f_f^{(0)} + d_f^{(1)}f_f^{(1)} + d_2^{(2)} = \frac{d_1^{(0)}}{\gamma_0}\left[\left(\frac{\gamma_2}{\gamma_0} - \frac{d_1^{(2)}}{d_1^{(0)}}\right) - \frac{\gamma_1}{\gamma_0}\left(\frac{\gamma_1}{\gamma_0} - \frac{d_1^{(1)}}{d_1^{(0)}}\right)\right] \quad \ldots [36]$$

$$d_0^{(4)}f_0^{(-1)} + d_0^{(3)}f_0^{(0)} + d_0^{(2)}f_0^{(1)} + d_0^{(1)}f_0^{(2)} + d_f^{(4)}f_f^{(-1)} + d_f^{(3)}f_f^{(0)} + d_f^{(2)}f_f^{(1)} + d_f^{(1)}f_f^{(2)} + d_2^{(3)} = \frac{d_1^{(1)}}{\gamma_0}\left[\left(\frac{\gamma_3}{\gamma_0} - \frac{d_1^{(3)}}{d_1^{(0)}}\right) - \frac{d_1^{(1)}}{d_1^{(0)}}\left(\frac{\gamma_2}{\gamma_0} - \frac{d_1^{(2)}}{d_1^{(0)}}\right) - 2\left(\frac{\gamma_2}{\gamma_0} - \frac{d_1^{(2)}}{d_1^{(0)}}\right)\left(\frac{\gamma_1}{\gamma_0} - \frac{d_1^{(1)}}{d_1^{(0)}}\right) + \left(\frac{\gamma_1^2}{\gamma_0^2} - \frac{d_1^{(2)}}{d_1^{(0)}}\right)\left(\frac{\gamma_1}{\gamma_0} - \frac{d_1^{(1)}}{d_1^{(0)}}\right)\right] \quad \ldots [37]$$

Four more relations among the $f_0^{(j)}$ and $f_f^{(j)}$ may be chosen arbitrarily so as to fix their values uniquely. Two possibilities have been mentioned previously: (a) the feedback loop operates only on a single capacitance so that either $f_0^{(j)} = 0$ or $f_f^{(j)} = 0$; (b) the two feedback loops are identical so that $f_0^{(j)} = f_f^{(j)}$; $j = -1, 0, 1, 2$. In each case only one pressure-sensing device and amplifier are required.

With the values of $f_0^{(j)}$, $f_f^{(j)}$ known, the behavior of the feedback circuit is determined for small s; the task is now to obtain general representations for $F_0(s)$ and $F_f(s)$ which agree with the known expressions for small s and vanish for large s so as to leave the original Satche diagram unchanged for large s. If, for instance, it were decided to control the oxidizer flow and leave the fuel flow uncontrolled, $f_f^{(j)} = 0$ and the $f_0^{(j)}$ are determined by successive application of Equations [34], [35], [36], and [37]. Then choose

$$F_0(s) = \frac{f_0^{(-1)}}{s}\left[\frac{1 - cs}{(1 - as)(1 - bs^2)}\right] \quad \ldots\ldots [38]$$

It is clear by reference to Equation [32] that the singular behavior as $s \to 0$ is correct. Furthermore for large s, $F_0(s)$ vanishes as $1/s^3$ which is probably strong enough. If the constants a, b, and c can be found so that the expansion of Equation [38] yields the first few coefficients in agreement with the known values $f_0^{(0)}$, $f_0^{(1)}$, and $f_0^{(2)}$, then Equation [36] will constitute a transfer function of the feedback loop, satisfactory for stabilizing the rocket against low-frequency oscillations regardless of the propellant time lag.

The power-series expansion of Equation [38] is

$$F_0(s) = \frac{f_0^{(-1)}}{s}\{1 + (a - c)s + [a(a - c) + b]s^2 + (a^2 - b)(a - c)s^3 + \ldots\} \quad \ldots [39]$$

which must be equal, term by term, to the first of Equations [32]. This condition determines the constants a, b, c directly as

$$\begin{aligned}
a^2 - \frac{f_0^{(2)}}{f_0^{(-1)}}a + \left(\frac{f_0^{(1)}}{f_0^{(-1)}} - \frac{f_0^{(2)}}{f_0^{(0)}}\right) &= 0 \\
b &= \frac{f_0^{(1)}}{f_0^{(-1)}} - a\frac{f_0^{(0)}}{f_0^{(-1)}} \\
c &= a - \frac{f_0^{(0)}}{f_0^{(-1)}}
\end{aligned} \quad \ldots [40]$$

where the $f_0^{(j)}$ are known. Substitution into Equation [38] then supplies the transfer function of the feedback loop to stabilize the system.

To illustrate application of the stabilization procedure, consider the unstable rocket for which the Satche diagram is shown in Fig. 6. For this example, the parameters have values

$$\begin{aligned} \alpha_0 &= \alpha_f = 1.0 \\ P_0 &= P_f = 1.0 \\ J_0 = 2.0 &\qquad J_f = 1.5 \\ \bar{r} = 2.50 &\qquad n = 0.6 \end{aligned}$$

The relations of Appendix 2 allow computation of the coefficients in the power expansions of the third-order determinants

$$\begin{aligned} d_1^{(0)} &= 2.50 & d_2^{(0)} &= 6.25 & d_0^{(1)} &= 3.01 \\ d_1^{(1)} &= 9.75 & d_2^{(1)} &= 6.85 & d_0^{(2)} &= 6.16 \\ d_1^{(2)} &= 9.95 & d_2^{(2)} &= 1.76 & d_0^{(3)} &= 2.89 \\ d_1^{(3)} &= 3.00 & d_2^{(3)} &= 0.02 & d_0^{(4)} &= 0.01 \end{aligned}$$

Now if, for small values of ω, the Satche diagram of the system may be moved to that indicated by the broken line in Fig. 16, the rocket motor will be stable against low-frequency oscillations. The curve $g_2(i\omega)$ will lie as shown if the γ_t are chosen

$$\begin{aligned} \gamma_0 &= -1.25 & \gamma_2 &= -0.25 \\ \gamma_1 &= -2.0 & \gamma_3 &= -1.0 \end{aligned}$$

By application of Equations [34] and [37]

$$\begin{aligned} f_0^{(-1)} &= -1.41 & f_0^{(1)} &= -3.87 \\ f_0^{(0)} &= -2.95 & f_0^{(2)} &= 5.05 \end{aligned}$$

which fixes the feedback loop for small values of ω. If further the transfer function is chosen to be of the form of Equation [38], the constants a, b, and c may be calculated from Equations [40]

$$\begin{aligned} a &= -0.8 & a &= -1.29 \\ b &= 1.08 & b &= 0.06 \\ c &= 1.29 & c &= 0.8 \end{aligned}$$

the two sets arising through the quadratic equation determining a. Choosing the first set (arbitrarily), the transfer function for the feedback loop in the oxidizer line is

$$F_0(s) = \frac{-1.41}{s} \frac{(1 - 1.29s)}{(1 + 0.8s)(1 - 1.08s^2)}$$

The Satche diagram for the stabilized motion is now easily computed through use of Equation [30] and the feedback transfer function found above. The result is shown in Fig. 16 along with the original Satche diagram and the power-series approximation for small values of ω. It is of interest to observe from Fig. 16 that the stabilized curve of $g_2(i\omega)$ and the corresponding series approximation diverge appreciably only as the value of ω exceeds unity. Thus the character of the Satche diagram is determined with sufficient accuracy by a few terms of its power-series expansion.

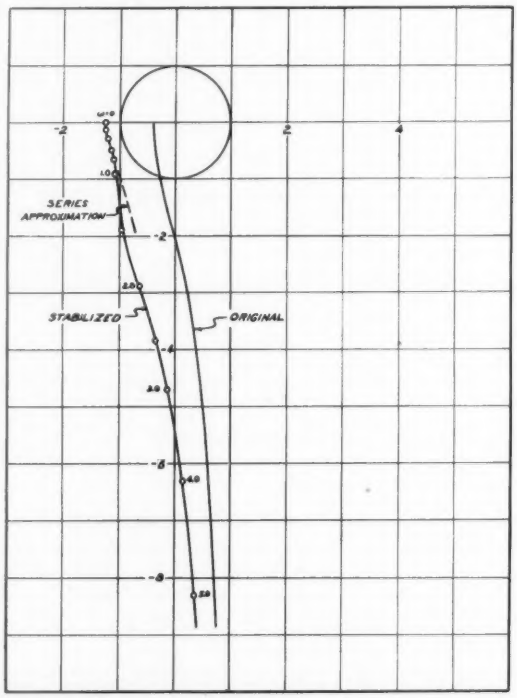

FIG. 16 COMPARISON OF STABILIZED AND UNSTABLE SATCHE DIAGRAMS, $\bar{r} = 2.5$, $n = 0.6$; $\alpha_0 = \alpha_f = 1.0$, $P_0 = P_f = 1.0$, $J_0 = 2.0$, $J_f = 1.5$

Concluding Remark

The present analytical results together with the initial work of Tsien (5) demonstrate conclusively that the low-frequency oscillations of a liquid propellant rocket motor may, in all cases, be stabilized by use of a feedback servo loop. Through use of the Satche diagram and the associated methods which have been described, a projected rocket configuration may be analyzed for possible unstable operation and the requirements for a stabilizing feedback loop determined. The application of these methods lies within common engineering practice. The concept of feedback stabilization removes restrictions on the propellant feed system and injector which would otherwise limit the freedom of the designer, with the consequence that he should be able to focus attention on improving combustion, reducing pumping loss, etc. This freedom is particularly important in the design of a rocket with variable thrust.

APPENDIX 1

Laplace Transform of the Rocket Stability Equations

The equation describing the combustion chamber pressure oscillation is

$$\frac{d\varphi}{dz} - (1 - n)\varphi + n\varphi(z - \delta) + \left[K\mu_0(z - \delta - 1) - \left(2K + H + \frac{1}{2}\right)\mu_0(z - \delta)\right] - \left[K\mu_f(z - \delta - 1) - \left(2K + H - \frac{1}{2}\right)\mu_f(z - \delta)\right] \quad [41]$$

while the equations of motion for the liquid in the oxidizer and fuel lines are

$$J_0 \frac{d\mu_0}{dz} + \left[\frac{1}{\alpha_0}\left(P_0 + \frac{1}{2}\right) + 1\right]\mu_0 + P_0\varphi + J_0 \frac{d^2\kappa_0}{dz^2} + \frac{1}{\alpha_0}\left(P_0 + \frac{1}{2}\right)\frac{d\kappa_0}{dz} = 0 \quad [42]$$

$$J_f \frac{d\mu_f}{dz} + \left[\frac{1}{\alpha_f}\left(P_f + \frac{1}{2}\right) + 1\right]\mu_f + P_f\varphi + J_f \frac{d^2\kappa_f}{dz^2} + \frac{1}{\alpha_f}\left(P_f + \frac{1}{2}\right)\frac{d\kappa_f}{dz} = 0 \quad [43]$$

Denoting the Laplace transforms of $\varphi(z)$, $\mu_0(z)$, $\mu_f(z)$, $\kappa_0(z)$, and $\kappa_f(z)$ by $\Phi(s)$, $M_0(s)$, $M_f(s)$, $K_0(s)$, and $K_f(s)$, respectively, the transformation of Equations [41], [42], and [43] is straightforward except for the terms involving a time lag. In general, the transform of $f(z - \delta)$ will be

$$\int_0^\infty f(z - \delta)e^{-sz}\,dz = \int_{-\delta}^\infty e^{-s\delta}f(z - \delta)e^{-s(z-\delta)}d(z - \delta) = e^{-s\delta}F(s) - e^{-s\delta}\int_{-\delta}^0 f(\xi)e^{-s\xi}\,d\xi$$

where $F(s)$ is the transform of $f(z)$. As is well known, when the variable is retarded the transform is modified through multiplication by an exponential factor $e^{-s\delta}$ and by the addition of an integral extending over the period of the time lag.

The equations then transform to

$$[s + 1 - n + ne^{-s\delta}]\Phi(s) + e^{-s\delta}\left[Ke^{-s} - \left(2K + H + \frac{1}{2}\right)\right] M_0(s) - e^{-s\delta}\left[Ke^{-s} - \left(2K + H - \frac{1}{2}\right)\right]M_f(s) = \varphi(0) + ne^{-s\delta}\int_{-\delta}^{0} \varphi(\xi)e^{-s\xi}\,d\xi + Ke^{-s(1+\delta)}\int_{-(1+\delta)}^{0} [\mu_0(\xi) - \mu_f(\xi)]e^{-s\xi}\,d\xi - (2K + H)e^{-s\delta}\int_{-\delta}^{0} [\mu_0(\xi) - \mu_f(\xi)]e^{-s\xi}\,d\xi - \frac{1}{2}\,e^{-s\delta}\int_{-\delta}^{0} [\mu_0(\xi) + \mu_f(\xi)]e^{-s\xi}\,d\xi \quad [44]$$

$$\left[J_0 s + 1 + \frac{1}{\alpha_0}\left(P_0 + \frac{1}{2}\right)\right] M_0(s) + P_0\Phi(s) + \left[J_0 s^2 + \frac{1}{\alpha_0}\left(P_0 + \frac{1}{2}\right)s\right] K_0(s) = J_0\mu_0(0) + J_0\frac{d\kappa_0}{dz}(0) + \left[J_0 s + \frac{1}{\alpha_0}\left(P_0 + \frac{1}{2}\right)\right]\kappa_0(0). \quad [45]$$

$$\left[J_f s + 1 + \frac{1}{\alpha_f}\left(P_f + \frac{1}{2}\right)\right] M_f(s) + P_f\Phi(s) + \left[J_f s^2 + \frac{1}{\alpha_f}\left(P_f + \frac{1}{2}\right)s\right] K_f(s) = J_f\mu_f(0) + J_f\frac{d\kappa_f}{dz}(0) + \left[J_f s + \frac{1}{\alpha_f}\left(P_f + \frac{1}{2}\right)\right]\kappa_f(0). \quad [46]$$

Stability analysis requires only the left-hand sides of these equations. Transient behavior of the rocket system, however, is determined by the complete equations where the right-hand sides, in usual problems, consist in the initial conditions of the dependent variables. For systems with time lag, such as the liquid propellant rocket, Equations [44], [45], and [46] show that in addition to initial conditions evaluated at $z = 0$, certain features of the behavior of the system must be known for a period preceding $z = 0$ equal in duration to the time lag. Physically this is clear, for due to the combustion time lag, the variation of chamber pressure $\varphi(z)$ cannot be described for $z > 0$ unless the behavior of the propellant flow is known for the period $-\delta \le z \le 0$.

APPENDIX 2

Power Series Representation of the Determinants

$$\mathfrak{D}_1(s) = d_1^{(0)} + d_1^{(1)}s + d_1^{(2)}s^2 + d_1^{(3)}s^3$$

Since this determinant, Equation [19], is a polynomial, this expression is exact.

$$d_1^{(0)} = (1 - n)\left[1 + \frac{1}{\alpha_0}\left(P_0 + \frac{1}{2}\right)\right]\left[1 + \frac{1}{\alpha_f}\left(P_f + \frac{1}{2}\right)\right]$$

$$d_1^{(1)} = \left[1 + \frac{1}{\alpha_f}\left(P_f + \frac{1}{2}\right)\right]\left[1 + \frac{1}{\alpha_0}\left(P_0 + \frac{1}{2}\right)\right] + (1 - n)J_0\left[1 + \frac{1}{\alpha_f}\left(P_f + \frac{1}{2}\right)\right] + (1 - n)J_f\left[1 + \frac{1}{\alpha_0}\left(P_0 + \frac{1}{2}\right)\right]$$

$$d_1^{(2)} = (1 - n)J_0J_f + J_0\left[1 + \frac{1}{\alpha_f}\left(P_f + \frac{1}{2}\right)\right] + J_f\left[1 + \frac{1}{\alpha_0}\left(P_0 + \frac{1}{2}\right)\right]$$

$$d_1^{(3)} = J_0J_f$$

$$\mathfrak{D}_2(s) = d_2^{(0)} + d_2^{(1)}s + d_2^{(2)}s^2 + d_2^{(3)}s^3 + \ldots$$

Referring to Equation [20], the coefficients are

$$d_2^{(0)} = n\left[1 + \frac{1}{\alpha_0}\left(P_0 + \frac{1}{2}\right)\right]\left[1 + \frac{1}{\alpha_f}\left(P_f + \frac{1}{2}\right)\right] + \frac{1}{2}\left\{P_0\left[1 + \frac{1}{\alpha_f}\left(P_f + \frac{1}{2}\right)\right] + P_f\left[1 + \frac{1}{\alpha_0}\left(P_0 + \frac{1}{2}\right)\right]\right\} - (K + H)\left\{P_f\left[1 + \frac{1}{\alpha_0}\left(P_0 + \frac{1}{2}\right)\right] - P_0\left[1 + \frac{1}{\alpha_f}\left(P_f + \frac{1}{2}\right)\right]\right\}$$

$$d_2^{(1)} = n\left\{J_0\left[1 + \frac{1}{\alpha_f}\left(P_f + \frac{1}{2}\right)\right] + J_f\left[1 + \frac{1}{\alpha_0}\left(P_0 + \frac{1}{2}\right)\right]\right\} + \frac{1}{2}\{P_0J_f + P_fJ_0\} + K\left\{P_0\left[1 + \frac{1}{\alpha_f}\left(P_f + \frac{1}{2}\right)\right] - P_f\left[1 + \frac{1}{\alpha_0}\left(P_0 + \frac{1}{2}\right)\right]\right\} + (K + H)\{P_0J_f - P_fJ_0\}$$

$$d_2^{(2)} = nJ_0J_f + K\{P_0J_f - P_fJ_0\} + \frac{K}{2}\left\{P_f\left[1 + \frac{1}{\alpha_0}\left(P_0 + \frac{1}{2}\right)\right] - P_0\left[1 + \frac{1}{\alpha_f}\left(P_f + \frac{1}{2}\right)\right]\right\}$$

$$d_2^{(3)} = \frac{K}{2}\{P_fJ_0 - P_0J_f\} + \frac{K}{6}\left\{P_0\left[1 + \frac{1}{\alpha_f}\left(P_f + \frac{1}{2}\right)\right] - P_f\left[1 + \frac{1}{\alpha_0}\left(P_0 + \frac{1}{2}\right)\right]\right\}$$

$$\mathfrak{D}_0(s) = d_0^{(0)} + d_0^{(1)}s + d_0^{(2)}s^2 + d_0^{(3)}s^3 + d_0^{(4)}s^4 + \ldots$$

Referring to Equation [27], the coefficients are

$$d_0^{(0)} = 0$$

$$d_0^{(1)} = \left(K + H + \frac{1}{2}\right)\frac{1}{\alpha_0}\left(P_0 + \frac{1}{2}\right)\left[1 + \frac{1}{\alpha_f}\left(P_f + \frac{1}{2}\right)\right]$$

$$d_0^{(2)} = \left(K + H + \frac{1}{2}\right)\left\{J_0\left[1 + \frac{1}{\alpha_f}\left(P_f + \frac{1}{2}\right)\right] + J_f\frac{1}{\alpha_0}\left(P_0 + \frac{1}{2}\right)\right\} + K\frac{1}{\alpha_0}\left(P_0 + \frac{1}{2}\right)\left[1 + \frac{1}{\alpha_f}\left(P_f + \frac{1}{2}\right)\right]$$

$$d_0^{(3)} = \left(K + H + \frac{1}{2}\right)J_0J_f + K\left\{J_0\left[1 + \frac{1}{\alpha_f}\left(P_f + \frac{1}{2}\right)\right] + J_f\frac{1}{\alpha_0}\left(P_0 + \frac{1}{2}\right)\right\} - \frac{K}{2}\frac{1}{\alpha_0}\left(P_0 + \frac{1}{2}\right)\left[1 + \frac{1}{\alpha_f}\left(P_f + \frac{1}{2}\right)\right]$$

$$d_0^{(4)} = KJ_0J_f - \frac{K}{2}\left\{J_0\left[1 + \frac{1}{\alpha_f}\left(P_f + \frac{1}{2}\right)\right] + J_f\frac{1}{\alpha_0}\left(P_0 + \frac{1}{2}\right)\right\} + \frac{K}{6}\frac{1}{\alpha_0}\left(P_0 + \frac{1}{2}\right)\left[1 + \frac{1}{\alpha_f}\left(P_f + \frac{1}{2}\right)\right]$$

$$\mathfrak{D}_f(s) = d_f^{(0)} + d_f^{(1)}s + d_f^{(2)}s^2 + d_f^{(3)}s^3 + d_f^{(4)}s^4 + \ldots$$

Referring to Equation [28], the coefficients are

$$d_f^{(0)} = 0$$

$$d_f^{(1)} = \left(K + H - \frac{1}{2}\right)\frac{1}{\alpha_f}\left(P_f + \frac{1}{2}\right)\left[1 + \frac{1}{\alpha_0}\left(P_0 + \frac{1}{2}\right)\right]$$

$$d_f^{(2)} = \left(K + H - \frac{1}{2}\right)\left\{J_f\left[1 + \frac{1}{\alpha_0}\left(P_0 + \frac{1}{2}\right)\right] + J_0\frac{1}{\alpha_f}\left(P_f + \frac{1}{2}\right)\right\} + K\frac{1}{\alpha_f}\left(P_f + \frac{1}{2}\right)\left[1 + \frac{1}{\alpha_0}\left(P_0 + \frac{1}{2}\right)\right]$$

$$d_f^{(3)} = \left(K + H - \frac{1}{2}\right)J_0J_f + K\left\{J_f\left[1 + \frac{1}{\alpha_0}\left(P_0 + \frac{1}{2}\right)\right] + J_0\frac{1}{\alpha_f}\left(P_f + \frac{1}{2}\right)\right\} - \frac{K}{2}\frac{1}{\alpha_f}\left(P_f + \frac{1}{2}\right)\left[1 + \frac{1}{\alpha_0}\left(P_0 + \frac{1}{2}\right)\right]$$

$$d_f^{(4)} = KJ_0J_f - \frac{K}{2}\left\{J_f\left[1 + \frac{1}{\alpha_0}\left(P_0 + \frac{1}{2}\right)\right] + J_0\frac{1}{\alpha_f}\left(P_f + \frac{1}{2}\right)\right\} + \frac{K}{6}\frac{1}{\alpha_f}\left(P_f + \frac{1}{2}\right)\left[1 + \frac{1}{\alpha_0}\left(P_0 + \frac{1}{2}\right)\right]$$

(Continued on page 81)

Stability and Control of Liquid Propellant Rocket Systems

Y. C. LEE,[1] M. R. GORE,[2] and C. C. ROSS[3]

Aerojet Engineering Corporation, Azusa, Calif.

Within the limitations of assumptions made in the analysis presented herein, it appears that the problem of stability and control of bipropellant liquid rockets may be investigated with respect to system dynamics, combustion time lag, and interaction of these two. For the gas-pressurized, bipropellant, liquid rocket system, stability criteria relating the system parameters have been established. Stability conditions for a typical pump-fed rocket are discussed. By the utilization of a suitable feedback control, it is theoretically demonstrated that bipropellant liquid rocket systems may be stabilized not only for system dynamics but also for any combustion time lag.

Nomenclature

A = area
C^* = characteristic velocity
C_f = frictional coefficient
c_p = specific heat at constant pressure
c_v = specific heat at constant volume
d = propellant line diameter
I = mass moment of inertia of turbine wheel
L^* = characteristic length of thrust chamber
l = propellant line length
l' = equivalent propellant line length
P = pressure
p = Laplace operator
R_c = gas constant of chamber gases
T_c = chamber gas temperature
t = time
V_c = chamber volume
v = velocity
w = weight rate of flow
θ = turbine speed
ρ = density
τ = combustion time lag
ω = frequency

(Bar over a symbol denotes equilibrium conditions.)

Subscripts

c = thrust chamber
d = propellant pump discharge or propellant tank
j = injector
f = fuel
ox = oxidizer
t = chamber throat

1 Introduction

(A) INSTABILITY in liquid-propellant rocket systems may be defined as operation in which uncontrolled variations in the system parameters occur. The rocket engineer is concerned with these variations because they may be of such magnitude as to cause poor performance of the propulsive unit or the vehicle which it propels. The rocket engineer would like to be able to design systems which are not only stable but also are free from large-amplitude transient oscillations. This paper suggests a method by which adequate stability and control of liquid propellant rocket systems may be achieved as part of a design procedure. The feasibility of such a method is demonstrated by the analysis presented herein.

(B) To facilitate discussion and analysis of the problem of stability and control, two mechanisms of instability may be distinguished. The first may be defined as one that involves only the dynamic behavior of the rocket feed system and its components. A rocket system is composed of many physical components, each characterized by its own dynamic behavior. Pumps, turbine, thrust chamber, and hydraulic flow through propellant lines are incapable of instantaneous response to changes in operating conditions. They are all characterized by a finite delay time. Time delay gives rise to phase shift and amplitude variation between system output and input, which are a function of the frequency of excitation. A disturbance such as a pulsation in propellant flow or chamber pressure may be of sufficient amplitude to initiate sustained oscillations in an unstable system.

(C) The second mechanism of instability is directly associated with the combustion phenomena of propellants in the thrust chamber. This mechanism of instability is generally referred to as combustion instability. There are two types of combustion instability. The first type involves pressure oscillations of frequencies low enough so that sound waves can traverse the thrust chamber several times during one oscillation. This type is generally referred to as "chugging" and usually occurs in the frequency range from 40 to 400 cps. The second type is associated with the motion of sound waves in the thrust chamber, and the observed frequencies of pressure oscillations are the characteristic frequencies of the various acoustic modes associated with a given chamber. This type is commonly called "screaming" instability and usually occurs in the frequency range from several hundred to several thousand cps. It is with the first type of instability, or chugging, that this paper is primarily concerned.

(D) The forcing function, or the driving mechanism, for the pressure oscillation of both chugging and screaming instability is associated with the atomization, mixing, and reaction processes of the propellants in the combustion chamber. The combustion mechanism depends on the fact that there is a great deal of energy available in the unreacted propellant components in the thrust chamber, and that a finite time is required to release this energy; or, to put it differently, there is a delay between the time when liquid fuel and oxidizer are injected into the thrust chamber and the time when these propellants are converted into gaseous combustion products at the steady-state chamber pressure and temperature. Instantaneous variations of any system parameter can change the instantaneous rate of energy release. If, for example, there is a pressure variation, and if the delay is of the proper magnitude, then the instantaneous increase or decrease of energy release due to the pressure change will be in the correct phase relationship with the resulting pressure oscillations, and these oscillations will increase in amplitude. Therefore, it appears that the rocket engineer is confronted with instability problems associated with the dynamic characteristics of the feed system and with the injection-combustion proc-

[1] Assistant Department Head, Study Department, Liquid Engine Division.
[2] Development Engineer, Physical Measurement Division.
[3] Manager, Liquid Engine Division. Member ARS.

Presented at the Fall Meeting of the AMERICAN ROCKET SOCIETY, September 9, 1952, Chicago, Ill.

esses of the thrust chamber and the interaction of these two.

(E) Increasing attention has been given recently to the problem of stability and control of liquid-propellant rockets. Particularly, the problem of combustion instability in liquid-propellant rockets has been exhaustively treated recently by Dr. M. Summerfield (1),[4] Dr. L. Crocco (2), and Dr. H. S. Tsien (3). Basically, the key to the theory lies in the concept of a time lag which exists during the process of propellant injection and transformation into high-temperature gases. Summerfield assumes that the time lag is constant, and Crocco postulates that the time lag is dependent upon chamber pressure. The assumption of a constant time lag implies that the system cannot become unstable or self-excited if the propellant flow is maintained constant. On the other hand, if the time lag is dependent upon chamber pressure, instability or self-excitation can result, even if the propellant flow is maintained constant. This represents the important and basic difference between Crocco's and Summerfield's work. Tsien, in his work, treated the same problem and attained the same results as Crocco by the use of an artifice of the Satche diagram (3). He further amplified his treatment of the problem by demonstrating the theoretical feasibility of achieving stabilization by means of feedback control in the propellant circuit.

(F) The first part of the present paper essentially extends Summerfield's work from a monopropellant to a bipropellant system for a simple gas-pressurized liquid-propellant rocket. The analysis of this system lends itself well to the servomechanism approach and may be treated most conveniently by the use of operational methods and the Nyquist criteria. Results of the analysis are given as stability boundaries relating the critical combustion time lag and critical frequency with the system parameters. The second part of this paper deals with a stability analysis of a rocket system, having fuel and oxidizer turbopumping plants. Both calibrated and feedback control systems are analyzed, and the effects of both system dynamics and combustion lag time are considered.

2 Gas-Pressurized Bipropellant System

(A) The gas-pressurized bipropellant rocket system is a simple system in which constant propellant-tank pressures are maintained by means of a pressure regulator, and propellants enter the thrust chamber through lines connecting the propellant tanks to the chamber. Fig. 1 is a schematic diagram of such a system.

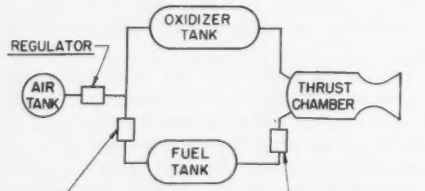

FIG. 1 BIPROPELLANT GAS-PRESSURIZED LIQUID ROCKET SYSTEM (SCHEMATIC)

(B) To facilitate the analysis of this system the following assumptions have been made: (a) A constant lag time, τ, exists between the time of propellant injection and time of equilibrium chamber pressure. (b) Propellant compressibility is negligible. (c) Propellant line elasticity is negligible. (d) System capacitance, such as trapped air in the lines or injector manifold, is negligible.

(C) The basic equations governing a monopropellant system have been developed by Summerfield (1). Those for a bipropellant system are presented as follows:

[4] Numbers in parentheses refer to References on page 81.

(a) The flow of oxidizer and fuel to the thrust chamber at a time $t-\tau$ must be equal to the rate at which the propellants are exhausted from the thrust chamber plus the rate at which they are stored in the chamber. Mathematically

$$w_{ox(t-\tau)} + w_{f(t-\tau)} = P_c \frac{A_t g}{C^*} + \frac{V_c}{R_c T_c} \frac{dP_c}{dt} \quad \ldots\ldots [1]$$

From energy considerations, the external work done on the propellant per unit time must be equal to the change in kinetic energy plus losses. For the fuel circuit

$$P_{df} A_{df} V_{df} - P_c A_{i_f} V_{i_f} = \frac{1}{2}\frac{w_f}{g} V_{i_f}^2 - \frac{1}{2}\frac{w_f}{g} V_{df}^2 + \frac{\rho_f l_f}{g} A_f V_f \frac{dV_f}{dt} + \frac{\rho_f l_{i_f}}{g} A_{if} V_{i_f} \frac{dV_{i_f}}{dt} + \frac{l'_f}{d_f} C_f \frac{w_f}{g} V_f^2$$

since

$$A_{df} V_{df} = A_i V_i = A_f V_f$$

The above equations may be simplified to

$$P_{df} - P_c = \frac{\epsilon_f w_f^2}{2\rho_f g A_{i_f}^2} + \frac{1}{g}\left(\frac{l_f}{A_f} + \frac{l_{i_f}}{A_{i_f}}\right)\frac{dw_f}{dt} \quad \ldots\ldots [2]$$

Similarly, for the oxidizer circuit

$$P_{dox} - P_c = \frac{\epsilon_{ox} w_{ox}^2}{2\rho_{ox} g A_{jox}^2} + \frac{1}{g}\left(\frac{l_{ox}}{A_{ox}} + \frac{l_{jox}}{A_{jox}}\right)\frac{dw_{ox}}{dt} \quad \ldots\ldots [3]$$

where

$$\epsilon_f = 1 - \left(\frac{A_{i_f}^2}{A_{df}^2}\right) + \left(\frac{A_{i_f}}{A_f}\right)^2 + C_f \frac{l'_f}{d_f}$$

$$\epsilon_{ox} = 1 - \left(\frac{A_{jox}}{A_{dox}}\right)^2 + \left(\frac{A_{jox}}{A_{ox}}\right)^2 + C_{ox} \frac{l'_{ox}}{d_{ox}}$$

(b) Inspection of Equations [1], [2], and [3] indicates that the system governed by them is analogous to a simple feedback servomechanism. In fact, the system may be represented by a block diagram, shown as Fig. 2. The inputs to the system are the tank pressures, P_{df} and P_{dox}. The output of the system is chamber pressure, P_c, which is compared with the input pressures. The error or difference between input and chamber pressures governs the propellant flow to the thrust chamber as described by Equations [2] and [3]. Since Equations [2] and [3] are nonlinear, small variations about an equilibrium point may be investigated. This is accomplished by linearization. The linearized system of equations results in

$$\left.\begin{aligned} w_{ox(t-\tau)} + w_{f(t-\tau)} &= \frac{A_t g}{C^*} P_c + \frac{V_c}{RT_c}\dot{P}_c \\ P_{df} - P_c &= \frac{2}{\bar{w}_f}(\bar{P}_{df} - \bar{P}_c) w_f + \frac{1}{g}\left(\frac{l_f}{A_f} + \frac{l_{if}}{A_{if}}\right)\dot{w}_f \\ P_{dox} - P_c &= \frac{2}{\bar{w}_{ox}}(\bar{P}_{dox} - \bar{P}_c) w_{ox} + \frac{1}{g}\left(\frac{l_{ox}}{A_{ox}} + \frac{l_{jox}}{A_{jox}}\right)\dot{w}_{ox} \end{aligned}\right\} \quad \ldots [4]$$

These equations may be expressed in operator form as the transfer functions appearing in Fig. 2.

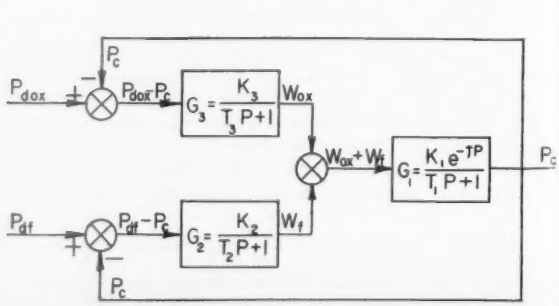

FIG. 2 BIPROPELLANT GAS-PRESSURIZED LIQUID ROCKET SYSTEM (BLOCK DIAGRAM)

$$G_1 = \frac{P_c}{w_{ox} + w_f} = \frac{K_1 e^{-\tau p}}{(T_1 p + 1)}$$

$$G_2 = \frac{w_f}{P_{df} - P_c} = \frac{K_2}{(T_2 p + 1)}$$

$$G_3 = \frac{w_{ox}}{P_{dox} - P_c} = \frac{K_3}{(T_3 p + 1)} \quad \text{.....[5]}$$

where T_1, T_2, etc., are time constants, and

$$T_1 = \frac{V_c C^*}{RT_c A_t g} = \frac{kL^*}{C^*}$$

$$K_1 = \frac{C^*}{A_t g}$$

$$k = \frac{1}{\gamma}\left(\frac{\gamma + 1}{\gamma}\right)^{\gamma + 1/\gamma - 1} \qquad \gamma = \frac{c_p}{c_v}$$

$$K_2 = \frac{\bar{w}_f}{2(\bar{P}_{df} - \bar{P}_c)}$$

$$T_2 = \frac{\bar{w}_f\left(\frac{l_f}{A_f} + \frac{l_{if}}{A_i}\right)}{2g(\bar{P}_{df} - \bar{P}_c)} = \frac{\bar{w}_f \alpha_f}{2g(\bar{P}_{df} - \bar{P}_c)}$$

$$K_3 = \frac{\bar{w}_{ox}}{2(\bar{P}_{dox} - \bar{P}_c)}$$

$$T_3 = \frac{\bar{w}_{ox}\left(\frac{l_{ox}}{A_{ox}} + \frac{l_{i_{ox}}}{A_{i_{ox}}}\right)}{2g(\bar{P}_{dox} - \bar{P}_c)} = \frac{\bar{w}_{ox}\alpha_{ox}}{2g(\bar{P}_{dox} - \bar{P}_c)}$$

$$\alpha_f = \frac{l_f}{A_f} + \frac{l_{if}}{A_{if}} \qquad \alpha_{ox} = \frac{l_{ox}}{A_{ox}} + \frac{l_{iox}}{A_{iox}}$$

From Equations [5], the system equation is

$$P_c = \frac{G_1 G_2 P_{df} + G_1 G_3 P_{dox}}{[1 + G_1(G_2 + G_3)]}$$

The characteristic equation, $F(p)$, is

$$F(p) = 1 + G_1(G_2 + G_3) = 0$$

$$1 + \frac{K_0(T_4 p + 1)e^{-\tau p}}{(T_1 p + 1)(T_2 p + 1)(T_3 p + 1)} = 0 \quad \text{.....[6]}$$

where

$$K_0 = K_1(K_2 + K_3) = \frac{\bar{P}_c}{2(\bar{w}_f + \bar{w}_{ox})}\left(\frac{\bar{w}_f}{\bar{P}_{df} - \bar{P}_c} + \frac{\bar{w}_{ox}}{\bar{P}_{dox} - \bar{P}_c}\right)$$

$$T_4 = \frac{K_2 T_3 + K_3 T_2}{K_2 + K_3} = T_3 \quad \frac{1 + \frac{\alpha_f}{\alpha_{ox}}}{1 + \bar{r}\left(\frac{\bar{P}_{df} - \bar{P}_c}{\bar{P}_{dox} - \bar{P}_c}\right)}$$

(c) T_1, T_2, T_3, and T_4 are time constants of the system. T_1 represents the time constant of the thrust chamber, T_2 represents the time constant of the fuel circuit, and T_3 the time constant of the oxidizer circuit. T_4 is a time constant associated with the coupling of the fuel and oxidizer circuits. K_0 is the static gain of the system.

(d) The fundamental criterion for the stability of this system is that $F(p)$ have no zeros in the right half of the complex p-plane; and system stability may be investigated by applying Nyquist's criteria to $Re^{-i\phi}$ where

$$Re^{-i\phi} = \frac{K_0(T_4 p + 1)e^{-\tau p}}{(T_1 p + 1)(T_2 p + 1)(T_3 p + 1)} \quad \text{.....[7]}$$

The system is unstable if $R > 1$ when the phase angle, $\phi = 180$ deg. The system is neutrally stable if the amplitude, $R = 1$ when $\phi = 180$ deg. It is to be noted that for a monopropellant system or for equal oxidizer and fuel tank pressures, K_0, the static gain of the system, reduces to

$$K_0 = \frac{\bar{P}_c}{2(\bar{P}_d - \bar{P}_c)}$$

and Equation [7] reduces to

$$Re^{-i\phi} = \frac{K_0 e^{-\tau p}}{(T_1 p + 1)(T_2 p + 1)}$$

This is a direct result of the fact that T_4, the coupling time constant, is equal to T_2 and T_3, the fuel and oxidizer circuit time constants, respectively.

(e) Based upon the criteria of stability, the following cases may be considered.

Case I: $\tau = 0$

For $\tau = 0$, the stability criteria are due entirely to system dynamics. The system is always stable for all values of K_0, T_1, T_2, T_3, and T_4, because:

First: If $K_0 \leq 1$, this system is stable for all values of T_1, T_2, T_3, and T_4. Since $T_4 = K_2 T_3 + K_3 T_2 / K_2 + K_3$, T_4 is always smaller than either T_2 or T_3. Therefore as $p = i\omega$ takes on all values of ω, the amplitude R is always smaller than unity. A phase shift of 180 deg is possible only as $\omega \to \infty$ and $R \to 0$.

Second: If $K_0 > 1$, the amplitude R can be greater than unity at some frequencies. But a phase shift of 180 deg is possible only as $\omega \to \infty$ and $R \to 0$.

Case II: $\tau \neq 0$

For this case, the stability criteria due to the interaction of combustion time lag and system dynamics may be investigated.

First: If $K_0 \leq 1$, this system is stable for all values of T_1, T_2, T_3, and T_4. Since T_4 is always smaller than either T_2 or T_3, and $e^{-\tau p}$ only contributes to phase shift, the amplitude R can never be greater than unity at any frequency. It is to be noted that this result is the same as that of a monopropellant system, investigated by Summerfield (1).

Second: If $K_0 > 1$, there always exists some τ regardless of values of T_1, T_2, T_3, and T_4 to cause a phase shift of 180 deg when $R = 1$.

(f) For the general case, it is desirable to establish the relationship which must exist among the system parameters in order that stable operation may be possible. The effect of combustion lag time, τ, upon system stability may be best investigated by a polar plot of $Re^{-i\phi}$. This plot is known as the Nyquist plot (4). As an example, Fig. 3 is a Nyquist plot of a system, having the following parameters:

$L^* = 30$ in. $\qquad C^* = 5100$ fps

$$\frac{\alpha_{ox}}{\alpha_f} = 1.275$$

$$\bar{r} = 3.52$$

$$T_1 = kL^*/C^* = 0.00114 \text{ sec}$$

$$T_3 = \frac{1}{2g}\frac{\bar{w}_f}{\bar{P}_{df} - \bar{P}_c}\alpha_f = 0.000472 \text{ sec}$$

$$K_0 = \frac{\bar{P}_c}{2(\bar{w}_{ox} + \bar{w}_f)}\left(\frac{\bar{w}_{ox}}{\bar{P}_{dox} - \bar{P}_c} + \frac{\bar{w}_f}{\bar{P}_{df} - \bar{P}_c}\right) = 1.19$$

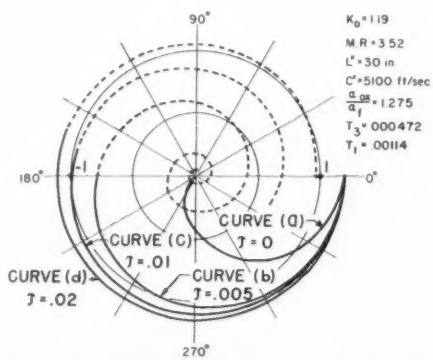

FIG. 3 NYQUIST PLOT, TYPICAL GAS-PRESSURIZED LIQUID ROCKET SYSTEM

It is evident from an inspection of curve (a) that stability exists for any value of K_0 if τ is assumed to be zero. For a fixed value of gain, curves (b), (c), and (d) demonstrate the effect that increasing lag time has on system stability. With τ equal to 0.005, the system is stable as indicated by curve (b). In the case of curve (d), for τ equal to 0.02 the system is unstable. For τ equal to 0.01, as shown by curve (c), the system is neutrally stable. It is of interest to note that the vector $Re^{-i\phi}$ "spins" forever about the origin due to the effect of $e^{-\tau p}$. The system response contains an infinite number of discrete higher frequencies as the vector "spins" every 2π radians and intersects with the real axis. The higher the frequency, the smaller the amplitude, indicating increasing attenuation with increasing frequency. However, it is possible that the system may respond to the higher frequencies, provided that the excitation, or forcing function, possesses high enough energy and is in phase with these modes.

(g) Neutral stability is characterized by a unique relationship among the system parameters and leads to the concept of a stability boundary. With all other parameters fixed, the relationship which must exist between any two parameters in order for $Re^{-i\phi}$ to pass through the -1 point may be established. The locus of all points satisfying this relationship is termed a stability boundary. If variations in more than two parameters are considered, families of stability boundaries may be found. For example, Figs. 4, 5, and 6 show a family of stability boundaries relating K_0 and τ as K_0 is varied for the system parameters given above. Fig. 4 shows a family of stability boundary curves for α_{ox}/α_f equal to 0.5 and for various values of $\bar{r}(\bar{P}_{df} - \bar{P}_c)/(\bar{P}_{dox} - \bar{P}_c)$. The region below the stability boundary curve represents the stable region, and that above the boundary the unstable. For typical rocket design, the parameter $\bar{r}(\bar{P}_{df} - \bar{P}_c)/(\bar{P}_{dox} - \bar{P}_c)$ is essentially equal to $\bar{r}$, the equilibrium mixture ratio. It appears that for this particular example, increasing the equilibrium mixture ratio tends to increase the region of stability for a given K_0. Or

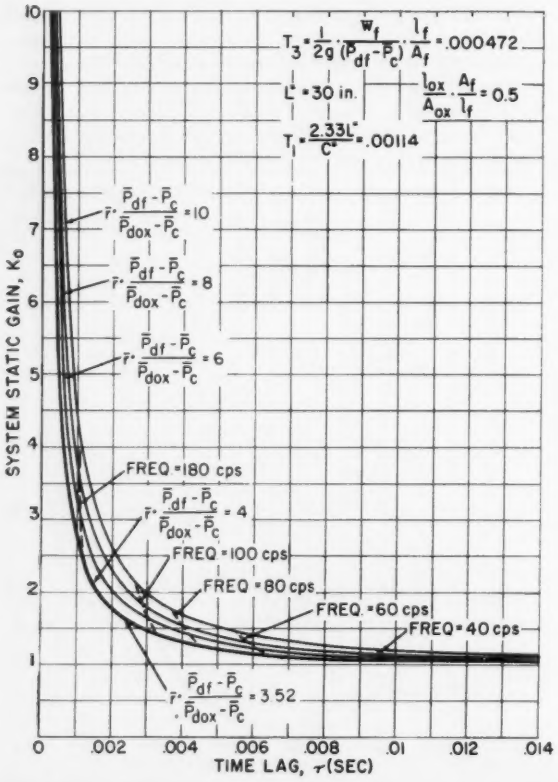
$T_3 = \frac{1}{2g} \cdot \frac{\bar{w}_f}{(\bar{P}_{df} - \bar{P}_c)} \cdot \frac{l_f}{A_f} = .000472$
$L^* = 30$ in.
$\frac{l_{ox}}{A_{ox}} \cdot \frac{A_f}{l_f} = 0.5$
$T_1 = \frac{2.33L^*}{C^*} = .00114$
$\bar{r} \cdot \frac{\bar{P}_{df} - \bar{P}_c}{\bar{P}_{dox} - \bar{P}_c} = 10$
$= 8$
$= 6$
$= 4$
$= 3.52$
FREQ = 180 cps
FREQ = 100 cps
FREQ = 80 cps
FREQ = 60 cps
FREQ = 40 cps
SYSTEM STATIC GAIN, K_0
TIME LAG, τ (SEC)
0 .002 .004 .006 .008 .01 .012 .014
1 2 3 4 5 6 7 8 9 10

FIG. 4 STABILITY BOUNDARY PLOT, $\alpha_{ox}/\alpha_f = 0.5$

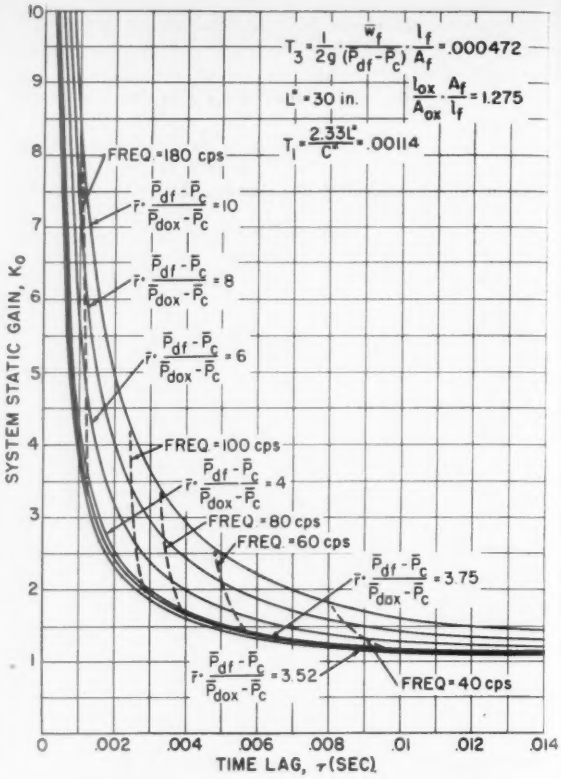
$T_3 = \frac{1}{2g} \cdot \frac{\bar{w}_f}{(\bar{P}_{df} - \bar{P}_c)} \cdot \frac{l_f}{A_f} = .000472$
$L^* = 30$ in.
$\frac{l_{ox}}{A_{ox}} \cdot \frac{A_f}{l_f} = 1.275$
$T_1 = \frac{2.33L^*}{C^*} = .00114$
$\bar{r} \cdot \frac{\bar{P}_{df} - \bar{P}_c}{\bar{P}_{dox} - \bar{P}_c} = 10$
$= 8$
$= 6$
$= 4$
$= 3.75$
$= 3.52$
FREQ = 180 cps
FREQ = 100 cps
FREQ = 80 cps
FREQ = 60 cps
FREQ = 40 cps
SYSTEM STATIC GAIN, K_0
TIME LAG, τ (SEC)
0 .002 .004 .006 .008 .01 .012 .014
1 2 3 4 5 6 7 8 9 10

FIG. 5 STABILITY BOUNDARY PLOT, $\alpha_{ox}/\alpha_f = 1.275$

for a given combustion time lag, higher values of K_0 may be tolerated as $\bar{r}$ increases. Figs. 5 and 6 illustrate the effect of α_{ox}/α_f on stability. Comparison of Figs. 4, 5, and 6 indicates that the higher the value of α_{ox}/α_f, the larger the stability region.

(h) The values of the parameters defining a point upon a stability boundary are such that the characteristic equation

$$1 + \frac{K_0(T_4p + 1)e^{-\tau p}}{(T_1p + 1)(T_2p + 1)(T_3p + 1)} = 0 \quad \ldots\ldots [8]$$

must be satisfied. To each point on the stability boundary there corresponds a frequency at which sustained oscillations occur, and this may be related to the system parameters if $p = i\omega$. And for small values of $\tau\omega$, the characteristic equation may be written

$$\frac{K_0(1 + i\omega T_4)(1 - i\tau\omega)}{(1 + i\omega T_1)(1 + i\omega T_2)(1 + i\omega T_3)} = -1$$

This equation provides an analytical means of locating points on the stability boundary. It can be shown that for the bipropellant system, the stability boundary is defined by the system parameters and the critical time lag, τ^*, as

$$\frac{T_1 + T_2 + T_3 + K_0(T_4 - \tau^*)}{T_1T_2T_3} = \frac{K_0 + 1}{T_1T_2 + T_1T_3 + T_2T_3 - K_0\tau^*T}$$

And the critical frequency at the boundary is

$$(\omega^*)^2 = \frac{K_0 + 1}{T_1T_2 + T_1T_3 + T_2T_3 - K_0\tau^*T_4}$$

For the monopropellant case, these equations reduce to

$$T_1 + T_2 = K_0\tau^*$$

and

$$(\omega^*)^2 = \frac{K_0 + 1}{T_1T_2}$$

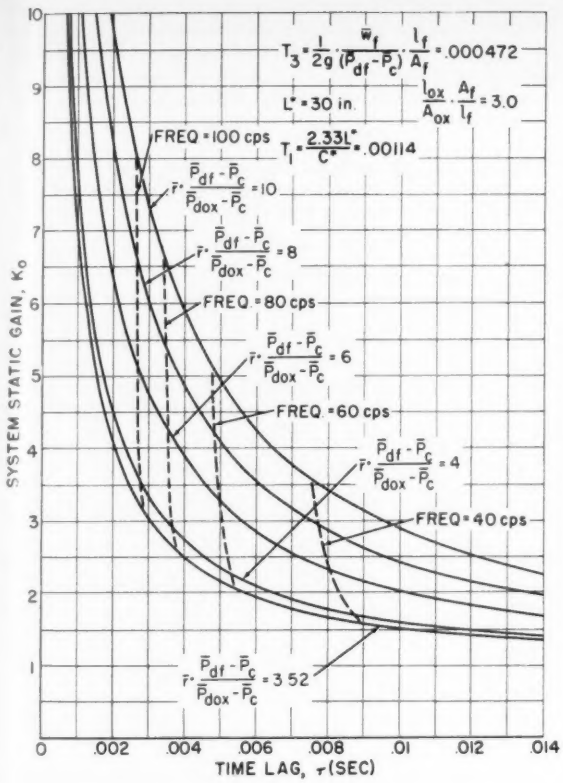

FIG. 6 STABILITY BOUNDARY PLOT, $\alpha_{ox}/\alpha_f = 3.0$

where $T_2 = T_3 = T_4$

This is the condition attained by Summerfield (1). However, it can be shown that the approximation $e^{-\tau p} = 1 - \tau p$, for small values of $\tau\omega$, is relatively poor in practical cases. From a Nyquist plot, the frequency at which the amplitude is unity may readily be obtained. And, at this frequency the additional phase shift resulting in marginal stability may be calculated. Since τ contributes only phase shift

$$\omega^*\tau^* = 180^\circ - \phi_1$$

where ϕ_1 is defined by

$$\frac{K_0(T_4p+1)}{(T_1p+1)(T_2p+1)(T_3p+1)} = Re^{-i\phi_1} \ldots\ldots [8']$$

To illustrate this point, the following example is given. For a bipropellant system having the following parameters

$T_1 = 0.00114$ sec
$T_2 = 0.000472$ sec
$T_3 = 0.00212$ sec
$T_4 = 0.000835$
$K_0 = 1.6$

The approximation yields the critical time lag, τ^*, of 0.0019 sec and the critical frequency, ω^*, of 215 cps. For an equivalent monopropellant system, having the same value of K_0, the time constant of the feed circuit is equal to $T_2 + T_3$ or 0.00259 sec, the thrust-chamber time constant, T_1, being the same. The critical time lag and critical frequency may be calculated

$$\tau^* = \frac{0.00114 + 0.00259}{1.6} = 0.0023 \text{ sec}$$

$$(\omega^*)^2 = \frac{(1.6+1)\times 10^6}{1.14 \times 2.59} = 0.88 \times 10^6$$

or $\omega^* = 150$ cps

It is seen that $\tau^*\omega^*$ is not small. On the other hand, if the complete Equation [8'] is used, for the bipropellant system, the critical frequency and time lag from Fig. 5 may be calculated as 80 cps and 0.004 sec, respectively.

3 Aspects of Stability and Control of a Pump-Fed Rocket

(A) A pump-fed rocket is one in which an oxidizer pump and fuel pump are employed to supply propellants to the thrust chamber. There are many types of pump drives. They differ only in the source of energy supply to the turbine. The turbine may derive its power from high-pressure air or hot combustion gases obtained from reaction of propellants. A typical pump-drive system is one in which the hot combustion gases from the thrust chamber may be employed to supply power to the turbine. This system is of particular interest from the standpoint of stability and control, because of the regenerative feature of such a system. The system is regenerative because the thrust chamber supplies combustion gases to drive the turbopumps, which in turn supply propellants that react in the thrust chamber and generate combustion gases to drive the turbopumps. The analysis presented herein will demonstrate that a system which may be unstable due to system dynamics and combustion time lag can be stabilized by the use of chamber-pressure feedback control.

(B) The analysis of the simple, gas-pressurized, bipropellant, liquid rocket system can readily be extended to a more complex system such as a regenerative pump-fed system. The rudimentary system is one in which an orifice that gives a calibrated hydraulic pressure drop in the hydraulic circuit is used to establish a thrust level. Fig. 7 shows a block diagram of such a calibrated system. In Fig. 7, G_5 represents the linearized turbine transfer function. If it is assumed that the drag, D, on the rotating parts is proportional to the square of the angular velocity, the equation for the turbine torque may be written as

$$T = I\ddot{\theta} + D(\dot{\theta})^2$$

If it is assumed that turbine torque is essentially proportional to chamber pressure for small variations of chamber pressures, then

$$K_T P_c = I\ddot{\theta} + D(\dot{\theta})^2$$

And the linearized turbine transfer function may be written as

$$G_5 = \frac{\dot{\theta}}{P_c} = \frac{K_5}{T_5 p + 1}$$

where

$$K_5 = \frac{K_T}{D} \text{ and } T_5 = \frac{I}{D}$$

G_6 and G_7 represent the linearized transfer functions of fuel

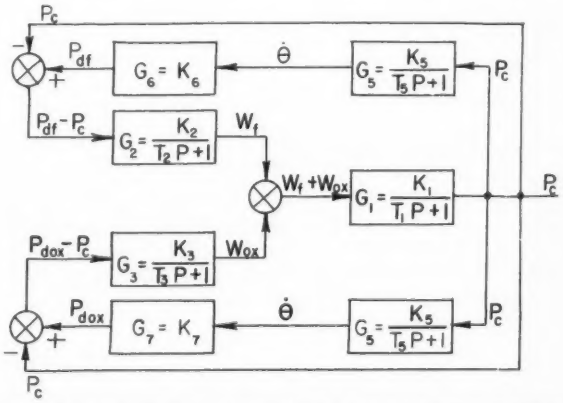

FIG. 7 REGENERATIVE CALIBRATED TURBOPUMPING SYSTEM (BLOCK DIAGRAM)

and oxidizer pumps. Since the pump discharge pressure is essentially proportional to the pump speed squared, the linearized pump-transfer functions may be written as

$$G_6 = \frac{P_{df}}{\dot{\theta}} = 2\bar{\theta}K_{Pf} = K_6$$

Similarly

$$G_7 = \frac{P_{dox}}{\dot{\theta}} = 2\bar{\theta}K_{Pox} = K_7$$

Therefore, the linearized equations governing the system are

$$G_1 = \frac{P_c}{w_f + w_{ox}} \qquad G_5 = \frac{\dot{\theta}}{P_c}$$

$$G_2 = \frac{w_f}{P_{df} - P_c} \qquad G_6 = \frac{P_{df}}{\dot{\theta}}$$

$$G_3 = \frac{w_{ox}}{P_{dox} - P_c} \qquad G_7 = \frac{P_{dox}}{\dot{\theta}}$$

The solution of these equations yields as a characteristic equation

$$1 + G_1[G_2(1 - G_5G_7) + G_3(1 - G_5G_6)] = 0 \ldots\ldots [9]$$

For symmetry, it is assumed that $G_7 = G_6$; Equation [9] then reduces to

$$1 + G_1(G_2 + G_3)(1 - G_5G_6) = 0$$

or

$$1 + \frac{K_0e^{-\tau p}(T_4p + 1)}{(T_1p + 1)(T_2p + 1)(T_3p + 1)} \cdot \frac{(1 - K_5K_6)\left(\frac{T_5p}{1 - K_5K_6} + 1\right)}{(T_5p + 1)} = 0 \quad [10]$$

In accordance with the Nyquist criteria, conditions of stability may be investigated by examining the behavior of $R_2e^{-i\phi_2}$ about the -1 point, where

$$R_2e^{-i\phi_2} = \frac{K_0e^{-\tau p}(T_4p + 1)}{(T_1p + 1)(T_2p + 1)(T_3p + 1)} \cdot \frac{(1 - K_5K_6)\left(\frac{T_5p}{1 - K_5K_6} + 1\right)}{(T_5p + 1)} \quad [11]$$

It is to be noted that Equation [11] is similar to Equation [7] except for the additional term

$$\frac{(1 - K_5K_6)\left(\frac{T_5p}{1 - K_5K_6} + 1\right)}{(T_5p + 1)}$$

which results from the inclusion of the turbine and pumps in the system. The effect of the addition of the turbine and pumps upon previously established conditions for stability of a gas-pressurized system may be investigated. There are three distinct cases:

Case I: $\quad K_5K_6 = 1$

In this case, Equation [11] may be reduced to

$$R_2e^{-i\phi_2} = \frac{K_0e^{-\tau p}(T_4p + 1)}{(T_1p + 1)(T_2p + 1)(T_3p + 1)} \cdot \frac{T_5p}{(T_5p + 1)}$$

and the effect of $T_5p(T_5p + 1)$ is to introduce a low-frequency phase lead. High-frequency behavior of the gas-pressurized system is not affected by the inclusion of turbine and pumps. The criteria for stability are essentially those established for the simple gas-pressurized system.

Case II: $\quad K_5K_6 < 1$

The conditions for stability are similar to those established for the gas-pressurized system except that conditions must now be imposed upon $K_0(1 - K_5K_6)$ rather than upon K_0 alone. The conditions for stable operation are somewhat less stringent than the gas-pressurized system, since $(1 - K_5K_6)$ is always <1. Not only is the phase lag caused by $(T_5p + 1)$ more than compensated by the phase lead due to $T_5p/(1 - K_5K_6) + 1$, but also a higher value of K_0 is permissible.

Case III: $\quad K_5K_6 > 1$

In this case, the system is a regenerative feedback one. For $\tau = 0$, necessary but not sufficient conditions for stability are that

$$|K_0(1 - K_5K_6)| < 1$$

and

$$|K_0[T_5 + T_4(1 - K_5K_6)]| < T_1 + T_2 + T_3 + T_5$$

(A) In a system defined by a given set of parameters, it is desirable to have some means of determining the maximum value of τ which the system may tolerate without instability due to combustion lag time. For this purpose, Equation [9] may be rewritten as

$$(T_1p + 1)(T_2p + 1)(T_3p + 1)(T_5p + 1) + K_0(1 - K_5K_6)(T_4p + 1)\left(\frac{T_5p}{1 - K_5K_6} + 1\right)e^{-\tau p} = 0$$

It is possible to define

$$G(p) = e^{-\tau p} - \left[-\frac{g_2(p)}{g_1(p)}\right]$$

where

$$g_1(p) = K_0(1 - K_5K_6)(T_4p + 1)\left(\frac{T_5p}{1 - K_5K_6} + 1\right)$$

$$g_2(p) = (T_1p + 1)(T_2p + 1)(T_3p + 1)(T_5p + 1)$$

The plot of $G(p)$ as p follows a contour about the right half of p-plane is known as a Satche diagram. A general discussion of the Satche diagram is included in Ref. (3). The vector $e^{-\tau p}$ maps into the unit circle; the points of intersection of $[-C_1(p)/g_2(p)]$ with this unit circle may be investigated, and the critical combustion lag time, τ^*, may be calculated from the relationship

$$\tau^*\omega^* = \phi^*$$

where ϕ^* is the phase angle introduced by $e^{-\tau p}$ at the point of intersection.

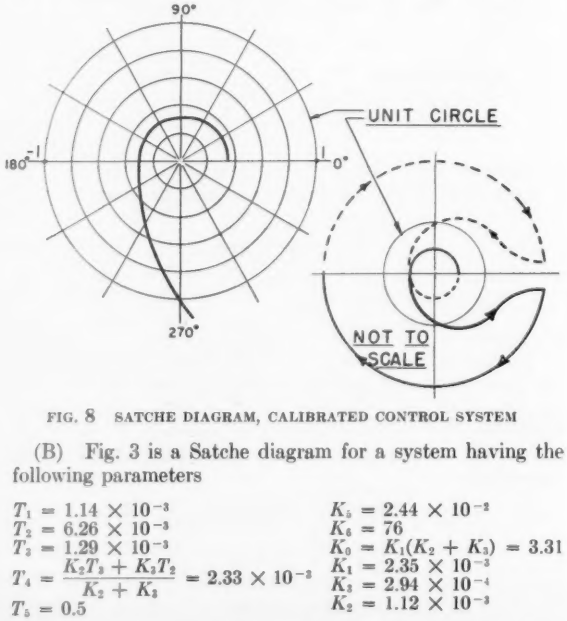

FIG. 8 SATCHE DIAGRAM, CALIBRATED CONTROL SYSTEM

(B) Fig. 3 is a Satche diagram for a system having the following parameters

$T_1 = 1.14 \times 10^{-3}$
$T_2 = 6.26 \times 10^{-3}$
$T_3 = 1.29 \times 10^{-3}$
$T_4 = \frac{K_2T_3 + K_3T_2}{K_2 + K_3} = 2.33 \times 10^{-3}$
$T_5 = 0.5$

$K_5 = 2.44 \times 10^{-2}$
$K_6 = 76$
$K_0 = K_1(K_2 + K_3) = 3.31$
$K_1 = 2.35 \times 10^{-3}$
$K_3 = 2.94 \times 10^{-4}$
$K_2 = 1.12 \times 10^{-3}$

This system is dynamically unstable because $K_5K_6 > 1$, and

the inequality of Case III is not satisfied. The condition for stability for all values of τ is that the curve $[-g_1(p)/g_2(p)]$ must never intersect the unit circle. This condition suggests the use of feedback not only to improve the system dynamic performance but also to make stable operation possible re-

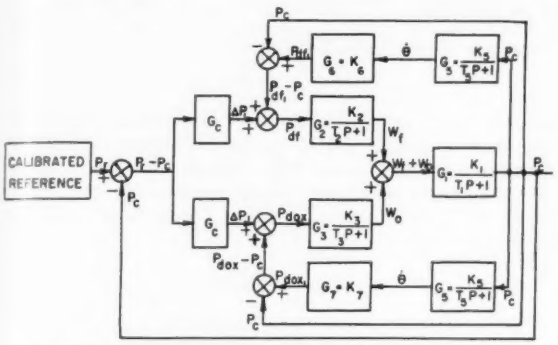

FIG. 9 FEEDBACK CONTROL SYSTEM (BLOCK DIAGRAM)

gardless of the magnitude of τ. If a feedback control system of the form shown in Fig. 9 is utilized, the system equations become

$$G_1 = \frac{P_c}{w_f + w_{ox}} \qquad G_6 = \frac{P_{df_1}}{\dot{\theta}} \qquad P_{df_1} + \Delta P_1 = P_{df}$$

$$G_2 = \frac{w_f}{P_{df} - P_c} \qquad G_7 = \frac{P_{dox_1}}{\dot{\theta}} \qquad P_{dox1} + \Delta P_1 = P_{dox}$$

$$G_3 = \frac{w_{ox}}{P_{dox} - P_c} \qquad P_e = P_R - P_c$$

$$G_5 = \frac{\dot{\theta}}{P_c} \qquad G_c = \frac{\Delta P_1}{P_e}$$

From which, for $G_6 = G_7$

$$\frac{P_c}{P_0} = \frac{G_c(G_2 + G_3)G_1}{1 + G_1(1 - G_5G_6)(G_2 + G_3)}$$

and the characteristic equation is

$$G_c(G_2 + G_3)\, G_1 + 1 + G_1(1 - G_5G_6)(G_2 + G_3) = 0$$

or

$$1 + G_1(G_2 + G_3)\{G_c + (1 - G_5G_6)\} = 0$$

which, upon substitution of the proper transfer functions, becomes

$$1 + \frac{K_0(T_4p + 1)e^{-\tau p}}{(T_1p + 1)(T_2p + 1)(T_3p + 1)} \left[G_c + \frac{(1 - K_5K_6)\left(\frac{T_5p}{(1 - K_5K_6)} + 1\right)}{(T_5p + 1)} \right] = 0 \ldots\ldots [12]$$

It is to be noted that Equation [12] is similar to Equations [6] and [10] except that the open-loop response of the simple gas-pressurized system is now modified by terms representing not only the turbine and pumps, but also the controller, represented by G_c.

If Equation [12] is rewritten

$$(T_1p + 1)(T_2p + 1)(T_3p + 1)(T_5p + 1) + e^{-\tau p}\left\{K_0(T_4p + 1)\left[G_c(T_5p + 1) + (1 - K_5K_6)\left(\frac{T_5p}{(1 - K_5K_6)} + 1\right)\right]\right\}$$

It is now possible to define

$$G'(p) = e^{-\tau p} - \left\{ - \frac{g'_2(p)}{g'_1(p)} \right\}$$

where

$$g'_1(p) = K_0(T_4p + 1)\left[C_c\,(T_5p + 1) + (1 - K_5K_6)\left(\frac{T_5p}{1 - K_5K_6} + 1\right)\right]$$

$$g'_2(p) = (T_1p + 1)(T_2p + 1)(T_3p + 1)(T_5p + 1)$$

(C) The value G_c may be selected so as to warp the plot of $[-g'_2(p)/g'_1(p)]$ in such fashion that intersection with the unit circle does not occur. For example, examination of the typical system shown in Fig. 8 indicates that G_c should be selected to alter only the low-frequency behavior of this system. In the frequency range from 0 to 550 rad/sec, G_c should be such that the amplitude of $[-g'_2(p)/g'_1(p)]$ is larger than unity. The selection of G_c would depend upon a particular system. One important consideration would be that the selection of G_c should be examined with respect to its practicability. Thus it is theoretically demonstrated that a liquid propellant rocket system may be stabilized completely independently of combustion time lag.[5]

[5] In his recent paper (5), Professor Frank E. Marble of California Institute of Technology provides in considerable detail an explanation of how one would determine the proper transfer function for the feedback controller, showing it is possible to stabilize the system for all combustion time lags.

References

1 "A Theory of Unstable Combustion in Liquid Propellant Rocket Systems," by M. Summerfield, JOURNAL OF THE AMERICAN ROCKET SOCIETY, vol. 21, September 1951, pp. 108–114.

2 "Aspects of Combustion in Liquid Propellant Rocket Motors, Part 1: Fundamentals. Low Frequency Instability With Monopropellants," by L. Crocco, JOURNAL OF THE AMERICAN ROCKET SOCIETY, vol. 21, November 1951, pp. 163–178.

3 Lecture Notes on Applications of Jet Propulsion Power Plants (unpublished), by H. S. Tsien, 1952.

4 "Principles of Servomechanisms," by Gordon S. Brown and Donald P. Campbell, New York, John Wiley & Sons, 1948, p. 170.

5 "Servo-Stabilization of Low-Frequency Oscillations in a Liquid Bipropellant Rocket Motor," by Frank E. Marble and Dale W. Cox, Jr., Daniel and Florence Guggenheim Jet Propulsion Center, California Institute of Technology, Pasadena, Calif. (see pp. 63–74 in this issue of the JOURNAL).

Servo-Stabilization of Low-Frequency Oscillations in a Liquid Bipropellant Rocket Motor

(*Continued from page 74*)

References

1 "Stability of Flow in a Rocket Motor," by D. F. Gunder and D. R. Friant, *Journal of Applied Mechanics* (Trans. ASME), vol. 17, 1950, pp. 327–333.

2 Discussion of Ref. 1, by M. Yachter, *Journal of Applied Mechanics* (Trans. ASME), vol. 18, 1951, pp. 114–116.

3 "A Theory of Unstable Combustion in Liquid Propellant Rocket Motors," by M. Summerfield, JOURNAL OF THE AMERICAN ROCKET SOCIETY, vol. 21, September 1951, pp. 108–114.

4 "Aspects of Combustion Stability in Liquid Propellant Rocket Motors, Parts I and II," JOURNAL OF THE AMERICAN ROCKET SOCIETY, vol. 21, November 1951, pp. 163–178; vol. 22, January-Febuary 1952, pp. 7–16.

5 "Servo-Stabilization of Combustion in Rocket Motors," by H. S. Tsien, JOURNAL OF THE AMERICAN ROCKET SOCIETY, vol. 22, September-October 1952, pp. 256–262.

6 Discussion by M. Satche of "Stability of Linear Oscillating Systems With Constant Time Lag," by H. I. Ansoff, *Journal of Applied Mechanics* (Trans. ASME), vol. 16, 1949, pp. 419–420.

7 "Transfer Functions of Rocket Nozzles," by H. S. Tsien, JOURNAL OF THE AMERICAN ROCKET SOCIETY, vol. 22, May-June 1952, pp. 139–143.

The Velocity of Sound in Some Rocket Propellant Liquids

GEORGE G. KRETSCHMAR[1]

U. S. Naval Ordnance Test Station, Inyokern, China Lake, Calif.

The velocity of sound in a number of rocket propellant liquids was obtained with ultrasonic frequencies. A quartz crystal driver was used in an ultrasonic interferometer. The interferometer was made with stainless steel parts, which permitted measurements to be made on concentrated nitric acid. Data were obtained for various samples of nitric acid, hydrazine, and the hydrocarbon mixtures, JP-3 and JP-4.

IT IS well known that early work on the velocity of sound goes back to the time of Newton who showed that the velocity is proportional to [elastic force/density]$^{1/2}$, and from this obtained a formula for the velocity of sound in air

$$c = [\text{pressure/density}]^{1/2}$$

This formula gives a value which is too low to check with experimental results. Laplace, about 1803, explained the discrepancy by pointing out that the rapidity of the pressure transformations does not permit temperature equalization to take place, so that Newton's formula should be modified by multiplying the velocity by $[\gamma]^{1/2}$ where γ is the ratio of the two specific heats (1).[2] Newton's formula should then be written

$$c = [\gamma \text{ pressure/density}]^{1/2}$$

The earliest tests of sound velocity in liquids were confined to long-distance tests in water (2). Also, considerable work was done in the early part of the present century using stationary waves in tubes, following the procedures of the well-known Kundt tube method as used for sound velocity measurement in gases (3).

There are considerable data on sound velocity in liquids available in the literature. There are, however, some notable gaps, particularly for some liquids used as rocket propellants. It was proposed that some of these missing data be obtained. The first attempts to obtain such data were made using audiofrequencies with simple equipment of the Kundt tube type. It was found advisable later, because of difficulties described below, to abandon the experiments using audiofrequencies, and to build entirely different apparatus, making use of ultrasonic frequencies.

The general formula for the propagation velocity of a plane wave in a fluid is (4)

$$c = [k/\rho]^{1/2}$$

For the case of a liquid medium, the elastic constant K is the volume elasticity or bulk modulus. By definition, $K = V \cdot dp/dV$, or it may be written in the reciprocal form, the compressibility, β, as $1/V \cdot dV/dp$. That is

$$c = [K/\rho]^{1/2} = [V/\rho \cdot dp/dV]^{1/2} = [1/\rho\beta]^{1/2}$$

If the isothermal compressibility is used, one must introduce the factor γ, the ratio of the two specific heats, just as in the corresponding case for the velocity of a longitudinal wave in a gas. Thus, the velocity of sound in a liquid is

$$v = [\gamma/\rho\beta_{is}]^{1/2} \text{ or } [1/\rho\beta_{ad}]^{1/2}$$

where β_{is} is the isothermal compressibility, and β_{ad} is the adiabatic compressibility. Most liquids are, however, so nearly incompressible that γ may be considered as unity. There are, however, some liquids having considerable compressibility, and some situations in which it may be advisable to take γ into account.

Experiments

The Kundt tube method, using audiofrequencies, appeared to be a natural and attractive method at the beginning of this work because the necessary equipment was readily available. There were tubes of various materials and lengths, a good audio oscillator, an amplifier, and a heavy-duty loudspeaker. The method chosen was to make use of a constant length tube with a variable applied frequency. The output of the oscillator was amplified and used to drive the speaker which was directly connected to a small piston fitted into one end of the tube. At the other end of the tube was fitted a piston containing a thin diaphragm, behind which was mounted a pair of barium titanate disks immersed in oil. The barium titanate disks, connected in push-pull, acting through a preamplifier and oscilloscope, made a sensitive pickup system.

First experiments with the Kundt tube equipment revealed a wealth of resonance points, most of which did not correspond to simple longitudinal modes of the liquid contained in the tube. It was very apparent that many spurious modes were excited. Probably many of these were due to transverse and longitudinal modes of the tube itself. An attempt to reduce these by using a thick-walled tube of stainless steel was unsuccessful. Also, surrounding the glass tube with a

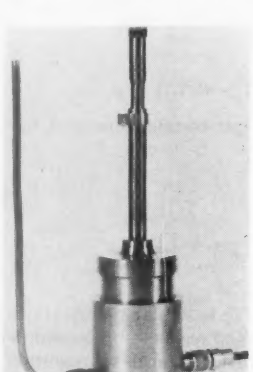

FIG. 1 ULTRASONIC INTERFEROMETER

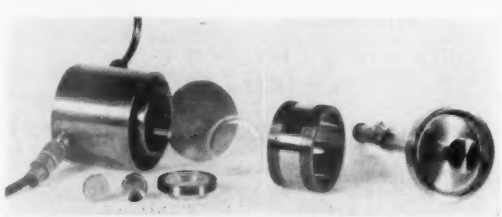

FIG. 2 ULTRASONIC INTERFEROMETER. DISASSEMBLED VIEW

Received September 19, 1952.

[1] Physicist, Research Department, Michelson Laboratory.

[2] Numbers in parentheses refer to References on page 84.

thick layer of wet sand did not sufficiently attenuate the unwanted modes.

Distilled water was used in order to have a liquid in which the sound velocity was accurately known. Working back from known values, it was possible to recognize the resonance points corresponding to the liquid column modes. But, without this help it was difficult if not impossible, to make a logical interpretation of the data.[3] Plotting of a complete

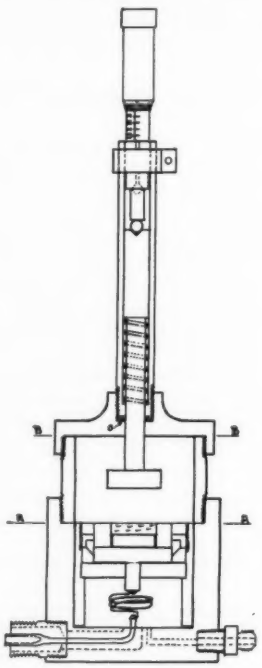

FIG. 3 INTERFEROMETER CROSS SECTION

set of data gave a completely ambiguous result, for one could select a number of sets of points, each of which would give a straight line relationship between the frequency and the number of half wave lengths, but each corresponded to a different value of the velocity of sound in the liquid.

It was at this point that the decision was made to drop the Kundt tube method and to build an ultrasonic interferometer, making use of a quartz crystal as the driving element (5, 6). Such an equipment makes use of standing waves just as in the Kundt tube. But, by making use of a rigid and accurately fitted moving plate and a good micrometer, a much higher degree of precision may be attained than with the Kundt tube, in spite of the much smaller size of the parts. There is, also, the additional advantage that a very small amount of liquid is required, and also the whole interferometer may be immersed in a constant temperature bath for accurate temperature control.

The instrument, as constructed, is shown in Fig. 1. On the left is the tube through which air pressure can be admitted below the pistonlike crystal holder. This enables one to compress the crystal slightly against the diaphragm. Fig. 2 is a disassembled view in which the quartz crystal appears as the solid disk on the left front. The transparent parts are insulators, machined from lucite. The piston can be seen projecting from the base cylinder. To the right are the stainless-steel cylinder and the cover which contains the movable plate and the micrometer head.

[3] Data have, however, been obtained by the method of resonances for a liquid contained in a large glass sphere. In a private communication, Mr. David Lieberman, of Aerojet Engineering Corporation, has informed the author that he obtained a value for the velocity of sound in nitric acid of 1.25×10^5 cm/sec by this method.

Fig. 3 is a detailed cross section of the interferometer. The stainless steel cylinder holds a 5-mil thick stainless-steel diaphragm against a shoulder in the base cylinder along the section AA. The crystal is just under and in contact with the diaphragm. The chamber is made tight with teflon gaskets at AA and BB; also a Vinylite O-ring around the stem of the movable plate prevents the escape of corrosive gases or fumes and effectively seals off the liquid compartment. The seals are made more secure and crystal contact is assured by spreading a thin layer of silicone grease on the gaskets and over the face of the crystal.

The crystal used was an X-cut quartz disk about 2 cm in diameter and about 6 mm thick. The resonant frequency was 512 kc. It was driven by a single 6L6 tuned amplifier stage which was in turn excited by the output of a General Radio Type 700-A wide range beat frequency oscillator.

Fig. 4 is a circuit diagram of the amplifier stage. The constants have been adjusted so that the tube operates with a plate current of approximately 50 milliamperes. In use there are slight variations of current in the plate circuit and this effect is made use of to determine the resonant positions. In order to follow these variations accurately, thus getting the positions of resonance with precision, a microammeter is introduced into the plate circuit, most of the current being neutralized by a bucking voltage across the microammeter. This part of the circuit is shown in more detail in Fig. 5. The microammeter is paralleled with an equivalent resistance of about 600 ohms so that the circuit may be first adjusted so that the microammeter will be on scale. The entire circuit was well shielded and the aluminum box grounded, but it was found necessary to leave the dry cell, used for producing the neutralizing voltage, outside of the box.

The frequency was determined and controlled with the aid of a Signal Corps Type BC 221 AH frequency meter. This was loosely coupled to the amplifier with a few turns wound around the crystal cable. Fig. 6 shows the interferometer in use with the required electronic gear. The voltage of the rectifier and the oscillator was stabilized with a Sorensen voltage regulator. The frequency meter can be seen at the

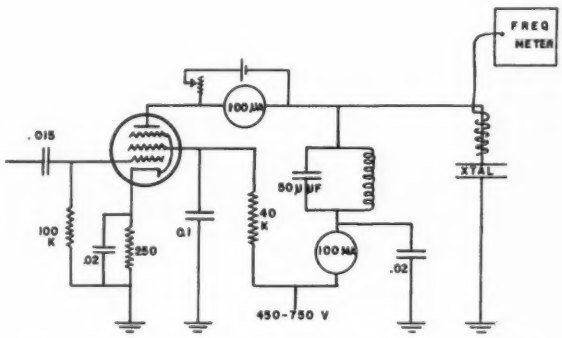

FIG. 4 CIRCUIT DIAGRAM OF 6L6 TUNED AMPLIFIER STAGE

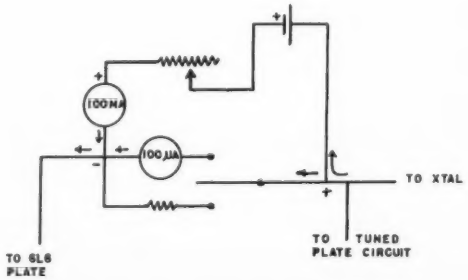

FIG. 5 NEUTRALIZING CIRCUIT AND MICROMETER INDICATOR

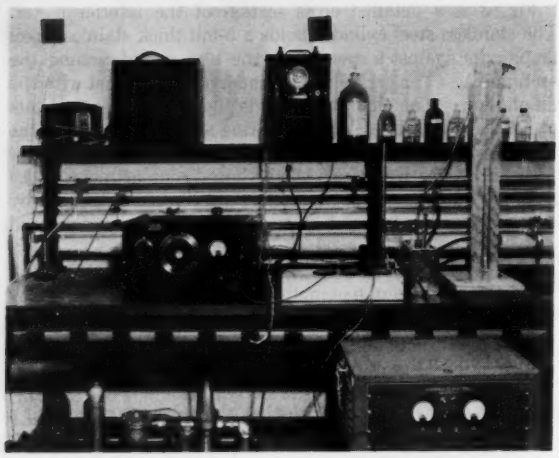

FIG. 6 INTERFEROMETER CONTAINED IN CONSTANT TEMPERATURE BATH; CONNECTED TO ACCESSORY ELECTRONIC EQUIPMENT

top of the photograph, and the coupling wire can also be seen. It will be observed, also, that the interferometer is immersed in a constant temperature bath. The pressure applied to the crystal is obtained from the air line and is controlled by a regulator and leak. A pressure of a few inches of mercury was needed for optimum crystal contact. The frequency meter was itself crystal-controlled with a standard 100-kc crystal, and the crystal was checked by beating with a 100-kc standard frequency signal available in the laboratory.

Results

Data were obtained on a number of rocket propellant liquids. A condensation of these data is given in Table 1. Specific gravity determinations were done on all the liquids studied, and these are included in the table. More data were taken on hydrazine than on other liquids studied because of the lack of sharpness of the resonances, with consequent greater uncertainty in wave-length measurements. The errors are estimated from the consistency of the data and the number of runs made on each liquid. All of the data were taken close to the resonant frequency of 512 kc per second.

TABLE 1 AVERAGE VALUES OF THE VELOCITY OF SOUND IN SOME ROCKET PROPELLANT LIQUIDS AT 512 KC
(Commercially available materials)

Liquid	Composition	Measured density at 25 C	Measured sound velocity at 25 C, m/sec
Hydrazine	(96 ± 1/2)% anhydrous	1.0096	2059 ± 6
RFNA[a]	HNO_3 77% min. NO_2 20% approx. H_2O 2 1/2 max.	1.585	1379.5 ± 1.4
RFNA[b]	HNO_3 90% min. NO_2 .... H_2O 10% max.	1.479	1340.4 ± 3
WFNA	HNO_3 97.08% NO_2 0.22% H_2O 1.91%	1.494	1239.2 ± 0.5
WFNA	HNO_3 97.52% NO_2 0.28% H_2O 2.11%	1.497	1239.7 ± 0.5
JP-3 Sample a	MIL-F-5624A[c]	0.7682	1233.8 ± 2
JP-3 Sample b	MIL-F-5624A	0.7590	1196.5 ± 1
JP-4 Sample a	MIL-F-5624A	0.7757	1242.2 ± 1
JP-4 Sample b	MIL-F5624A	0.7762	1242.3 ± 1

[a] Reagent grade, A.C.S. Specifications, Code 1122.
[b] Reagent grade, A.C.S. Specifications, Code 1121.
[c] Specifications may be obtained from Air Materiel Command, Wright-Patterson Air Force Base, Dayton, Ohio.

Also, the errors are estimated from the consistency of the data and the number of runs made on each liquid. All of the data were taken close to the resonant frequency of 512 kc per second.

As a check on the over-all accuracy of the interferometer, measurements were made on distilled water at 25 C. The average of three measurements made is 1498.22 m/sec. This may be compared with the recently published value of Barthel and Nalle, which is 1496.2 ± 0.2 m/sec, and that of Willard, which is 1498 ± 1 m/sec at 25 C (7, 8).

Acknowledgment

I am indebted to Dr. Saul Pollock for the suggestion that we obtain sound-velocity data on rocket propellant liquids for use in connection with studies of rocket instability. Dr. Pollock did, in fact, initiate the experiments making use of the Kundt tube apparatus. I am grateful to Dr. A. B. C. Anderson for calling my attention to the superior advantages of using ultrasonic frequencies, and for supplying the quartz crystals used in the interferometer. Ensign C. D. Hendricks, Jr., USNR, gave considerable help and advice in the adjustment of the electronic circuits. Also, my thanks are due to Lowell Criddle of the Physics Model Shop for his careful work in machining stainless-steel parts for the interferometer. The Aerojet Engineering Corporation, Azusa, Calif., furnished a number of the liquid samples used in the measurements.

References

1 "Acoustics," by Alexander Wood, Interscience Publishers, New York, 1941, pp. 243–244.
2 Idem., p. 265.
3 Idem., p. 268.
4 "Acoustics," by G. W. Steward and R. B. Lindsay, D. Van Nostrand Co., New York, 1930, p. 27.
5 "Ultra Sonics and their Scientific and Technical Applications," by Ludwig Bergman (translated by H. S. Hatfield), John Wiley & Sons, New York, 1938, pp. 109–110.
6 "The Physical Properties of Liquids, The Sonic Interferometer," by E. Freyer and J. C. Hubbard, *Journal of the American Chemical Society*, vol. 51, 1929, p. 759.
7 "A Precise Recording Ultrasonic Interferometer and its Applications to Dispersion Tests in Liquids," by R. Barthel and A. W. Noble, *Journal of the Acoustical Society of America*, vol. 24, 1952, p. 8.
8 "Temperature Coefficients of Ultrasonic Velocity in Solutions," by G. W. Willard, *Journal of the Acoustical Society of America*, vol. 19, 1947, p. 235.

ARS 1953 Junior Award Competition

Papers are now being invited for consideration for the 1953 Junior Award, to be presented at the ARS 8th Annual Convention to be held in December 1953.

The winning paper will be judged mainly on the basis of content which should reflect original thought and effort. The age of authors of papers should not exceed 25 years.

Please refer to page 57, this issue of the JOURNAL, for acceptable scope of subject matter. Manuscripts are to be prepared in accordance with style instructions on inside back cover.

Papers must be received no later than October 1, 1953, and should be clearly marked, "Submitted for Junior Award Competition."

Send papers to: The Secretary, American Rocket Society, 29 West 39th Street, New York 18, N. Y.

On Maximum Evaporation Rates of Liquid Droplets in Rocket Motors[1]

S. S. PENNER[2]

Daniel and Florence Guggenheim Jet Propulsion Center, California Institute of Technology, Pasadena, Calif.

Upper limits have been estimated for the rate of evaporation of small liquid droplets in representative rocket combustion chambers. The droplets are assumed to be isothermal at all times. The droplet temperature as a function of time is determined by an appropriate heat balance. The calculations are useful in determining the significance of inelastic collisions between liquid droplets for complete combustion. Radiant heat transfer to moving liquid droplets is considered briefly.

I Introduction

EXPERIMENTAL studies of liquid fuel rockets have shown that the performance of many bipropellant systems is dependent on the type of injection system employed. The results indicate the importance of (*a*) the size of the liquid droplets at the point of injection, and (*b*) the relative directions of injection of the separate streams of fuel and oxidant.

These experimental findings suggest a combustion mechanism in liquid fuel rockets which may be represented schematically as follows:

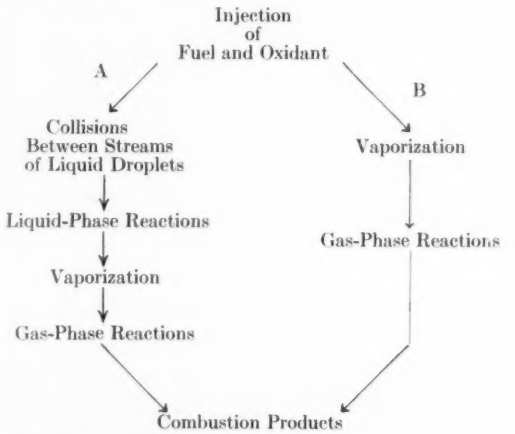

Mechanisms A and B generally occur concurrently in a motor chamber. For any given set of conditions, either mechanism A or mechanism B may be of greater importance.

An indication regarding the relative importance of mechanisms A and B may be obtained by determining whether liquid droplets are in a given motor chamber for a sufficiently long period of time to vaporize completely without the occurrence of exothermic liquid-phase reactions. If the time required for the complete vaporization of the liquid droplets is greater than the time spent by the liquid droplets in the motor chamber, then liquid-phase reactions must occur, provided complete combustion takes place in the rocket chamber. It is therefore of interest to determine the minimum time required for the evaporation of liquid droplets in a rocket chamber.[3]

The evaporation of liquids and solids has been studied both experimentally and theoretically (1–11).[4] Extended theoretical investigations of vaporization under idealized conditions have been carried out by Fuchs (5). A general treatment for the calculation of droplet lifetimes in combustion chambers has been described by Wentzel (6). Application of the results of these studies on evaporation to the special conditions existing in a rocket chamber cannot readily be made. The treatment of Wentzel (6), although applicable in principle, requires knowledge of a number of empirically determined parameters which are not generally available. Furthermore, there are indications that the usual laws which govern the evaporation of liquid droplets may not be valid for droplets of exceedingly small size. For example, Probert (1) indicates that the rate of evaporation of very small droplets is proportional to the diameter of the evaporating droplet rather than to the square of the diameter. Studies on comparatively large drops (0.5 mm in radius) (4) led to the conclusion that the treatment of Fuchs (5) for the rate of evaporation of drops is essentially correct. The work of Fuchs, in so far as it applies to very low Reynolds numbers, has been criticized recently (11). Finally, a study of evaporation rates for falling and burning droplets by Topps (12) shows a complicated dependence for evaporation rate on size and Reynolds number.

In view of the obvious complexity of the problem, no attempt was made to carry through a complete treatment of the rate of evaporation of liquid droplets in a rocket chamber. Instead, an approximate treatment has been employed which is designed to estimate a reasonable upper limit for the rate of droplet vaporization in a rocket chamber. A discussion of the maximum and minimum rates of evaporation, under conditions somewhat different from those of interest for the present study, has been given previously (13).

The results of the present investigation emphasize the importance of droplet size. For example, at least 1.58×10^{-3} sec is required before the radius of an aniline droplet decreases from 5×10^{-3} cm to 2.5×10^{-3} cm. However, more than 1×10^{-2} sec is required before an aniline droplet initially

Received July 14, 1952.

[1] This paper presents the results of one phase of research carried out at the Jet Propulsion Laboratory, California Institute of Technology, under U. S. Army Ordnance Department Contract No. W-04-200-ORD-1482. The original manuscript was distributed as Progress Report No. 9-13 by the Jet Propulsion Laboratory in September 1947.

[2] Assistant Professor of Jet Propulsion. Formerly with Jet Propulsion Laboratory, California Institute of Technology, Pasadena Calif.

[3] It should be noted particularly that the present investigation was undertaken with the modest objective of approximating minimum lifetimes of droplets rather than with the idea of obtaining a realistic estimate of the complicated evaporation processes involved in heterogeneous combustion. For recently published reports on heterogeneous combustion see, for example, J. E. C. Topps, *J. Inst. Petrol.*, vol. 37, 535 (1951); G. A. E. Godsave, National Gas Turbine Establishment Reports Nos. R. 66, March 1950, and R. 87, April 1951, Pyestock, Hants, England; D. B. Spalding, *Fuel*, vol. 29, 2, 25, 1950; vol. 30, 121, 1951.

[4] Numbers in parentheses refer to References on page 88.

1×10^{-2} cm in diameter decreases to one half of its original diameter. The rate of evaporation is, of course, dependent on the nature of the evaporating compound. Thus octane is found to evaporate more rapidly than aniline under similar experimental conditions. The transfer of radiant energy to a moving liquid droplet is discussed. The analysis shows that the maximum possible temperature rise associated with the absorption of radiant energy increases as the droplet diameter is decreased.

II Outline of Theory

The rate of droplet vaporization depends upon the nature of the evaporating liquid and upon the heat transferred to the liquid droplets after injection into the combustion chamber. The minimum life of a liquid droplet in a rocket chamber may be calculated by using an upper limit for the heat transfer and also for the isothermal rate of decrease of droplet radius with time.

The order of magnitude of the upper limit for the isothermal rate of decrease of droplet radius with time can be calculated from the Knudsen equation, which may be written in the form (14–16)

$$-dr/dt = (p_s/\rho_l)(M/2\pi RT)^{(1/2)} \quad [1]$$

where r is radius of the evaporating droplet, t time, p_s saturated vapor pressure of the evaporating liquid at a given temperature, ρ_l density of the evaporating liquid, M molecular weight of the evaporating compound, T temperature, R gas constant. An upper limit for the heat transfer to the liquid droplets is obtained by maximizing the product $h\Delta T$ in the relation

$$Q = 4\pi r^2 h \Delta T \quad [2]$$

where Q is rate of heat transfer to a spherical droplet of radius r, h is over-all coefficient of heat transfer to a liquid droplet evaluated at the mean film temperature, ΔT is mean temperature difference between the gases surrounding the liquid droplet and the liquid droplet itself.

The order of magnitude of the value of h may be ascertained from an empirical relation determined as the result of heat transfer studies between air and spheres (17, p. 237),[5] viz.,

$$(2hr/k_f) = 0.33(2rG/\mu_f)^{0.6} \quad [3]$$

where k_f is thermal conductivity of the hot gases at temperature T_f, G = mass rate of flow of air past the liquid droplets, μ_f = viscosity of hot gases at the temperature T_f, $T_f = T + 0.5\,(T_c - T)$ where T is the droplet temperature (assumed to be uniform), T_c = temperature of the hot gases. At a chamber temperature of 3000° K and a pressure of 300 psi, it is found that Equation [3] leads to values of $2hr/k_f$ of about 4 for the largest droplets ($r = 10^{-2}$ cm in radius), even if the droplets move at 100 fps relative to the gases in the chamber. For very small droplets, on the other hand, $0.33\,(2rG/\mu_f)^{0.6} < 2$. However, the theoretical lower limit for $2hr/k_f$ is 2 in a stagnant medium unless the spheres have diameters of the same order of magnitude as the mean free path in the fluid. Therefore, it is evident that $2hr/k_f$ for small droplets does not differ greatly from 2, and considering the fact that the gases at the head end of the rocket chamber move, on the average, in the direction of the droplets,[6] it appears likely that even for $r = 10^{-2}$ cm, the approximation $h = k_f/r$ will yield a reasonable estimate for heat transfer to the droplet.[7] Thus we set

[5] It should be noted that the conclusion reached by using Equation [3] is the same as that obtained from the elegant treatment on heat transfer to spheres for very low Reynolds numbers given by Kronig and Bruijsten (11).

[6] Representative estimates of gas velocities near the injector are of the order of 50 fps.

[7] This last conclusion does not make allowance for the possible occurrence of turbulent motion near the injector.

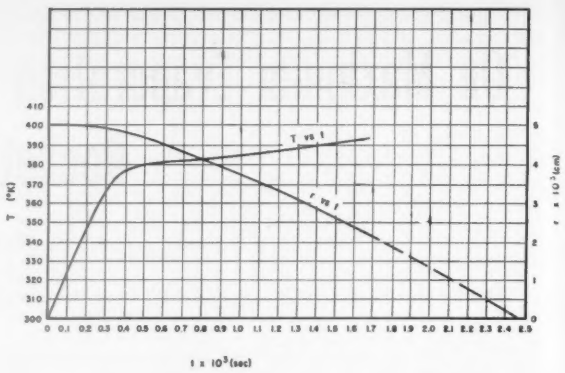

FIG. 1 TEMPERATURE-VS.-TIME AND RADIUS-VS.-TIME DATA FOR AN ANILINE DROPLET IN A NITRIC-ACID-ANILINE ROCKET MOTOR ($T_c = 3000°$ K, $T_0 = 300°$ K, $r_0 = 5 \times 10^{-3}$ CM).

$$\Delta T = 3000 - T \text{ with } h = k_f/r \quad [3a]$$

The rate of temperature rise with time, $(dT/dt)_1$, of a spherical droplet receiving the energy Q is

$$(dT/dt)_1 = Q(4\pi r^3/3)^{-1}(\rho_l C_l)^{-1} = 3h\Delta T/r\rho_l C_l \quad [4]$$

where C_l is the heat capacity per unit weight of the evaporating liquid. The liquid droplet is cooled as the result of evaporation. The rate of decrease of temperature with time associated with the cooling effect of evaporation is given according to the relation

$$-(dT/dt)_2 = (3\Delta H_{vap}/C_l M r)(-dr/dt) \quad [5]$$

where ΔH_{vap} is the heat of vaporization of the liquid per mole, and $(-dr/dt)$ is given by Equation [1]. The net rate of change of temperature with time is therefore

$$dT/dt = (3k_f \Delta T/r^2 \rho_l C_l) - (3\Delta H_{vap}/rMC_l)(-dr/dt) \quad [6]$$

where use has been made of Equation [3a].

Reference to Equation [6] indicates that the temperature of an evaporating liquid droplet changes continuously with time. Since the first term on the right-hand side of Equation [6] varies nearly inversely with the square of the radius, whereas the second term varies inversely as the first power of the radius, it is apparent that the droplet temperature will rise rapidly for very small droplets. For moderately large droplet sizes, Equation [6] is found to lead to quasi-steady-state temperatures.

III Calculation of Minimum Lifetimes of Droplets

Equations [1] and [6] can be solved numerically without difficulty. A representative calculation is outlined below for the evaporation of aniline in a nitric-acid-aniline rocket operating at a chamber temperature of 3000° K.

The aniline droplets are chosen to have an initial diameter of 5×10^{-3} cm. They are injected at an initial temperature of 300° K with an average velocity of 100 fps into a rocket chamber 1 ft in length. The droplet velocity is assumed to remain constant. Thus the droplets remain in the rocket chamber for 0.01 sec. It is therefore of interest to determine the temperature and radius of the aniline droplets as a function of time for 0.01 sec.

The gaseous combustion products in the nitric-acid aniline rocket consist predominantly of NO, CO, CO_2, H_2O, and N_2. Approximate calculations for these components lead to a value for μ_f of about 0.157 lb/hr-ft (p. 411 of Ref. 17) at the temperature $T_f = 300 + 0.5\,(3000 - 300) = 1650°$ K. For the specified composition, it is found (p. 415 of Ref. 17) that $C_p\mu_f/k_f \simeq 0.76$. Since $C_p \simeq 0.50$ Btu/lb-°F (p. 406 of Ref.

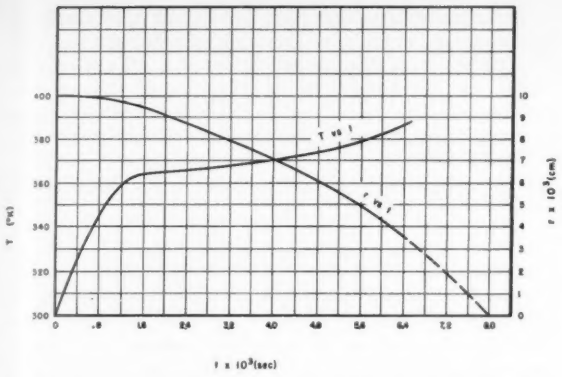

FIG. 2 TEMPERATURE-VS.-TIME AND RADIUS-VS.-TIME DATA FOR AN ANILINE DROPLET IN A NITRIC ACID-ANILINE ROCKET MOTOR ($T_c = 3000°$ K, $T_0 = 300°$ K, $r_0 = 1 \times 10^{-2}$ CM).

17), it follows that $k_f \simeq 0.104$ Btu/hr-ft-°F $= 4.30 \times 10^{-4}$ cal/sec-cm-°K.

For approximate calculations the numerical values of k_f, ρ_l, C_l, and ΔH_{vap} are assumed to be independent of temperature. Since the droplet temperature does not vary greatly with time, the error introduced by this simplification is not large. Thus, $T_c = 3000°$ K, $\rho_l \simeq 1.02$ gm/cm³, $C_l \simeq 0.53$ cal/gm-°C, $M = 93.12$ gm/mole, $\Delta H_{vap} \simeq 12{,}000$ cal/mole (18).

Introduction of the numerical values into Equation [6] leads to the desired result

$$dT/dt = 2.38 \times 10^{-3}[(3000 - T)/r^2] - (730/r)(-dr/dt) \quad [6a]$$

The values of $-dr/dt$ may be calculated directly from Equation [1] by use of measured values for the vapor pressure of aniline. For numerical work it is convenient to express $-dr/dt$, as a first approximation, by the relation $\log(-dr/dt) \simeq A - B/T$, where A and B are nearly independent of temperature. For aniline it is found that

$$\log(-dr/dt) \simeq 7.09 - 2.60 \times 10^3 T^{-1} \quad [7]$$

Temperature-time and radius-time curves can be constructed from Equations [6a] and [7] by using a straightforward iteration procedure. Representative results for aniline, hydrazine, and octane are shown in Figs. 1 through 5. The same numerical value for k_f was employed for all of the calculations.

IV Results

The results plotted in Figs. 1 to 5, inclusive, exhibit the expected behavior. The temperature of the liquid droplets increases rapidly at first, then reaches a quasi-steady state, and finally rises very rapidly after the droplet radius has become sufficiently small. The droplet radius decreases continuously with time, very slowly at first, and then at an ever-increasing rate as the droplet temperature rises. From Figs. 1 to 5 it is possible to ascertain the minimum lifetimes of droplets for a number of different droplet sizes and liquids. The calculated results may be compared by evaluating the half life, $t_{(1/2)}$, of the liquid droplets, i.e., the time required to decrease the droplet diameters to one half of their original value.[8] Relevant data are summarized in Table 1.

Reference to the results summarized in Table 1 shows that an aniline droplet with an initial radius of 1×10^{-2} cm cannot evaporate in 0.01 sec unless heat transfer to the liquid droplet is considerably greater than that calculated from

[8] The numerical value of $t_{(1/2)}$ is always greater than one half the time required for complete evaporation of a given droplet. Calculation of the time required for complete evaporation is somewhat laborious.

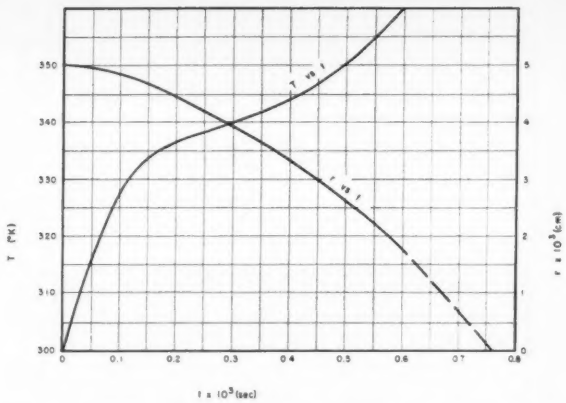

FIG. 3 TEMPERATURE-VS.-TIME AND RADIUS-VS.-TIME DATA FOR AN OCTANE DROPLET SURROUNDED BY HOT GASES AT 3000° K ($T_0 = 300°$ K, $r_0 = 5 \times 10^{-3}$CM).

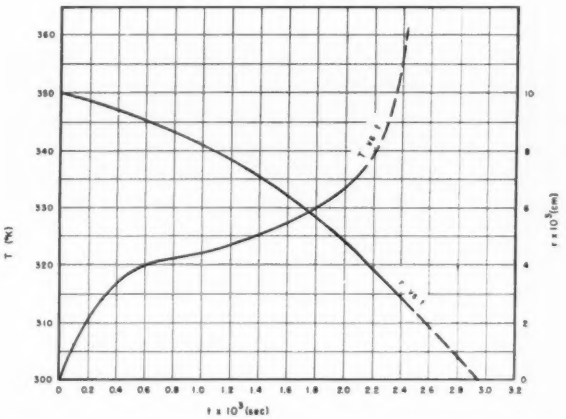

FIG. 4 TEMPERATURE-VS.-TIME AND RADIUS-VS.-TIME DATA FOR AN OCTANE DROPLET SURROUNDED BY HOT GASES AT 3000° K ($T_0 = 300°$ K, $r_0 = 1 \times 10^{-2}$ CM).

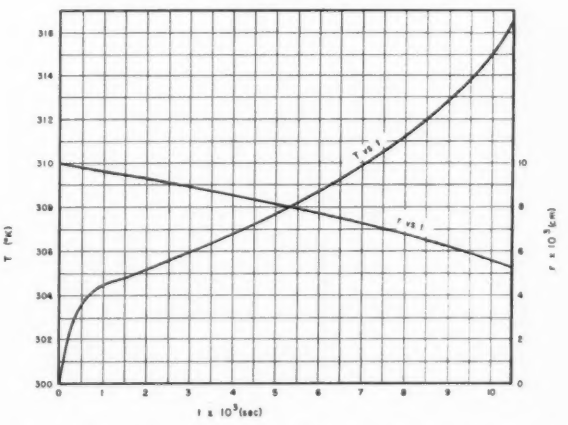

FIG. 5 TEMPERATURE-VS.-TIME AND RADIUS-VS.-TIME DATA FOR A HYDRAZINE DROPLET SURROUNDED BY HOT GASES AT 3000° K ($T_0 = 300°$ K, $r_0 = 1 \times 10^{-2}$ CM).

Equations [2] and [3]. Since only lower limits for the droplet lifetimes have been calculated, it is not possible to draw definite conclusions for the smaller droplet sizes for aniline. The evaporation of octane is seen to proceed more rapidly and at lower droplet temperatures than the evaporation of aniline. Hydrazine appears to evaporate somewhat more

TABLE 1 MINIMUM HALF-LIFE OF LIQUID DROPLETS
($T_c = 3000°$ K, $T_0 = 300°$ K, $h = k_f/r$, $k_f = 4.3 \times 10^{-4}$ cal/sec-cm-°K)

Compound	$r_0 \times 10^3$ (cm)	$t^a_{(1/2)} \times 10^3$ (sec)	$T^b_{(1/2)}$ (°K)
Aniline	5	0.158	392
	10	0.560	370
Octane	5	0.052	352
	10	0.188	333
Hydrazine	10	1.07	317

[a] $t_{(1/2)}$ = time required for the droplet diameter to decrease to one half of its original value.
[b] $T_{(1/2)}$ = droplet temperature at $t_{(1/2)}$.

slowly than aniline. Because of the uncertainties which exist with regard to droplet size distribution in rocket motors,[9] it is not possible at this time to draw definite conclusions with regard to the importance of liquid phase reactions in given rocket motors. However, it is evidently desirable to extend the calculations presented in this discussion to larger droplets by using the known size and velocity distributions in combustion chambers in conjunction with realistic heat transfer equations.

V Radiation Heating of Liquid Droplets

Equations for the heat transfer by radiation to a liquid droplet moving along the axis of a rocket motor chamber have been derived previously (19). It was shown that the radiant energy, I_T, received per square centimeter of surface during the residence time t_r in the rocket chamber, is given by the approximate relation

$$I_T = [2/a(a+L)]\int_\lambda I^0_\lambda d\lambda \int_0^{t_r} dt \left\{\int_0^a [1 - \exp\{-k_\lambda \rho[a^2 + (L - vt)^2]^{(1/2)}\}]\alpha d\alpha + \int_0^{L-vt} \{1 - \exp[-k_\lambda \rho(a^2 + x^2)^{(1/2)}]\}a\,dx\right\} \ldots\ldots [8]$$

where a is radius of cylindrical motor chamber (cm); L length of chamber (cm); I^0_λ radiant energy (cal/cm²-sec) emitted by a blackbody radiator in the wave-length region between λ and $\lambda + d\lambda$, the blackbody being at the same temperature as the radiating gases surrounding the moving liquid droplet; t is time (sec); t_r residence time of the liquid droplet in the motor chamber (sec); ρ density of the hot radiating gases (gm/cm³); k_λ spectral mass absorptivity of the gases (cm²/gm); v linear flow velocity of the moving liquid droplets (cm/sec).

Approximate calculations of heat transfer by radiation to moving liquid droplets have been carried out for the case where $a = 7$ cm, $L = 30$ cm, $T_c = 3000°$ K, $\int I^0_\lambda d\lambda = 115$ cal/cm²-sec, $t_r = 0.01$ sec, $k_\lambda = 40$ cm²/gm, $\rho = 2 \times 10^{-3}$ gm/cm³, $v = 3 \times 10^3$ cm/sec. Evaluation of I_T from Equation [8] for the specified numerical values leads to the result $I_T = 0.733$ cal/cm². The maximum possible radiant energy, I'_T, incident on a liquid droplet surrounded by blackbody radiators for 0.01 sec, is $I'_T = 1.15$ cal/cm² if the blackbody radiators are at 3000° K. This is only about 1.6 times the value calculated from Equation [8]. However, the calculated value of I_T may not be significant, since the assumed value of $k_\lambda = 40$ cm²/gm may be too high for a liquid fuel rocket operating at a pressure of 300 psi (19).

The temperature rise ΔT of a spherical liquid droplet of radius r, caused by incident radiation $I_{T\lambda}$ cal/cm² in the wavelength region between λ and $\lambda + d\lambda$ is given by the relation (19)

$$\Delta T_R = (3/rC_l\rho_l)\int_\lambda I_{T\lambda}[1 - \exp(-2K_\lambda r)]d\lambda \ldots\ldots [9]$$

[9] Dr. J. M. Schmidt, of JPL, CalTech, estimates the radius of aniline droplets at the point of injection into a nitric-acid-aniline rocket as probably lying between 5×10^{-3} and 5×10^{-2} cm. Our analysis does not apply to the largest droplets.

where K_λ is the absorption coefficient (in cm⁻¹) of the liquid droplet for light in the wave-length region between λ and $\lambda + d\lambda$. Evaluation of ΔT_R by use of Equation [9] can be performed only if K_λ is known as a function of wave length. Experimental determination of K_λ could be carried out in the same manner as was done previously for double-base rocket propellants (20).

If an average value $\overline{K}$ may be used for K_λ, then ΔT_R is given by the relation

$$\Delta T_R = 3I_T[1 - \exp(-2\overline{K}r)](rC_l\rho_l)^{-1} \ldots\ldots [10]$$

For very small droplets and weak absorbers $[1 - \exp(-2\overline{K}r)] \simeq 2\overline{K}r$. Therefore

$$\Delta T_R \simeq 6I_T\overline{K}/C_l\rho_l \ldots\ldots [11]$$

The radiation temperature rise of small droplets, which are not blackbody absorbers, is therefore approximately proportional to $\overline{K}$. An upper limit may be estimated for ΔT_R by treating the absorbing liquid droplet as a blackbody. In this case

$$\Delta T_{R_{max}} = 3I_T/rC_l\rho_l \simeq 2.2r^{-1}, °\text{K} \ldots\ldots [11a]$$

if $C_l\rho_l \simeq 1$ cal/cm³-°K, and $I_T = 0.733$ cal/cm².

It can be seen from Equation [11a] that the maximum possible temperature rise of liquid droplets caused by the absorption of radiant energy increases as the droplet size decreases. If Equation [11a] holds, then $\Delta T_{R_{max}} \simeq 300°$ K for $r = 5 \times 10^{-2}$ cm, and $\Delta T_{R_{max}} = 300°$ K for $r = 5 \times 10^{-3}$ cm. In order to evaluate the relative importance of radiant heat transfer, we may compare the coefficient $\Delta T_R/t_r$ with $(dT/dt)_1$ as given by Equation [4]. For very small droplets it appears that the *equilibrium* transfer of radiant energy in a rocket motor is probably not very significant. However, the quantitative effects of chemiluminescent radiation may well be important and merit extensive further study.

References

1 "The Influence of Spray Particle Size and Distribution in the Combustion of Oil Droplets," by R. P. Probert, *Philosophical Magazine*, vol. 37, 1946, pp. 94–105.

2 "Experiments on the Rate of Evaporation of Small Spheres as a Method of Determining Diffusion Coefficients—The Diffusion Coefficient of Iodine," by B. Topley and R. W. Whytlaw-Gray, *Philosophical Magazine*, vol. 4, 1927, pp. 873–888.

3 "A Study of the Evaporation of Small Water Droplets," by H. G. Houghton, *Physics*, vol. 4, 1933, pp. 419–424.

4 "The Rate of Evaporation of Droplets. Evaporation and Diffusion Coefficients and Vapor Pressures of Dibutyl Phthalate and Butyl Stearate," by R. S. Bradley, M. G. Evans, and R. W. Whytlaw-Gray, *Proceedings of the Royal Society of London*, vol. 186A, 1946, pp. 368–390.

5 "Rate of Evaporation of Small Droplets into a Gaseous Atmosphere," by N. Fuchs, *Physikalische Zeitschrift der Sowjetunion*, vol. 6, 1934, pp. 224–243.

6 "Ignition in a Diesel Motor," by W. Wentzel, *Forschung auf dem Gebiete des Ingenieurwesens*, vol. 6, 1935, pp. 105–115.

7 "Rates of Evaporation. IV. The Rate of Evaporation and Vapour Pressure of Rhombic Sulfur," by R. S. Bradley, *Proceedings of the Royal Society of London*, vol. 205A, 1951, pp. 553–563.

8 "The Rate of Evaporation of Droplets. V. Evaporation Characteristics of Some Branched-Chain Hydrocarbons and a Straight-Chain Fluorocarbon," by R. S. Bradley and G. C. S. Waghorn, *Proceedings of the Royal Society of London*, vol. 206A, 1951, pp. 65–72.

9 "Vaporization of Small Sulfur Droplets," by H. F. Johnstone and D. K. Eads, *Industrial and Engineering Chemistry*, vol. 42, 1950, pp. 2293–2298.

(*Continued on page 98*)

Combustion Studies in Rocket Motors

KURT BERMAN[1] and SAMUEL H. CHENEY, JR.[1]

General Electric Company, Malta Test Station, Ballston Spa, N. Y.

Investigation of combustion instability was continued with 3-in. diam, 1200-lb thrust rocket motors. The study was carried out both with normal developmental motors and the slit-window motor. Pictures of shock propagation axially along the motor are presented. The reactants used were ethyl alcohol and liquid oxygen.

Introduction

IN A PREVIOUS paper (1),[2, 3] experiments with a rocket motor having a full-length observation window were described. Special emphasis was devoted to the presentation of photographs showing combustion under unstable operation. It is the purpose of this paper to describe some recent experiments both with the window-motor assembly and normal developmental water-cooled motors which present further data on the phenomenon of instability. The reactants used in all experiments were ethyl alcohol and liquid oxygen.

Water-Cooled Body Experiments

As was pointed out in (1), two general types of instability have been observed with 3-in. diam motors: (a) A high-frequency type of instability of about 1400–1700 cps, and (b) a low-frequency type of about 200–300 cps. As mentioned in (1), 3-in. modified impinging head assemblies tend toward high-frequency instability as the chamber pressure is lowered. In order to study the effect of chamber length on the frequency of oscillation incurred in this type of instability, a modified impinging injector head was assembled with a 41-deg convergent half angle, 1.75-in. throat diam, and 15-deg divergent half-angle nozzle and various lengths of 3-in. diam cylindrical water-cooled chambers. The normal instrumentation was supplemented by a GM-type Dynagage pressure pickup[4] mounted in a boss inserted in the $^5/_{16}$-in. diam igniter hole of the head. The diaphragm of the gage was located approximately $2^1/_2$ in. from the head face. With the various assemblies, the chamber pressure was lowered sufficiently (to approximately 270 psig) to induce the unstable operating condition.

Two general modifications of high-frequency chamber pressure oscillations were encountered: (*a*) The type shown in Fig. 1a which has been arbitrarily designated as "sinusoidal-type," and (*b*) the oscillations illustrated in Fig. 1b which have been designated as "shock-type." The latter type was invariably accompanied by large chamber heat-transfer rates (1.5 to 2.5 times normal). Since a run is usually terminated as soon as a predetermined heat-transfer rate is reached, this caused the shutdown of most tests in which instability was characterized by shock-type oscillations. In one test the motor was permitted to run under unstable conditions for 29 sec. Although there was considerable mechanical shock on the motor assembly, as evidenced by the fact that several gage connections were broken, and the body heat-transfer rate was quite high (>2 Btu/in.^{2} sec), the motor was unharmed. The nozzle heat transfer rate during this run was about 25 per cent higher than normal. It appears therefore that the high heat-transfer rates obtained with shock-type oscillations are not caused by local hot spots.

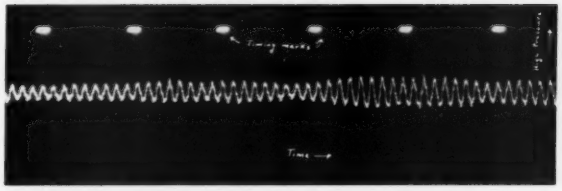

FIG. 1a DYNAGAGE CHAMBER PRESSURE RECORD OF "SINUSOIDAL" OSCILLATIONS

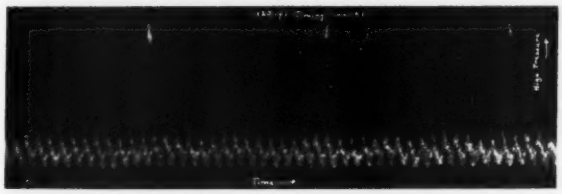

FIG. 1b DYNAGAGE CHAMBER PRESSURE RECORD OF "SHOCK-TYPE" OSCILLATIONS

Since the Dynagages are calibrated statically for pressure and are temperature-sensitive, all pressure amplitude measurements must be accepted with some degree of caution. The peak-to-peak amplitude of the shock-type oscillations ranged from 200 to 500 psi.

Sinusoidal-type oscillations were generally much smaller in amplitude, usually not much larger than 100 psi peak-to-peak. No abnormal heat-transfer rate seemed to be associated with sinusoidal-type oscillations. Shock-type instability was always preceded by periods of sinusoidal oscillations. A Dynagage record of the transition period is shown in Fig. 2.

The frequency of the oscillations varied with chamber length. The predominant components of the frequency spectrum were the fundamental and a second harmonic. Sinusoidal oscillations were considerably lower in frequency than the shock type. For example, with the $21^3/_4$-in. assembly, the frequency of the sinusoidal oscillations was 830 to 860 cps, while for the shock-type, the frequencies ranged from 930

FIG. 2 DYNAGAGE CHAMBER PRESSURE RECORD OF TRANSITION FROM SINUSOIDAL TO SHOCK-TYPE OSCILLATIONS

Presented at the 7th Annual Convention of the AMERICAN ROCKET SOCIETY, New York, N. Y., December 3, 1952.

[1] Research Engineer. Member ARS.

[2] Numbers in parentheses refer to the References on page 95.

[3] Since the present paper was written, a paper was presented at the Fourth Symposium on Combustion (September 1952) essentially confirming the results of (1). See (2).

[4] Manufactured by Photocon Research Products, Pasadena, Calif.

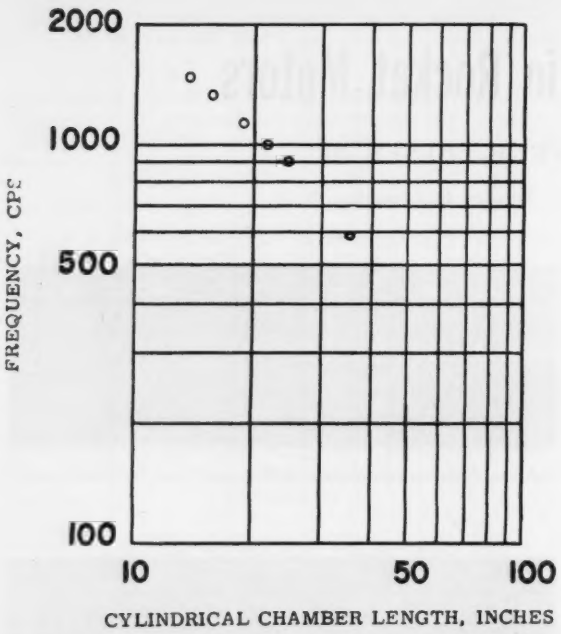

FIG. 3 FUNDAMENTAL FREQUENCY OF SHOCK-TYPE CHAMBER PRESSURE OSCILLATIONS VERSUS CYLINDRICAL CHAMBER LENGTH

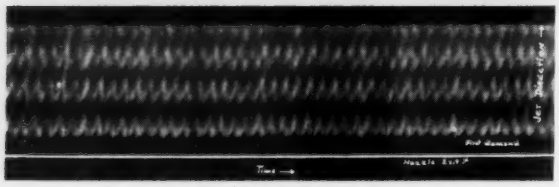

FIG. 4 SLIT PHOTOGRAPH OF JET AT UNSTABLE OPERATION

to about 1000 cps. In Fig. 3 the full-stage "shock-type" fundamental frequency is plotted as a function of the cylindrical chamber length.

A General Radio Type 651 continuous strip camera was used in some experiments to photograph the rocket motor jet. The camera viewed the jet through a slit and the film motion was perpendicular to the jet axis. Photographs of the diamonds during stable and unstable operation are illustrated in Figs. 4 and 5. The frequency of the diamond oscillation corresponded to that of the fundamental chamber oscillation frequency recorded by the Dynagage.

As the operating chamber pressure for a fixed motor assembly is lowered, the propellant flow rate and hence the head pressure drop decreases. To determine whether the onset of instability is primarily a function of chamber pressure or head pressure drop, experiments were performed keeping the mass flow through the motor constant and changing the chamber pressure by using nozzles of various throat diameters. Of course the gas velocity in the chamber changes also as the throat to chamber area is varied. This factor is believed to be of minor importance as a stability parameter in the present tests.

Motor assemblies consisted of a modified impinging head, a $15^1/_2$-in. long, $4^1/_2$-in. diam water-cooled body, and nozzles of 2.5, 3.0, 3.5, and 3.75-in. throat diam. The $4^1/_2$-in. diam assembly was used, since insufficient 3-in. diam assemblies were available to extend the experiments over a wide range of chamber pressure. In Fig. 6 the chamber pressure is plotted versus the total flow rate of propellants. Runs in which intermittent instability was experienced are indicated. Although the severity of the instability decreased with increasing throat diameter, it is interesting to note that the instability region begins when the total flow rate is below a definite value (about 9 lb/sec in this specific instance). This seems to indicate that head pressure drop is a more important factor in determining stable operation with the modified impinging head than is the chamber pressure.

Window Motor Tests

Modified Impinging Head, 41-Deg Convergent Nozzle, 17-In. Chamber Tests

Photographs of unstable combustion obtained with the 10-in. long window-motor chamber were presented in (1). In order to continue the investigation at various chamber lengths, the window motor was attached to standard 3-in. diam water-cooled bodies. To date, tests have been conducted with two lengths of composite chamber: one about 17 in., the other approximately 21 in. long. Two different injector heads were employed—a modified impinging and a conventional impinging head of the types described in (1). The effect of the convergence angle of the nozzle was introduced as a variable by using 1.75-in. throat diam nozzles having either a 10 or a 41-deg convergent section. A few tests were also conducted with a "stove-pipe motor" (i.e., one having no nozzle). The equipment and procedures were otherwise identical to those described in (1), except that the instrumentation was supplemented by the use of Dynagages to measure chamber pressure and, at times, alcohol line-pressure oscillation frequencies. Timing marks of either 120 cps or 240 cps were provided on the film edge by means of an externally excited spark gap.

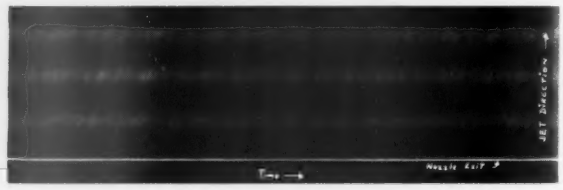

FIG. 5 SLIT PHOTOGRAPH OF JET AT STABLE OPERATION

Since the slit window extended only along the window motor portion of the composite chamber, the sole means of studying the flow field along the entire length of the cylindrical motor section was to exchange the chamber sections so that the window motor would at alternate times form either the upstream or downstream portion of the chamber.

Figs. 7a–7c are a strip film record showing the transition

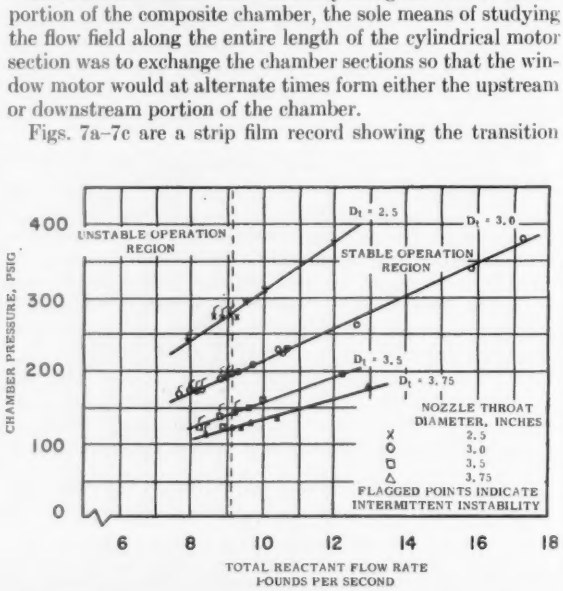

FIG. 6 CHAMBER PRESSURE VERSUS PROPELLANT FLOW RATE OF $4^1/_2$-IN. DIAM ROCKET MOTORS WITH VARIOUS THROAT DIAMETERS

Fig. 7a

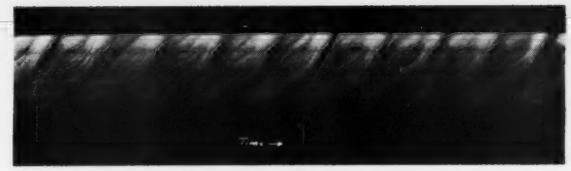

FIG. 7b

FIG. 7c

Figs. 7A, 7B, 7C

RADIATION PATTERN OF TRANSITION FROM SINUSOIDAL TO SHOCK-TYPE OSCILLATION. MODIFIED IMPINGING HEAD, 41° CONVERGENT NOZZLE, $16^{5}/_{8}$-IN. LONG CHAMBER WITH WINDOW-MOTOR FORMING UPSTREAM PORTION. SLIT LENGTH, $8^{21}/_{32}$-IN.; SHOCK FREQUENCY, 1200 CPS

FIG. 8a

FIG. 8b

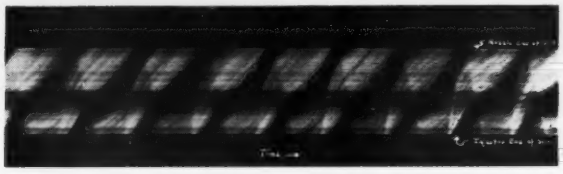

FIG. 8c

Figs. 8A, 8B, 8C

RADIATION PATTERN OF TRANSITION FROM SINUSOIDAL TO SHOCK-TYPE OSCILLATION. MODIFIED IMPINGING HEAD, 41° CONVERGENT NOZZLE, $17^{3}/_{8}$-IN. LONG CHAMBER WITH WINDOW-MOTOR FORMING DOWNSTREAM PORTION. SLIT LENGTH, $8^{21}/_{32}$-IN.; SHOCK FREQUENCY, 1140 CPS; NOZZLE ENTRANCE 1 IN. DOWNSTREAM OF SLIT END. FILM SPEED ABOUT 40 FT/SEC

from sinusoidal to shock-type oscillations with a $16^{5}/_{8}$-in. long chamber, the modified impinging head, and a 41-deg convergent half-angle nozzle. The window motor formed the upstream portion of the chamber. Figs. 8a–8c show the transition period near the nozzle, obtained with the reassembled motor having the window motor forming the downstream portion of the chamber. The nozzle end of the slit ended roughly 1 in. upstream of the nozzle entrance. Since it was necessary to insert a special adapter between the bodies, the total cylindrical chamber length was $17^{3}/_{8}$ in. Otherwise the assembly and operating conditions in the two tests were identical. The chamber pressure was approximately 275 psig. A sketch of the composite flow field, based on the photographs obtained at the two locations of the window motor, is shown in Fig. 9. The black streaks are drawn in for reference purposes.

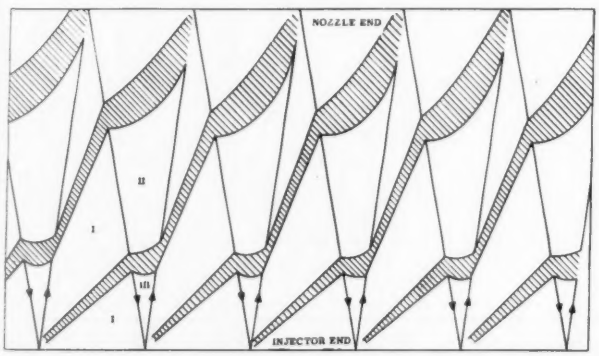

FIG. 9 COMPOSITE SKETCH OF SHOCK-WAVE RADIATION PATTERN AS SEEN IN WINDOW-MOTOR PHOTOGRAPHS

The radiation pattern of the sinusoidal oscillations, as shown in Figs. 7a–7c, is, except for the frequency, almost identical to the one obtained with the 10-in. long window motor chamber alone and shown in Figs. 10a, 10b of (1). In both cases one observes pressure waves propagating upstream. The path of the pulse is made evident by the sharp deceleration which the gas stream undergoes immediately upon passage of the wave. In addition, the radiation intensity of the gas increases behind the pulse. No downstream moving pulses are discernible. The transition to shock oscillations occurs within a short time interval as upstream moving pulses become more sharply defined and, finally, the first evidence of a downstream moving pulse can be observed. Within a fraction of a second, a fully developed shock-wave radiation pattern becomes established. The frequency of the oscillations obtained from the film record and Dynagages agree. For the $16^{5}/_{8}$-in. long motor the sinusoidal oscillation frequency is 1080–1140 cps, while the shock-type frequency ranges from 1200–1230 cps. Concurrent with the reflection of each shock wave at the injector, a nonluminous region commences, which moves downstream at the existing gas velocity. This probably represents a cool mixture, consisting of an off-ratio fuel-oxidizer composition. It may be noticed that the radiation intensity emitted by the gas (except for the dark region), immediately after passage of the shock, increases considerably. This is probably caused by the higher pressure and temperature existing behind the shock front. In addition, it is quite feasible that the shock by its impulsive action initiates further combustion. The dark nonluminous region, on the other hand, seems to undergo no radiation increase as it passes through the shock. The upsteam-moving pulse is quite strong, as evidenced by the fact that the gas velocity

at times is actually reversed in direction immediately behind the shock.

The shock velocity, within the accuracy of measurement, appears constant in the regions bounded by the nonluminous streak. After passage through the nonluminous region the shock has a higher velocity.

As described in (1), the tangent of the slope angle enters into the calculation of the velocity, and since the angles of the shock path approach 90 deg, a comparatively small error in angle measurement will cause a large error in the velocity calculation. The measurements are probably no better than ±10%. After reflection from the injector, the shock starts downstream at an absolute velocity of about 3900 ft/sec. After passage through the nonluminous region, its velocity is approximately 4700 ft/sec. The absolute shock velocity after returning from the nozzle is about 2600 ft/sec. After passing through two nonluminous regions, the shock approaches the injector at a velocity of approximately 3300 ft/sec.

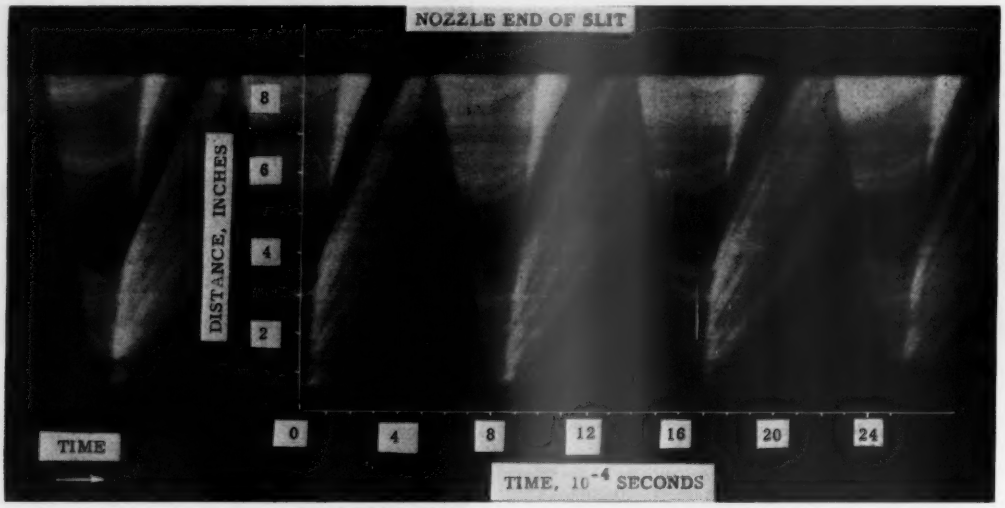

ALL INDICATED VELOCITIES ARE IN FEET PER SECOND

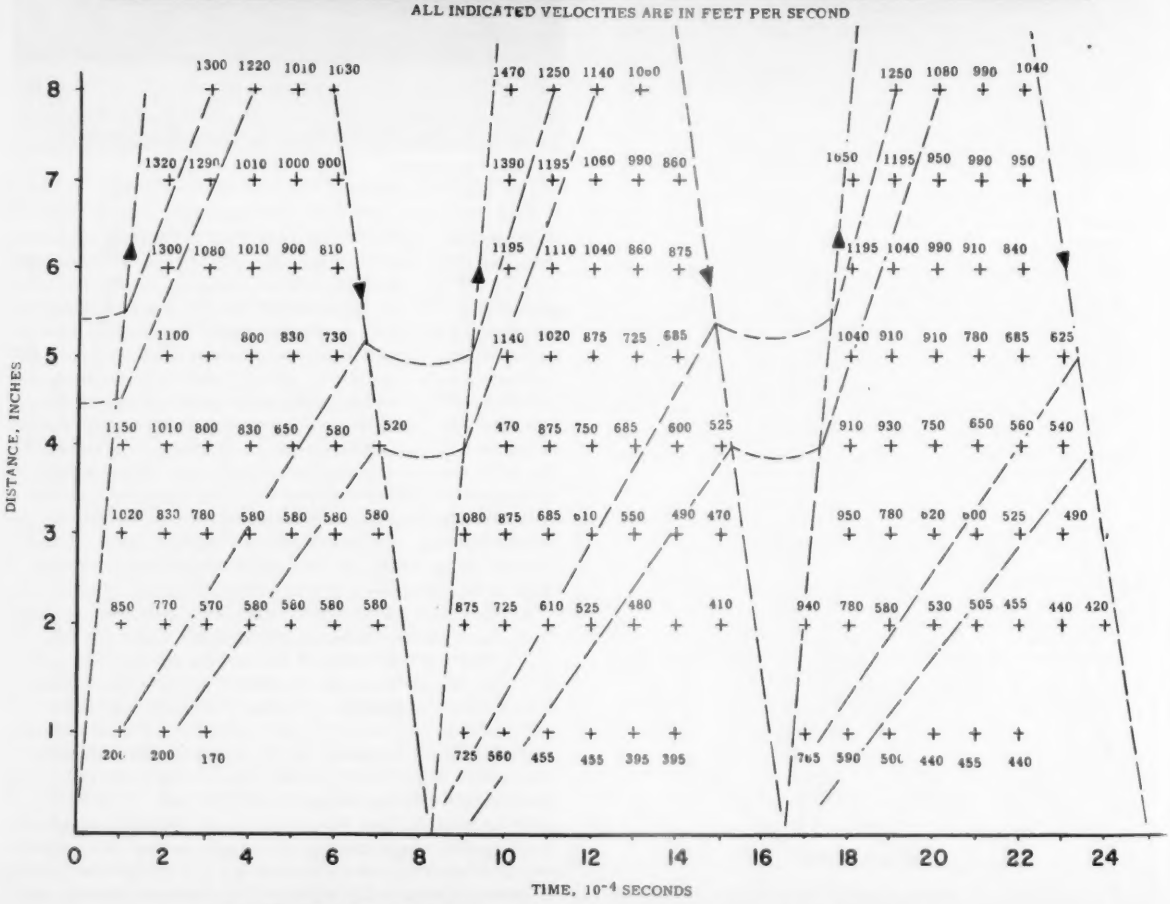

FIG. 10 VELOCITY DISTRIBUTION IN FLOW FIELD AHEAD AND BEHIND SHOCK FRONT

The strip film records furnish the velocity distribution of the flow field. Assuming nonviscous flow theory, it is possible therefore to determine the pressure gradients existing in the motor. The partial derivative of the pressure with respect to the distance x along the axis of the slit is determined from the momentum equation

$$\frac{\partial u}{\partial t} + u\frac{\partial u}{\partial x} = -\frac{1}{\rho}\frac{\partial p}{\partial x} \quad \ldots\ldots\ldots\ldots [1]$$

where

ρ = density at any point x at time t
u = flow velocity at any point x at time t
p = static pressure at any point x at time t

The partial derivative of pressure with respect to time is derived by using the continuity equation

$$u\frac{\partial \rho}{\partial p}\frac{\partial p}{\partial x} + \rho\frac{\partial u}{\partial x} = -\frac{\partial \rho}{\partial p}\frac{\partial p}{\partial t} \quad \ldots\ldots\ldots\ldots [2]$$

where it has been assumed that a $p - \rho$ relationship exists. Since $\sqrt{\partial p/\partial \rho}$ is the sonic velocity a, Equation [2] can be rewritten, after substituting the value $\partial p/\partial x$ from Equation [1], in the form

$$\frac{1}{\rho}\frac{\partial p}{\partial t} \equiv u\frac{\partial u}{\partial t} - (a^2 - u^2)\frac{\partial u}{\partial x} \quad \ldots\ldots\ldots\ldots [3]$$

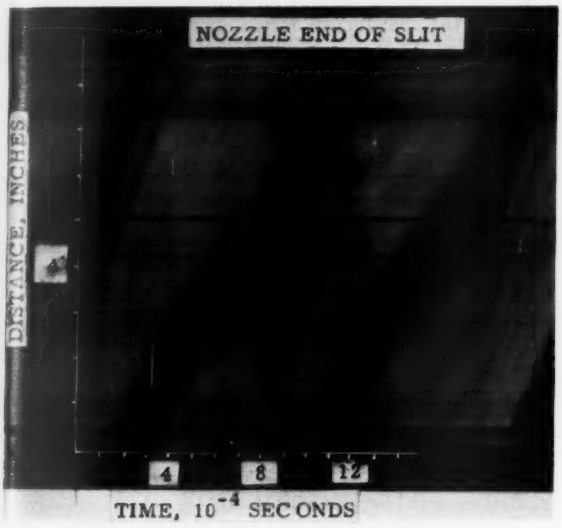

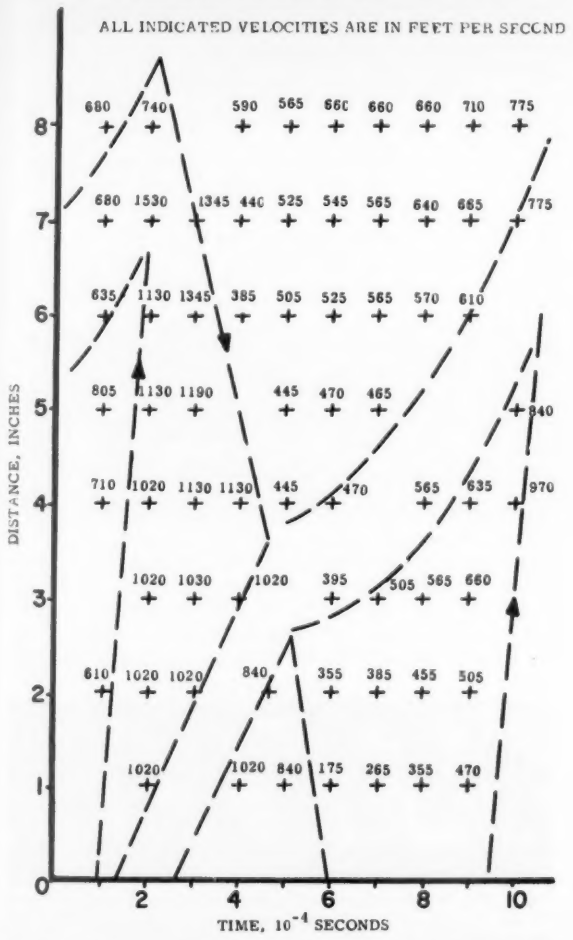

FIG. 11 VELOCITY DISTRIBUTION IN FLOW FIELD AHEAD AND BEHIND SHOCK FRONT

In Figs. 10 and 11 the velocities at selected points of the flow field are indicated. In region I (Fig. 9), i.e., in the region between the downstream moving shock and the returning shock, u $(\partial u/\partial x)$ is positive, while $\partial u/\partial t$ is negative. Calculating the value of the gradients from the rather crude grid, it appears that $\partial u/\partial t$ and u $(\partial u/\partial x)$ have almost identical magnitudes. Since $1/\rho$ $(\partial p/\partial x)$ is therefore calculated as the difference of two large numbers, the possible error of the calculated value is very large. The calculations seem to indicate that $1/\rho$ $(\partial p/\partial x)$ is so small that it is difficult to say what the sign of the pressure gradient is. Since the indicated flow velocity is always subsonic, Equation [3] shows that $\partial p/\partial t$ is always negative and therefore the pressure at a fixed point x decreases with time. In region II, $\partial u/\partial t$, $\partial u/\partial x$, and u are positive. Therefore, $\partial p/\partial x$ is negative. Assuming a sonic value of a = 3000 ft/sec, it appears that $\partial p/\partial t$ is also negative. In region III, $\partial u/\partial t$ and $\partial u/\partial x$ are greater than zero; however, the gas velocity changes from a negative value, immediately after the passage of the shock, to a positive value. Since the time interval is so short, it becomes very difficult to establish an adequate grid to calculate the derivatives. It seems, though, that $\partial p/\partial x$ is positive immediately after the passage of the shock, and then becomes negative. $\partial p/\partial t$ appears to be negative. Qualitatively, at least, it appears that the static pressure of the gas stream behind the downward moving shock decreases with time. The upstream moving shock is trailed by a rarefaction.

The shock strength of the pulses is another quantity which can be approximated from the velocity gradient across the shock. Considering the pressure pulse as a steady one-dimensional normal shock, and neglecting any heat release caused by combustion, the pressure ratio p_2/p_1 can be calculated at any given point. Using the normal shock equation (3)

$$\frac{p_2}{p_1} = \frac{\dfrac{\gamma+1}{\gamma-1}\dfrac{U_1^2}{a^{*2}} - 1}{\dfrac{\gamma+1}{\gamma-1} - \dfrac{U_1^2}{a^{*2}}} \quad \ldots\ldots\ldots\ldots [4]$$

γ = specific heat ratio of combustion gases
a^* = critical speed of sound = $\sqrt{U_1 U_2}$
U_1 = velocity relative to shock of undisturbed gas immediately before entrance into shock front
U_2 = velocity relative to shock of gas immediately after passage through shock
p_1 = pressure of undisturbed gas immediately before entrance into shock front
p_2 = pressure of gas immediately after passage through shock front

Assuming γ = 1.3, it is found that the shock strength p_2/p_1 is approximately 1.5.

FIG. 12 RADIATION PATTERN OBTAINED WITH ASSEMBLY CONSISTING OF MODIFIED IMPINGING INJECTOR, 10° CONVERGENT NOZZLE, AND 17-IN. LONG CHAMBER. WINDOW-MOTOR FORMS UPSTREAM PORTION OF CHAMBER. FILM SPEED ABOUT 40 FT/SEC

Modified Impinging Head, 10-Deg Nozzle, 17-In. Long Body Test

The 41-deg convergent nozzle was replaced with a 10-deg convergent, 1.75-in. throat diam nozzle. The operating conditions were made similar to those of the 41-deg convergent nozzle assembly when the shock-type oscillations occurred. The run was smooth. The chamber pressure was then lowered about 20 psi and the test repeated. Although the run was unstable, no shock-type oscillations were in evidence. A photograph of the combustion pattern is shown in Fig. 12. The frequency of the oscillations is about 1000 cps.

Conventional Impinging Head, 41-Deg Nozzle, 17-In. Long Body

Pictures of the radiation pattern obtained with the conventional impinging head and a 10-in. long window assembly were presented in (1). Oscillations of 240–340 cps were observed then during the first oxygen-full alcohol period.

Five test runs were made with the 17-in. long assembly; two with the window motor at the nozzle end, and three with the window motor at the injector end of the composite chamber. When the chamber pressure was lower than about 310 psig, the combustion became very unstable throughout the run. Severe shock-type oscillations were evidenced, preceded by sinusoidal-type oscillations. For the $17^3/_8$-in. assembly, the sinusoidal frequency was about 800–850 cps while the shock type was approximately 1100 cps; while for the $16^5/_8$-in. assembly the shock-type frequency was about 1150 cps. Figs. 13, 14a, and 14b represent strip film records of the sinusoidal and shock-type oscillation, respectively. It may be noticed that the radiation pattern is not as uniform as the one obtained with the modified impinging head. The nonluminous region seems to drift with time. It appears that with each succeeding cycle of shock reflection at the injector, the nonluminous region seems to commence at a different location, and thus there appears to be a phase shift between the motion of the nonluminous region and the shock path until finally several of the dark streaks almost merge with each other to form an extended nonluminous region. Then the cycle repeats itself. Its approximate period is 200–300 cps

FIG. 13 RADIATION PATTERN OF SINUSOIDAL OSCILLATIONS OBTAINED WITH ASSEMBLY CONSISTING OF CONVENTIONAL IMPINGING HEAD, 41° CONVERGENT NOZZLE, AND 17-IN. LONG CHAMBER. WINDOW-MOTOR FORMS UPSTREAM PORTION OF CHAMBER. FILM SPEED ABOUT 75 FT/SEC

Conventional Impinging Head, 10-Deg Nozzle, 17-In. Long Motor

All runs with this assembly were unstable. However, the instability was of the sinusoidal type and had a frequency of about 800 cps. The instability was somewhat random, i.e. it disappeared for a while and then started up again. An example of the radiation pattern is shown in Fig.15

21-In. Long Motor Assemblies

The radiation patterns obtained with the 21-in. assemblies had the general appearance described for the 17-in. assemblies except that the shock oscillation frequency was lower (950–1000 cps). However, intermittent shock-type oscillations were obtained with the 10-deg nozzle assembly.

"Stove-Pipe" Assembly with Conventional Impinging Head

Two test runs were made with a 21-in. long "stove-pipe" assembly at chamber pressures of about 125 psig. The flow rates at these chamber pressures are equal to those for a conventional 1.75-in. throat diam motor operating at a pressure of 300 psi. Both runs were unstable on full stage operation. The Dynagage chamber pressure record showed sinusoidal-type oscillations at a frequency of 650 cps. A Dynagage had also been placed in the alcohol line, about $^3/_4$ ft upstream of the injector inlet. The frequency of oscillations agreed with the chamber pressure oscillations; however, the alcohol oscillations were of considerably higher amplitude. A portion of the pressure record is reproduced in Fig. 16. The strip-film record is shown in Fig. 17. The radiation pattern is composed of regions of weak and strong radiation which alternate at a frequency of about 650 cps. There is no evidence of any shock-type oscillation.

Summary

The present study seems to confirm that high-frequency instability in small-diameter motors corresponds to the propagation of finite pressure disturbances axially along the motor. In (1), it was postulated that the unsteady combustion cycle is initiated by the rapid ignition of a mass of combustible mixture near the injector head. It was conjectured

Fig. 14a Window-Motor Forming Upstream Portion of Chamber

Fig. 14b Window-Motor Forming Downstream Portion of Chamber

RADIATION PATTERN OF SHOCK-TYPE OSCILLATIONS OBTAINED WITH ASSEMBLY CONSISTING OF CONVENTIONAL IMPINGING HEAD, 41° CONVERGENT NOZZLE, AND 17-IN. LONG CHAMBER

that the lower chamber pressure would increase the quenching distance, and hence, stable flame holding between the injector jets would become impossible. The present study appears to indicate that these assumptions are incorrect. The fact that the initiation of unstable operation is dictated more by the head pressure drop than the chamber pressure is a point which definitely invalidates the quenching-distance consideration, although it does in no way depreciate the fundamental assumption that the low-velocity gas region existing between the liquid fuel and oxidizer jets, in the vicinity of the injector holes, is the flame-stabilizing or holding zone of a rocket motor.

It is also pertinent to notice that in case of relatively weak oscillations (i.e., sinusoidal oscillations), the upstream-moving pulse is always evident while a downstream moving pulse is hardly discernible. It almost appears as if the sonic nozzle acts not only as a reflector for the pulse but also as an amplifier. On reaching and reflecting from the injector the pressure pulse might be expected to influence the mass flow into the motor as well as the oxidizer to fuel ratio, if the two propellant components have different properties such as density and sonic velocity. As was pointed out in the discussion of the strip-film records, the nonluminous gas region, commencing with each reflection of a pulse from the injector, is believed to be such an off-ratio, cold-gas region. At the entrance to the nozzle, this cold gas has therefore a different Mach number from the warmer gas which preceded it, since no sharp velocity gradient (in time) $\partial u/\partial$ is apparent at the nozzle end of the strip film. The possibility of pressure pulse formation caused by this unsteady gas Mach number entrance condition into the nozzle is a topic which merits further analysis.

The shock waves are apparently not established instantaneously, as might be expected from a detonation, but build up gradually from finite pulses which gain in strength. Whether the energy gain is the result of heat addition by combustion or a result of amplification caused by the nozzle is a question which for the moment cannot be answered. It has, however, been found that, generally, shock formation is much more prevalent with longer motor chambers than shorter ones. It was found impossible to make unstable a $5^3/_4$-in. long water-cooled assembly, consisting of the modified impinging head and the 41-deg convergent nozzle. With a 10-in. long assembly, as reported in (1), only sinusoidal oscillations were obtained.

FIG. 15 RADIATION PATTERN OBTAINED WITH CONVENTIONAL IMPINGING INJECTOR, 10° CONVERGENT NOZZLE AND 17-IN. LONG CHAMBER. WINDOW-MOTOR FORMED DOWNSTREAM PORTION OF ASSEMBLY. FILM SPEED ABOUT 40 FT/SEC

The importance of the shape of the convergence section of the nozzle on the severity of instability is illustrated by the data. This possibility has been recognized previously (4). Unfortunately our present equipment did not permit the photographic investigation of the phenomenon occurring in the nozzle. The reflection of shock waves from solid surfaces has only recently been studied intensively, especially by Bleakney (5) and associates at Princeton University. If the results obtained from two-dimensional studies can be used as an analogy for three-dimensional studies, it appears that, in general, the mode of reflection is a function of the shock strength and the angle of incidence, which is defined as the angle between the normals to the shock wave and the wall. From the data presented by Bleakney and White (6), it appears that with the 41-deg nozzle one would probably get a "regular" reflection for the shock strength obtained in the present investigation, while for the 10-deg nozzle it would be of the Mach type. The detailed mechanism of the shock reflection at the sonic nozzle, especially under conditions of nonuniform flow, is a problem which requires experimental investigation.

FIG. 16 DYNAGAGE PRESSURE RECORD OBTAINED WITH 21-IN. LONG "STOVE-PIPE" MOTOR

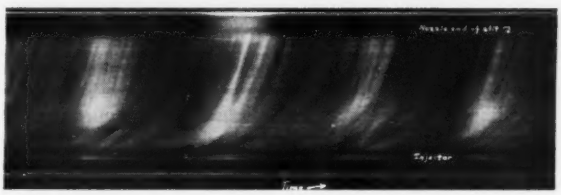

FIG. 17 RADIATION PATTERN OBTAINED WITH 21-IN. LONG "STOVE-PIPE" MOTOR WITH CONVENTIONAL IMPINGING INJECTOR HEAD. WINDOW-MOTOR FORMED UPSTREAM PORTION OF CHAMBER ASSEMBLY. FILM SPEED ABOUT 40 FT/SEC

Conclusion

It has been established that high-frequency combustion instability in small-diameter motors is the result of pressure pulse propagation along the length of the motor. The frequency of oscillation is a function of the cylindrical chamber length of the motor. The severity of unstable operation is increased by low injector head pressure drop, long chamber lengths, and large nozzle convergent angle. In the case of very large-scale oscillation, the radiation pattern obtained on the strip film shows the existence of shock waves. The flow field ahead and behind the shock front has been measured.

Acknowledgments

This work was performed as part of Project Hermes. We wish to thank Army Ordnance for permission to publish the results. The assistance of numerous individuals at the Malta Test Station of Project Hermes made the execution of these experiments possible. Special thanks are due to Dr. G. E. Moore and Mr. E. H. Hull.

References

1 "Combustion Studies With a Rocket Motor Having a Full-Length Observation Window," by K. Berman and S. B. Logan, JOURNAL OF THE AMERICAN ROCKET SOCIETY, vol. 22, March-April 1952, pp. 78–85.

2 "Experimental Investigation of Combustion Instability in Rocket Motors," by H. Ellis, I. Odgers, A. J. Stosick, N. Van de Verg, and R. S. Wick, presented at the Fourth International Symposium on Combustion, Boston, Mass., September 1952.

3 "Introduction to Aerodynamics of Compressible Fluid," by Liepmann and Puckett, John Wiley and Sons, New York, N. Y., 1947, p. 40.

4 Private Communication by R. H. Johnson, General Electric Research Laboratory.

5 See, for example, "Interaction of Shock Waves," by W.

Bleakney and A. H. Taub, *Reviews of Modern Physics*, vol. 21, October 1949, pp. 584–605.

6 Technical Report II-10, by W. Bleakney and M. White, Princeton University, Department of Physics Contract N6ori-105, Task Order II, August 21, 1951, Fig. 3.

DISCUSSION

By SIN-I CHENG[5]

Daniel and Florence Guggenheim Jet Propulsion Center, Princeton University, Princeton, N. J.

Dr. Berman and Mr. Cheney are to be congratulated for their important experimental information in confirming the basic postulate of the linearized, small-perturbation analysis for the stability of combustion system in rockets.

There has been considerable dispute on the feasibility of making linearized stability analysis for the high-frequency oscillations encountered in rough burning rocket motors. After Berman's presentation at the ARS 7th Annual Convention, a written comment was read in which the shock-type oscillation is considered as a definite indication of nonlinearity and cannot be analyzed by linearized treatment. It seems that, by "rough burning," we mean combustion with large amplitude pressure oscillations whose nonlinearity is obvious. The existence of the shock-type oscillation does not add any new information in this respect. In fact, any measurable or observable quantities must be of finite magnitude and cannot be treated with linearized analysis in the strict sense. It is, therefore, apparent that the properties of the large pressure oscillations in rough burning rockets cannot be analyzed on a linearized basis. However, this is not what one is most interested in at the present time. One knows rough burning is undesirable and one wants to avoid it. Any knowledge of the behavior of the nonlinear oscillations in rockets and how they cause damage is, of course, very valuable. But one is more interested in finding why such nonlinear oscillations can occur in rockets which seem to be designed for smooth operation, and how they can develop in rockets that burn smoothly in the early stage of operation and then become rough. Once one knows why and how, one can seek to avoid or suppress it.

It does not seem likely that oscillations of large amplitudes are introduced into the combustion system or burned gas flow system from without. It is, therefore, postulated that oscillations of large amplitudes are the result of rapid amplification of unstable small perturbations of certain frequency range which invariably are present in the system as "random noise." These random noises are sufficiently small so that the stability of these small random disturbances in the system can be determined by linearized analysis based on certain excitation mechanisms. If disturbances in certain frequency range become unstable when the mechanisms of excitation overcome the mechanisms of damping, they will grow in magnitude with time. When these disturbances are sufficiently amplified, new damping or exciting mechanisms of nonlinear nature gradually come into play, and finally a definite finite magnitude is reached when damping balances excitation. Based upon such a postulate as to the origin and the course of development of the nonlinear oscillations, the instability of small disturbances becomes a necessary condition prior to the existence of oscillations of large amplitudes or rough combustion. The best justification of the contemplated course of development is to be able to record experimentally the oscillations during the intermediate stages, and to follow the course of amplification that leads to the final stage of large amplitude oscillations. This experimental justification is found in the present work of Berman and Cheney. In their experiments it is consistently found that shock-type oscillations are always preceded by sinusoidal-type oscillations which are of considerably smaller amplitudes. The authors are cautious in giving the absolute magnitudes of the two types of oscillations, but it is reasonable to believe that the relative magnitudes of the two types of oscillations are qualitatively correct. There are several radiation patterns of transition, but it is rather unfortunate that Berman and Cheney have not given more detailed records of the transition processes. A series of such records following the development more closely, such as those given by Schubauer and Skramstad on the amplification of pulses in unstable laminar boundary layer, would be very impressive.

It is found that shock-type oscillation has higher frequency than the preceding sinusoidal oscillation. This is not surprising because of its larger propagation speed which results in a smaller characteristic time for the wave to travel the length of the combustion chamber. It does not seem likely that this change of frequency has anything to do with the basic mechanism of instability.

In a recent theoretical investigation (7, 8)[6] on the high-frequency combustion instability of the intrinsic type in liquid propellant rockets, it is found that the ratio of the length l_{sub} of the subsonic portion of the de Laval nozzle to the combustion chamber length L is an important parameter involved in the boundary condition at the exit of the combustion chamber. If the ratio l_{sub}/L is reduced while other parameters remain unchanged, the rocket is found to be more unstable. This theoretical deduction is confirmed by Berman and Cheney's experimental results, that both larger combustion chamber length and larger nozzle converging angle are destabilizing. The theory also predicts that the fundamental mode is the most unstable mode in the series of higher frequency oscillations, and that each higher mode is more stable than the preceding lower modes. Experiments presented in this paper show that the fundamental and the second mode are predominating. The qualitative trends of the theoretical deduction agree with the experimental results. The presence of other modes at finite magnitudes may well be due to the nonlinear coupling of oscillations of different frequencies when the fundamental and the second mode are sufficiently amplified.

Berman and Cheney put forth several interesting ideas. The nonluminous gas region commencing with each reflection of a pulse from the injector end seems to indicate the importance of the difference in the responses of the fuel and the oxidizer lines to the pressure change at the injector end. Whether this fact has fundamental importance in the stability behavior of small disturbances in the system seems to be worth further investigation. In an effort to explain the "superficially stronger" upstream moving waves reflected from the nozzle in the radiation streak records, they also propose the excitation mechanism, that "the sonic nozzle acts not only as a reflector but also as an amplifier." Since no combustion is supposed to take place in the nozzle, and the steady flow in the nozzle is considered to be isoenergetic, the pressure wave cannot possibly gain energy in the course of its reflection from the nozzle. The reflected wave must not be stronger than the incoming wave in order to conform to the energy principle. In fact, normally incident compression shock is reflected as expansion from open end and as weaker shock from a closed wall. The three-dimensional reflection is much more complicated but will not create energy in the course of reflection. The fact that the reflected wave moving in upstream direction appears to be stronger in the radiation streak is probably due to a simple geometrical reason which becomes more significant when the angle between the radiation streak and the time axis becomes larger. If this angle is initially

Received December 30, 1952.

[5] Assistant Professor of Aeronautical Engineering.

[6] Numbers in parentheses refer to the References at end of this discussion.

(*Continued on page 98*)

Technical Notes

Comment on "An Approximate Theory of Porous, Sweat, or Film Cooling With Reactive Fluids" by L. Crocco[1]

ANDREW E. ABRAMSON[2]

National Advisory Committee for Aeronautics
Lewis Flight Propulsion Laboratory, Cleveland, Ohio

The paper by L. Crocco presents a very interesting approach to a rather complicated mechanism. Evaluation of the validity of the simplifying assumptions used in the analysis remains for future work; however, the assumptions appear to be in line with conventional assumptions used for analysis of this type.

Whereas the paper is applicable to various types of cooling, it was reviewed only with reference to liquid film cooling, as data for this type of cooling are available from experiments conducted at the NACA Lewis Flight Propulsion Laboratory.

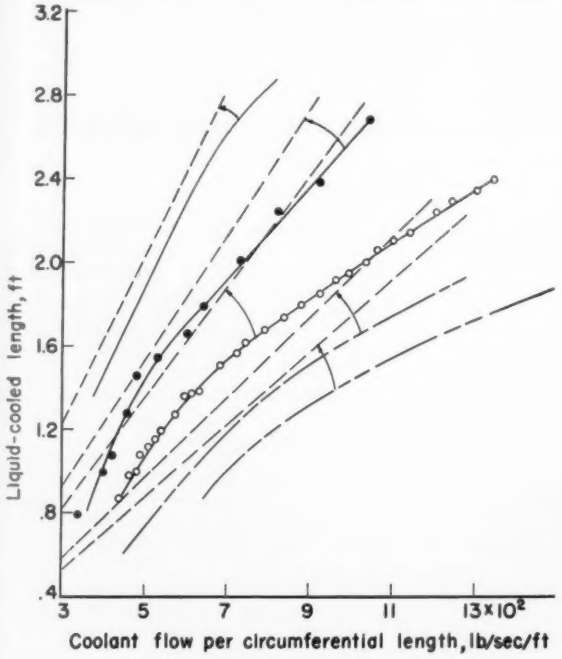

FIG. 1. VARIATION OF LIQUID-COOLED LENGTH WITH WATER FLOW PER UNIT CIRCUMFERENCE

Legend	Gas temperature (°F)	Gas mass velocity (lb/(sec)(sg ft))	Reynolds number
●	900	57.9	8.18×10^5
○	900	70.2	9.90
———	900	42.5	6.00 } NACA
– – –	1400	45.3	5.25 } RM
———	1600	43.6	4.70 } E50F19
– – – –	Theoretical results corresponding to experimental conditions		

[1] JOURNAL OF THE AMERICAN ROCKET SOCIETY, vol. 22, November–December 1952, pp. 331–338.
[2] Aeronautical Research Scientist.

The assumption of a smooth liquid surface limits the range of liquid coolant flow rates to which the results of this analysis can be applied. The results of a visual investigation of annular liquid flow with concurrent gas flow, NACA RM E51013 (now unclassified), indicate that a smooth liquid surface is encountered at only the relatively low liquid flow rates. It is questionable whether liquor or coolant flow rates of this magnitude are practical for film cooling application to rocket engines.

The expression used for the evaluation of the friction coefficient (i.e., $C_F = 0.046\ Re^{-0.2}$) does not appear to be valid for the flow system encountered in liquid film cooling. Investigations of the pressure drop encountered in a two-phase two-component flow reported by Lockhardt and Martinelli (in *Chemical Engineering Progress*, January 1949) and by Bergelin (in *Chemical Engineering*, May 1949) indicate the friction coefficient would be larger than given by the previous relation.

A comparison of the theoretical results for the inert coolant with experimental results obtained from a gasoline-air burner test rig is given in Fig. 1. The experimental results are taken in part from NACA RM E50F19 (now unclassified), and the remainder from data to be published in the near future. The theory predicts a longer liquid cooled length than observed experimentally, and gives the best agreement at the low coolant flow rates which correspond to a smooth liquid surface. In applying the theory, the term $h_g - h_0$, which appears in Equation [18] of Crocco's paper, was evaluated as the change in enthalpy of the coolant vapor in going from its boiling point to the free stream temperature. The paper does not indicate clearly whether the term $h_g - h_0$ is referred to the main gas stream or the coolant vapor. The above interpretation seems the most logical and gives a closer agreement with the experimental results.

JOURNAL BINDERS AVAILABLE

Handsome binder holds six issues (one year)

Approximately 8½" x 11½"
Blue leatherette with stamped letters
Simple metal rack, easy to assemble

Keeps Journal securely in place
Stands erect on bookshelf
Convenient to carry
Individual copies cannot be misplaced
Back issues protected against damage

Price $2.00

Please order from
Secretary
American Rocket Society
29 West 39th Street
New York 18, N. Y.

EDITOR'S NOTE: This section of the JOURNAL is open to short manuscripts describing new developments or offering comments on papers previously published. Such manuscripts are published without editorial review, usually within two months of the date of receipt. Requirements as to style are the same as for regular contributions. (See inside back cover.)

GROVE
SELF-ACTUATED
CONTROLS AND REGULATORS
for
High pressure liquids and gases
•
Pressure Reducing
Back Pressure
Relief and By-Pass
Manual Valves
•
Special light weight units
for air-borne service.
•
Special materials for corrosive
or low-temperature applications.
•
GROVE CONTROLS, INC.
6529 Hollis Street
Emeryville GROVE SIMPLICITY ACCURACY SAFETY California

WANTED
ENGINEERS and
SCIENTISTS

Unusual opportunities for outstanding and experienced men.

These top positions involve preliminary and production design in advanced military aircraft and special weapons, including guided missiles.

IMMEDIATE POSITIONS INCLUDE:

★ Boundary layer research scientists . . .
★ Electronic project engineers . . .
★ Electronic instrumentation engineers . . .
★ Radar engineers . . .
★ Flight-test engineers . . .
★ Thermodynamicists . . .
★ Servo-mechanists . . .
★ Electro-mechanical designers . . .
★ Electrical installation designers . . .

Excellent location in Southern California. Generous allowance for travel expenses.
Write today for complete information on these essential, long-term positions. Please include résumé of your experience & training. Address inquiry to Director of Engineering,

NORTHROP AIRCRAFT, INC.
1041 E. Broadway, Hawthorne (Los Angeles County), Cal.

Combustion Studies in Rocket Motors

(*Continued from page 96*)

60 deg, a given velocity change of the particle that could turn the velocity vector in the radiation record for 15 deg in the upstream direction can only turn the velocity vector for 7½ deg in the downstream direction. While an upstream shock will almost cause flow reversal, a downstream shock of equal strength can hardly turn the velocity vector through 15 deg. In extreme cases, if the initial angle is as big as 80 deg, a shock which is strong enough to cause flow reversal if moving upstream may hardly be discernible when it is moving downstream.

References

7 "High Frequency Combustion Instability in Rockets with Concentrated Combustion," by L. Crocco and S. I. Cheng, presented at the Eighth International Congress on Theoretical and Applied Mechanics, Istanbul, Turkey, August 1952 (to appear in a later issue of the JOURNAL OF THE AMERICAN ROCKET SOCIETY).

8 "High Frequency Combustion Instability in Rockets with Distributed Combustion," by L. Crocco and S. I. Cheng, presented at the Fourth International Symposium on Combustion, Boston, Mass., September 1952.

On Maximum Evaporation Rates of Liquid Droplets in Rocket Motors

(*Continued from page 88*)

10 "Principles of Spray Drying. Part I: Fundamentals of Spray-Dryer Operation; Part II: Elements of Spray-Dryer Design," by W. R. Marshall, Jr., and E. Setzer, *Chemical Engineering Progress*, vol. 46, 1950, pp. 501–508, 575–584.

11 "On the Theory of the Heat and Mass Transfer from a Sphere in a Flowing Medium at Low Values of Reynolds Number," by R. Kronig and J. Bruijsten, *Applied Science Research*, vol. A2, 1951, pp. 439–446.

12 "An Experimental Study of the Evaporation and Combustion of Falling Droplets," by J. E. C. Topps, *Journal of the Institute of Petroleum*, vol. 37, 1951, pp. 535–553.

13 "An Analysis of the Factors Affecting the State of Fuel and Air Mixtures," by M. Gilbert, J. N. Howard, and B. L. Hicks, *NACA Technical Note* no. 1078, Washington, D. C., May 1946.

14 "Die Maximale Verdampfungs-geschwindigkeit des Quecksilbers," by M. Knudsen, *Annalen der Physik*, vol. 47, 1915, pp. 697–708.

15 "On the Kinetics of Evaporation," by S. S. Penner, *Journal of Physical Chemistry*, vol. 56, 1952, pp. 475–479.

16 "Kinetic Theory of Gases," by E. H. Kennard, McGraw-Hill Book Co., Inc., New York, N. Y., 1938.

17 "Heat Transmission," by W. H. McAdams, McGraw-Hill Book Co., Inc., New York, N. Y., 1942.

18 "The Apparent Energy of the N—N Bond as Calculated from Heats of Combustion," by C. M. Anderson and E. C. Gilbert, *Journal of the American Chemical Society*, vol. 64, 1942, pp. 2369–2372.

19 "Some Considerations of the Effect of Radiation on the Performance of Liquid Fuel Rockets," by S. S. Penner and S. Weinbaum, *Journal of the Optical Society of America*, vol. 38, 1948, pp. 599–603, 840.

20 "Mass Emissivity of Powder Gases in Solid Fuel Rockets," by S. S. Penner, *Journal of Applied Physics*, vol. 19, 1948, pp. 278–285; "Effect of Radiation on the Rate of Burning of Solid Fuel Rocket Propellants," by S. S. Penner, *Journal of Applied Physics*, vol. 19, 1948, pp. 392–398; "Qualitative Experimental Verification of the Change of Burning Rate of Rocket Powder with Radiation Path Length," by S. S. Penner, *Journal of Applied Physics*, vol. 19, 1948, pp. 511–513. See also "Studies of Radiation Phenomena in Rockets," by J. Beek, Jr., W. H. Avery, M. J. Dresher, F. T. McClure, and S. S. Penner, ABL Final Report P-2, OSRD Report No. 5817, June 1946.

Jet Propulsion News

C. F. WARNER, Purdue University, *Associate Editor*

with the assistance of W. G. BOHL

Rockets

A COMPLETELY redesigned and re-engineered Viking high-altitude rocket, one of a series built by The Glenn L. Martin Company for the Naval Research Laboratory, equalled the previous single-stage altitude mark of 135.6 miles when launched at the White Sands Proving Ground, Las Cruces, N. Mex. Shorter by some six feet and of slightly greater diameter, with completely new control, fuel, and electronics systems, Viking No. 9's most readily distinguishable external feature was smaller, triangular fins. The power plant, made by Reaction Motors, Inc., was of the same type used on previous Vikings, liquid oxygen and alcohol, with a 20,000-lb thrust. Fig. 1 shows a Viking just after take-off. White cloud at right is steam from water in pit under launching stand, vaporized by tremendous heat from rocket engine. Up to the time of this firing, the altitude record for single-stage rockets was held by Viking No. 7, which was also launched at White Sands on August 7, 1951. A WAC Corporal launched from the nose of a German V-2 in a two-stage operation has reached about 250 miles.

Vikings are being used by NRL scientists to extend knowledge of (1) the physical state of the earth's atmosphere to as great a height as possible, the temperatures, pressures, densities and composition being principal objects of study; (2) the fundamental nature and properties of the ionosphere and those processes which lead to its formation; (3) solar and terrestrial radiation; and (4) the physics of high-energy particles by high-altitude cosmic ray studies. This information is expected to be of practical benefit to radio communication, meteorology, and the guided missile program, as well as to the basic physical sciences. Four additional rockets have been ordered by NRL from The Glenn L. Martin Company.

✦ ✦ ✦

SOME details of the rockets currently being developed by Oerlikon in Switzerland have recently been revealed. In addition to their first powder rockets, which have a diameter of 3.15 in. and a length of 24 in., they are producing several versions of a 2.2-lb contact detonating rocket. All of these solid rockets may be fired from fighter and bomber aircraft, or from ground-stationed antiaircraft units.

A longer range rocket with a proximity fuse is also under development. A small turbine driven by the exhausted rocket gases powers an electric generator. Current from the generator supplies power to a miniature radar instrument which continuously measures the distance of the rocket from the target and ignites the warhead at the correct instant.

One of the Oerlikon guided missiles, guided to the target by the guide-beam method, has four small wings and is powered by a nitric acid motor. These antiaircraft missiles have a length of 16.4 ft, a combustion cut-off speed of 2460 fps, and are said to reach an altitude of 66,000 ft. The gross weight of the missile, including a 44-lb war head, is 550 lb.

Aircraft

AN Air Force North American F-86D Sabrejet interceptor powered by a GE turbojet was recently flown to a new official world's speed record of nearly 700 mph by Air Force Capt. J. Slade Nash. The F-86D combines high speed with all-seeing radar and new electronic equipment to enable it to operate in any kind of weather. The "all-weather" engine makes possible the successful completion of missions under severe icing conditions. "Icing up" has been a serious problem in jet operation. Supercooled water droplets, striking the air inlet at the nose of the engine, form into ice crystals and, within seconds, can block passage of air into the engine. This problem has been overcome by giving the engines "hot noses." Air, at temperatures high enough to melt any ice crystals, is bled from the compressor and piped to passages in the nose.

(Photograph courtesy of The Glenn L. Martin Company

FIG. 1 VIKING NO. 9 RISING FROM LAUNCHING STAND

✦ ✦ ✦

THE Republic Aviation Corporation's XF-91, powered by a GE J-47 turbojet and a Reaction Motors rocket engine, recently flew faster than sound in level flight. Thus the XF-91 became the first U. S. plane designed for warfare to achieve a level flight speed of greater than Mach 1. The necessary additional thrust was supplied by the rocket motor.

Republic also recently delivered its first production model of the F-84F Thunderstreak fighter bomber to the Air Force. The Thunderstreak, capable of speeds over 700 mph, is powered by the Curtiss-Wright built British Sapphire engine. The F-84F is said to be able to carry a small atom bomb to a range of more than 2000 miles.

✦ ✦ ✦

THE Swedish Air Force claims that its new two-seated fighter, the Saab-32, powered by a Rolls-Royce Avon, has a top speed of 700 mph. The Saab-32 is armed with rocket pro-

EDITOR'S NOTE: The information reported in this Section has been selected from approved news releases originating with the Department of Defense, private manufacturers, universities, etc., and from published news accounts in journals and newspapers. The reports are considered generally reliable, although no attempt has been made to verify them in detail.

jectiles, bombs, and cannon. The fighter has a span of 41 ft and an over-all length of about 46 ft.

✦ ✦ ✦

THE new Handley Page crescent-wing jet bomber, the H.P. 80, powered by four Sapphire turbojet engines, has been ordered into quantity production for the British Bomber Command. No details as to performance or dimensions are available. However, the maker claims that no other bomber can fly as far or as fast with its bomb load.

✦ ✦ ✦

THE world's first delta-wing seaplane, the XF2Y-1 "Sea Dart," a jet-powered experimental aircraft built for the Navy by Consolidated Vultee Aircraft Corporation, is shown in Fig. 2 as it began preflight trials on San Diego Bay. Two Westinghouse J-34 turbojet engines power the present Sea Dart, but it is thought that two J-46's will be used eventually. It is reported that ten additional Sea Darts have been ordered at a reported cost of $2,250,000 each.

To provide better rough-water landing and take-off characteristics, the XF2Y-1 is equipped with retractable hydro-skis. This marks the first application of the hydro-ski to a combat type aircraft in this country and, according to Navy officials, may well be the first such application in the world. The new hydro-ski will enable high-speed aircraft to operate from water, grass, ice, and snow. The NACA, Navy, Air Force, the Research Division of All-American Airways, and the Edo Corporation developed the hydro-ski in a six-year joint research program. The Canadian bush pilots originated the idea when they used their winter snow skis to land on water during periods of melting ice. The watertight fuselage of the Convair XF2Y-1 enables it to float on the water. However, the hydro-skis take all of the water impact shock during landing and take-off. At take-off, the extended hydro-skis are under water as the XF2Y-1 begins its run (Fig. 3). The plane's cambered surface provides hydrodynamic lift and lifts the fuselage out of the water; then the lower V-shaped surfaces of the skis provide the lift. The final take-off run is made on the skis. When landing, the extended skis take the initial water impact and carry the plane as it loses speed until it sinks and floats on its fuselage.

The use of the hydro-ski will enable high-speed coastal defense aircraft to operate without the necessity of constructing expensive runways. When fitted with small integral wheels, the hydro-skis will enable an aircraft to land upon the water and taxi up a beach. This type of landing gear would be of great value to aircraft operating from an invasion beach head.

Turbojet Engines

SWEDEN'S newest turbojet, the 9000-lb thrust Dovern, will soon go into production at the underground plant of Svenska Flaygmotor AB near Trollhättan. The Dovern has undergone extensive flight tests in a modified Avro Lancaster. This new turbojet was developed from the 3300-lb thrust Skuten. Other more powerful engines are currently under development by Svenska Turbin-fabriks AB Ljungström (STAL) of Finspong.

✦ ✦ ✦

THE Société National d'Étude et de Construction de Moteurs d'Aviation (SNECMA) of Paris has been flight-testing a "jet deviator" which turns the turbojet engine thrust

FIG. 2
CONVAIR "SEA DART"
WATER-BASED INTERCEPTOR
(Photograph courtesy of Convair)

FIG. 3
"SEA DART"
AT START OF
TAKE-OFF RUN
(Photograph courtesy of Convair)

through an angle of approximately 120 degrees toward the front of an aircraft. This forward-directed thrust effects a braking action which permits landing in much shorter distances. Although design and performance data are secret, SNECMA claims that they hope to be able to land a jet plane without the use of wheel brakes. It is reported that the deviator consists of from eight to ten small jet nozzles mounted in a circle in the engine nacelle. A mechanical device deflects a portion of the engine exhaust gases to these nozzles which turns the gases forward. So far the deviator has only been tested on a Vampire.

✦ ✦ ✦

TOP officials of the British deHavilland Engine Company, Ltd., recently inspected the General Electric Company's jet-engine manufacturing facilities at Evendale, Ohio, in conjunction with a "full interchange" of aircraft engine experience and knowledge agreement between the two companies. The agreement between deHavilland and the General Electric Company provides for an exchange of both current and future information in the aircraft gas-turbine field with the exception of aircraft nuclear propulsion. The deHavilland Company has developed such engines as the Goblin, in the 3000–3500 lb of thrust category, and the Ghost, rated at 5000 lb, which powers the jet-propelled transport, the Comet.

Jet Assisted Take-Off

IT IS reported that the Flying Tiger Air Line is seeking C.A.A. approval to install Marboré II turbojets on all of its C-46 aircraft. Flying Tigers carried out the first American tests of the engine as a standby unit to provide extra thrust on take-off and to serve as an emergency power plant in the event of failure of one of the regular engines. It is produced in the United States by Continental Aviation and Engineering Corporation, under license from the developers, Société Turbomeca of Bordes, France.

The engine, 82 in. long and 25 in. in diam, is mounted under the fuselage between the wheels in a streamlined fairing. It delivers 880-lb thrust at sea level, and at 5000 ft it provides the C-46 with a 100 per cent power increase for climb. The engine uses the same fuel as the regular piston engine.

Surface Cooling at High Speeds

A STUDY of the air-resistance heating effect encountered by supersonic aircraft and missiles has been under way for some time at the NACA Ames Aeronautical Laboratory. Major contributions to the knowledge of aerodynamic heating are expected from tests of the Bell X-2 stainless-steel supersonic aircraft. The tests of the X-2 will provide a check on the theoretical and scale model work.

Aerodynamic heating, directly related to the boundary layer surrounding the aircraft, increases with speed. It has been estimated that this boundary layer may reach a temperature of 500 F for a plane flying 2000 mph at altitude, and 1200 F at 3300 mph. The boundary-layer friction may also account for approximately one half of the aircraft's drag at Mach 3. During a flight of short duration, the heat generated may not have time to penetrate beyond the surface skin of the aircraft or missile. The German V-2 is an example of high-speed short-duration flight. Aircraft designed for prolonged high-speed flight will need some type of cooling. Water cooling may be practicable in some cases. The water can be evaporated at the hot skin of the missile or aircraft and vented overboard.

It has recently been discovered that the regions of laminar flow in the boundary layer can be increased by cooling. Laminar flow reduces both skin friction and aerodynamic heating. Experimental work at Ames is directed toward extending the regions or areas of laminar flow at supersonic speeds. The amount of cooling required for laminar flow is of critical importance. At the present time, both the skin friction and the heat transfer rates have been investigated by the NACA at speeds up to Mach 3 for both laminar and turbulent flows.

FIG. 4 INSTALLATION OF G. E. TAIL CONE THERMOCOUPLES

Thermocouple Controls

A VITAL component of automatic electronic controls for F-86D jet interceptor planes is being manufactured by the General Electric Company's Meter and Instrument Department. Thermocouples, mounted in the tail cone of the J47-GE-17 jet engine, transmit temperature changes to the electronic control. The control system automatically regulates fuel flow to provide optimum performance of the jet power plant under all flight conditions.

Sustained accurate measurement of the jet-engine exhaust gas temperature previously had been prevented by mechanical difficulties caused by the terrific buffeting of the gases which often approached the speed of sound. This problem was overcome by G-E engineers after five years of research and testing. The new thermocouple responds rapidly to temperature changes, is highly accurate, and retains its characteristics in spite of severe operating conditions. The couples (Fig. 4) operate over a temperature range, 1000 to 1900 F.

New Facilities

PURDUE University has begun construction of the University-financed Jet Propulsion Laboratory No. 2. The Laboratory, when completed, will contain three rocket-motor research cells and control rooms, a classroom, drafting room, instrument laboratory, and a hydraulic laboratory. In addition, the new building will house the administrative offices of the jet propulsion personnel, and a technical library. A wing, to be added to the building in the future, will house air-burning jet propulsion engine laboratories.

At present, jet propulsion research at Purdue is being conducted in Rocket Laboratory No. 1 (housing four rocket-

motor test cells, control rooms, and a machine shop) and in the Gas Turbine Laboratory. The research projects are being sponsored by ONR, Squid, and USAF.

✦ ✦ ✦

REACTION Motors, Inc., in co-operation with the Navy Department, announced that it is undertaking a $3,500,000 to $4,000,000 construction program to provide new engineering, research, laboratory, and administrative facilities. The new facilities, which will include a 60,000-sq ft machine shop, will be financed in part by the Company and in part by a government facilities contract.

Reaction Motors' new construction program continues a story of rapid growth and achievement for this rocket concern. RMI, the oldest rocket company in the United States, last year celebrated its tenth anniversary. RMI rocket engine applications include the famous Air Force (Bell) X-1, first supersonic airplane; the Navy (Douglas) D-558-II Skyrocket, present world speed (1238 mph) and altitude (79,494 ft) record holder for piloted aircraft; the Air Force (Republic) XF-91, turbojet and rocket-powered interceptor airplane which is the first combat-ready aircraft to travel at supersonic speeds; the Navy (Fairchild) Lark subsonic missile; and the Navy (Martin) Viking high-altitude sounding rocket, present world speed (4100 mph) and altitude (136 miles) record holder for single-stage missiles.

Mr. Charles W. Newhall, Jr., executive vice-president of the Company, stated that plans for Reaction Motors' new facilities call for work to be started this year with a completion date some time in late 1953. The new plant will be in the Rockaway-Lake Denmark vicinity. It will provide complete, modern buildings, laboratories, and equipment for all phases of the development and fabrication of rocket engines and related components, and for a variety of other aircraft and guided missile auxiliaries. In addition to Reaction Motors' new facilities, substantial additions and improvements are being made to the present test facilities leased and operated by the Company at the Naval Air Rocket Test Station, Lake Denmark, Dover, N. J.

✦ ✦ ✦

IN A new fuel test laboratory just completed at Northrop, engineers can stand on the ground and observe fuel mechanisms of jet aircraft operating under conditions that in flight would whisk them in a matter of minutes from searing desert sea-level temperatures to the thin, cold atmosphere found at 80,000 ft. Northrop built the fuel test facility because, in the current era of high-speed aircraft and guided missiles, it is easier and more economical to "bring" the weather into the laboratory than it is for engineers to take their elaborate testing equipment to high altitude.

Housing several full-scale fuel system mockups, including one of the U. S. Air Force's "grand slam" Scorpion F-89D rocket-armed all-weather interceptor, this facility provides reproduction of atmospheric conditions at any altitude up to 80,000 ft above sea level within temperatures ranging from −85 degrees to +170 degrees.

✦ ✦ ✦ ✦

TESTING equipment ten miles up in the sky without ever leaving the ground is now possible in this new turbopump altitude test chamber at General Electric's Aircraft Gas Turbine Division facilities here. This chamber is one of the many testing facilities used to test equipment under the severest conditions which could be encountered in actual flight. Simulated altitudes over 60,000 ft can be obtained, as well as simulated aircraft climb rates in excess of 20,000 fpm and climb rate angles as high as 60 degrees. Used primarily for testing reheat (afterburner) fuel pumps for jet engines under varied conditions and altitudes, this chamber has a volume of approximately 950 cu ft and can accommodate a 470-gal capacity fuel tank. Engineers can observe pump operation under all conditions of altitude by watching through observation ports provided in the sides of the chamber. The entire end of the chamber can be removed to permit the installation of larger equipment to be tested under altitude conconditions.

✦ ✦ ✦ ✦

A NEW altitude test chamber—largest in the United States, and probably largest in the world—has recently been completed at the McDonnell Aircraft Corporation in St. Louis, Mo. This addition to the company's expanding engineering facilities in the physical laboratory is designed to simulate altitudes up to 70,000 ft and has a temperature range of −100 F to +165 F. Relative humidity can be controlled from 15 per cent to 95 per cent at dew point temperatures above 35 F. The unit will provide McDonnell engineers with the exact answers to many of the functional problems faced when aircraft equipment is operated under conditions of extreme heat, cold, altitude, or humidity. Despite the initial cost of the installation, considerable saving may be effected by "de-bugging" all equipment well ahead of the actual flight-test program.

✦ ✦ ✦ ✦

THE world's two most powerful motors and two smaller "giants" to drive the world's largest rotating machine are nearing completion at the East Pittsburgh plant of the Westinghouse Electric Corporation. The four motors—two rated at 83,000 hp each, and the smaller pair rated at 25,000 hp each—will be installed tandem fashion in a rotating machine almost two-football-fields long to be used in new wind tunnels of the U. S. Air Force.

In addition to the 216,000-hp four-motor drive, the gargantuan rotating machine will have five tremendous compressors, which are under construction at the Westinghouse plant in Sunnyvale, Calif. The entire unit is slated for installation in transonic and supersonic wind tunnels being built at the Arnold Engineering Development Center in Tullahoma, Tenn. The Center is under the command and supervision of the Air Research and Development Command, responsible for the over-all U. S. Air Force research and development program.

Prior to this order from the Air Force, the most powerful motors were those built for the Grand Coulee Dam by Westinghouse and rated at 65,000 hp each. The 83,000-hp giants each will stand $21\frac{1}{2}$ ft high and weigh 225 tons. Their 122-ton rotors will spin at the dizzy rate of 600 rpm. Some 31 miles of copper wire are used in their windings. From end to end it will measure about 500 ft, and the four-motor drive alone will weigh more than 1000 tons.

✦ ✦ ✦ ✦

The Aluminum Company of America has been awarded a contract to install a 20,000-ton extrusion press under a lease agreement with the Air Force. The 20,000-ton press will be installed in the Alcoa Lafayette, Ind., plant where a 14,000-ton press is currently being installed. These presses will be used to extrude ribbed shapes for aircraft wing sections. The internal strains will be relieved and the shapes will be straightened by a 3,000,000-lb stretcher capable of straightening shapes having a cross section of 60 sq in. The larger press will be capable of extruding shapes weighing $2\frac{1}{4}$ tons.

Theodore Von Kármán to Lecture at Princeton

The Department of Aeronautical Engineering of Princeton University announces that Professor Theodore von Kármán, world-famous aerodynamicist, is scheduled to deliver three guest lectures on the subject, "Aerothermodynamics and Combustion Theory," on Tuesday, Wednesday, and Friday, March 24, 25, and 27, 1953, at 8:00 p.m., in Frick Auditorium. The Daniel and Florence Guggenheim Jet Propulsion Center at Princeton is sponsoring the lectures. A general invitation to attend has been extended to those outside of Princeton University who are interested in scientific aspects of combustion phenomena.

American Rocket Society News

H. K. WILGUS, *Associate Editor*

Final Report of the Ad Hoc Space Flight Committee of the American Rocket Society

THIS Committee was authorized and constituted by the ARS Board of Directors at the meeting of February 4, 1952. The basic task of the Committee was briefly outlined in the Minutes of the meeting as follows:

"The Ad Hoc Space Flight Committee is to investigate and recommend to the Board the ways in which the American Rocket Society can best serve its members and fulfill the aims outlined in its By-Laws for activity in the field of space flight, satellite space stations, astronautics, etc., and to define the extent to which the American Rocket Society should become active in these fields."

A better understanding of the Committee's comments and recommendations requires a brief restatement of certain background information.

Our Society, as originally incorporated in April 1931, under the name of the "American Interplanetary Society," was empowered to engage in the following activities:

"The promotion of interest in and experimentation toward interplanetary expeditions and travel; the mutual enlightenment of its members in matters bearing on the astronautical, physical and other problems pertinent to man's ultimate conquest of space; the stimulation by expenditure of funds and otherwise of American scientists toward a solution of the problems which at present bar the way toward travel among the planets; the raising of funds for research and experimentation; and such other activities as the Society may from time to time deem necessary or valuable in connection with the general aim of hastening the day when interplanetary travel shall become a reality."

In 1934 the present name of the Society was adopted, and in 1947 the charter powers were changed to read as follows:

"The purpose of the Society shall be to aid and encourage by all suitable means the development and application of the principle of jet propulsion as applied to rockets, aircraft, water and underwater craft and to all other appropriate and practical devices; to aid and encourage the development of the sciences and engineering techniques pertaining thereto, and to create increasingly wide interest in the field of jet propulsion and rocketry among both technicians and laymen, to the end that jet propulsion in all its various forms shall rapidly and permanently be developed for the ultimate good of man; the preparation, collection, correlation and dissemination, by publication or otherwise, of facts, information, articles, books, pamphlets and other literature pertaining to jet propulsion, rocketry and subjects relating thereto; the establishment of a library containing such literature for the information of members, scientists and others to whom the privileges of such library may be granted by the Society; the collaboration or affiliation with other organizations, whether technical or otherwise, in any manner, and to any extent which, in the judgment of the Society or of the Board of Directors, will best aid in accomplishing its objectives; the raising of funds for research and experimentation, and such other activities as the Society or the Board of Directors may from time to time deem necessary or desirable in connection with the foregoing."

Throughout its deliberations the Committee has borne in mind the basic purposes and powers of the Society.

The great interest in the subject of space flight, which undoubtedly motivated the creation of the Society, was necessarily subordinated to the practical problems on hand attending the preparation for World War II, the conduct of the war, and the post war developments in a world still filled with turmoil. A real interest in the subject of space flight, however, has always persisted among many members of the Society. This interest has gained momentum during the past three years, and has been demonstrated by the attendance of Society delegates at the International Astronautical Congresses held in London (1951) and Stuttgart (1952); the adherence of the Society to the International Astronautical Federation; the direct expressions of many members of the Society, such as the remarks of Commander R. C. Truax during the 1951 Honor's Night Dinner, and so on. The Committee was constituted on a special and temporary basis, as a result of this interest.

The work of the Committee was initiated by each member submitting proposed agendas for study and discussion. The agendas were then disseminated on a random basis to a third of the membership of the Society for comment and viewpoints. The replies evidenced uniform interest in the subject of space flight among the membership of the Society.

A formal meeting of the Committee was held in Washington, D. C., on May 17, 1952, and the proceedings were recorded verbatim. Many informal meetings were held by groups of Committee members, and numerous consultations were held with leading scientists. A second formal meeting was held in Washington, D. C., on November 21, 1952. A third and final formal meeting was held at noon on Thursday, December 4, 1952, to consider comments of the Society membership on this report.

FINDINGS

With respect to technical and other substantive matters, the Committee finds as follows:

(a) Space flight is a basic challenge to the progress of mankind and its achievement will ultimately prove to be worth the cost and effort required; but it is not possible to spell out in hard economic terms at the present time the extent of the physical and social returns that will flow from the conquest of space. We have insufficient information at the present time on which to base considered judgment concerning the utility or feasibility of various widely publicized proposals advocating space ships as military weapons, as reconnaissance or bombing platforms, as missile guidance adjuncts, as television relays, as weather observation stations, for basic physical experiments, or for astrophysical observations.

(b) Successful flight from the earth and return of satellite, lunar, and interplanetary space ships will some day be technically feasible. Judgment is withheld on the technological feasibility of establishing large, inhabited, satellite stations. No opinion is offered as to the date when successful space flight might be achieved. The rate of progress will be determined to a great extent by the amount and quality of effort that is focused on the project, and perhaps to an even larger degree by unforeseen fundamental problems that may arise as the program proceeds. It is believed, however, that space flight of inhabited vehicles may be achieved during this century if mankind is in a position diligently to undertake the task.

(c) The development of a rocket-propelled space ship requires the successful solution of many basic problems involved in the development of long-range guided missiles. In this respect, a space flight program cannot be divorced from the current military program for guided missiles. A space flight project, if initiated under present world conditions, would require the efforts of many of the very engineers and scientists now engaged in the development of guided missiles, and consequently must be carefully evaluated in that light.

(d) For the purpose of building up experience and knowledge in an orderly fashion, the following projects should be emphasized and supported, in the sequence indicated: High-altitude sounding rockets for scientific purposes; ground-to-ground unmanned guided vehicles; orbital (satellite) unmanned vehicles; manned satellite vehicles; manned, returnable, lunar, or interplanetary vehicles. The development of manned, long-range, ground-to-ground vehicles similar to present rocket-propelled aircraft is not considered a prerequisite for achieving interplanetary flight, although data obtained from such projects could serve as a useful adjunct to the technology of guided rocket vehicles. The development of a one-way rocket to the moon is considered a waste of effort, although interesting from a publicity and educational standpoint. Encouragement and support should be given to a high-

altitude rocket research program, such as that carried out by the Army, Navy, and Air Force, and co-ordinated by the Upper Atmosphere Research Panel.

(e) Key factors in the achievement of space flight are recognized as money, competent personnel, a recognized long-range program, and continued public enthusiasm and support. Key problems, as understood today, in the establishment of an unmanned satellite or space vehicle are (not in order of importance): Reliability of a vehicle's mechanical and electronic systems, radiation hazards, aerodynamic heating upon re-entry into the earth's atmosphere, automatic solution of navigation problems, effects of prolonged weightlessness upon humans, recovery of spent stages, communications, telemetering, and minimum weight designs of all components.

RECOMMENDATIONS

With regard to the position of the Society and measures that it might take to promote the early achievement of space flight, the Committee recommends the following:

(a) The Society should on appropriate occasions take a public stand in favor of realistic research and development looking toward the achievement of space flight. This stand should be based upon the set of beliefs outlined in the findings above. It should refrain from lending support to sensational projects motivated by a desire for publicity or private gain.

(b) The Society should implement its stand by:

Encouraging the presentation of high quality technical papers on space flight at National and Sectional meetings of the Society.

Publication of contributed technical articles on all aspects of space flight in the JOURNAL.

Encouraging scientific and technical effort on space flight problems on the part of any group competent to perform such work.

Co-operating with other nonprofit organizations having sound programs along the lines indicated in the Findings above.

Advocating the expenditure of government funds, if no adequate private financing is available, to support work on the problems of space flight, to the extent that such effort is compatible with national security.

Bringing such matters to the attention of the public through various media in a manner calculated to promote sound public thinking on the subject.

Fostering international co-operation and exchange of ideas on the subject of space flight through the medium of the International Astronautical Federation, United Nations Educational, Scientific and Cultural Organization, and International Council of Scientific Unions.

Maintaining a continuous program of co-operation with existing foreign rocket societies and encouragement of formation of such societies in countries where they do not at present exist.

Establishing a permanent Society space-flight committee which will meet at regular intervals for the purpose of recommending to the National Board of Directors methods of implementing the aforesaid objectives effectively.

(c) The Society should point out the need for a realistic survey of the technical problems standing in the way of space flight. The support of appropriate governmental agencies should be solicited in order to consider the extent of these problems. A survey of this kind may serve to stimulate research in the required directions. At this stage of man's knowledge the Committee believes that a study program of all phases of space flight, supported by the government, possibly by the National Science Foundation, would provide a sound basis for a vehicle construction program in the least possible time. Such a study would tend to "clear the air" of some of the sensational concepts engendered by unprincipled or uninformed fiction writers. Further, such a study would elicit support of competent professional engineers and scientists who at present are fearful of supporting projects which are incompletely thought out. At the same time, recognition of excellent work by United States and foreign experts would inspire even greater efforts.

(d) The Society should not presume to conduct practical research or development under its own auspices on the subject of space flight, but rather to function as a "catalyst" for such activity on the part of private industry, universities, private research institutions, and governmental agencies.

(e) The Society should refrain from endorsing any specific development proposal in preference to other competitive proposals, but should offer a forum at its meetings and in its JOURNAL for the open discussion of each proposal. For the present, the Society should take the position that to decide upon a specific design is less important than the promotion of broad technical analysis of all the problems involved. Similarly, the Society should not be associated with activities conducted primarily for the purpose of publicity, such as science fiction movies, television or radio shows of a fictional character, and the like, unless such efforts represent a sincere attempt to educate the public. The cost and difficulty inherent in the achievement of space flight must never be underplayed.

(f) The Society should promote the view that, to the extent that world political conditions permit, and with due regard to United States security, the conquest of space should be carried out on an international basis. The Society should reiterate its adherence to the aims of the International Astronautical Federation as a specific step in this direction.

Finally, the Committee is of the view that exploratory space flight as a speculative venture into the unknown should be regarded as the ultimate objective of a reasonable effort on the part of the United States and mankind as a whole. It is a logical function of the Society and its constituted committee to recommend ways of synthesizing existing unconnected activities with the objective of directing such efforts toward a unified space flight program.

Respectfully submitted: Andrew G. Haley, *Chairman;* F. C. Durant, III, R. W. Porter, Milton W. Rosen, Kurt R. Stehling, Franki van der Wal, John R. Youngquist. November 25, 1952.

Separate Report by R. W. Porter

While generally in agreement with the other members of the Committee on the foregoing report of November 25, I would like to see the conclusions more specifically worded. For example, I believe that the following statement of policy should be adopted by the Society: "The American Rocket Society recommends that exploratory space flight as a speculative venture into the unknown should be regarded as the ultimate objective of a reasonable effort on the part of the United States of America. It further recommends that actual design or construction of satellite or space vehicles should not be undertaken until the present war emergency is resolved, and that such work should be regarded as one of several large projects into which our national effort could be directed when no longer urgently needed for military work."

In furtherance of the above policy, the following should be adopted as specific objectives of the Society.

a To seek and publish articles of sound scientific content on the subject of satellite and space flight.

b To encourage discussion of satellite and space flight in Section and National meetings of the Society.

c To foster international co-operation and exchange of ideas on the subject of space flight through the medium of the IAF and UNESCO.

d To carry on a continuing campaign of encouragement and support for the high-altitude rocket research program being carried out by the Army, Navy, and Air Force, co-ordinated by the Upper Atmosphere Research Panel. In particular, to interest this Panel in problems related to space flight.

e To urge the National Science Foundation to give serious consideration at this time to the possibility of establishing within its organization the initial phase of a long-range space-flight project, and if successful, to assist the Foundation in obtaining financial support by all means at the Society's disposal.

f To establish a permanent space-flight committee which will meet at regular intervals for the purpose of implementing the above objectives effectively.

The Society should not sponsor any individual projects except as indicated above, nor should it seek association at this time with activities conducted primarily for the purpose of publicity, such as science fiction movies, TV or radio shows of a fictional character, and the like.

Admiral Bolster Addresses Joint Meeting at Northeastern New York Section

ON JANUARY 13, 1953, a meeting sponsored jointly by the ARS Northeastern New York Section and the Schenectady Chapter of the ASME, was held at Union College, Schenectady, N. Y. Over 200 persons attended to hear the guest speaker, Admiral Calvin M. Bolster, Chief of Naval Research.

Admiral Bolster, in discussing "Aspects of Current Rocket Research," described

AT THE JOINT MEETING OF ARS NORTHEASTERN NEW YORK SECTION AND ASME SCHENECTADY CHAPTER, JANUARY 13, 1953

Left to right: Commdr. F. W. Kinsley, USN, Office of Inspector of Naval Machinery, Schenectady, N. Y.; K. Berman, vice-president, ARS Northeastern New York Section; G. M. Ketchum, chairman, ASME Schenectady Chapter; R. W. Porter, ARS National Board of Directors; Admiral Calvin M. Bolster, Chief of Naval Research, who was guest speaker; and F. M. Cooper, president, Northeastern New York Section.

the workings of the Bureau of Naval Research, and recounted the latest developments in jet-assisted take-offs. His talk was illustrated with films of experiments with jet-assisted aircraft, and concluded with movies of a recent Viking firing.

Admiral Bolster, an active member of the ARS as well as of the Institute of the Aeronautical Sciences, is a noted aviator in both heavier and lighter-than-air craft. In 1947 he was chosen to the post of Deputy Chief of Naval Research, and was made Chief in 1951.

Joint ARS-IAS Rocket Propulsion Session

THE American Rocket Society, in cooperation with the Institute of the Aeronautical Sciences, held a technical session on rocket propulsion on the opening day of the IAS Annual Meeting, January 26–29, 1953, at the Hotel Astor, New York, N. Y. Mr. F. C. Durant, III, president of the American Rocket Society, served as chairman of the session, which was attended by more than 130 persons. Three technical papers constituted the program.

The first paper, "The Effect of Fluid Properties on the Spray Formed by Two Impinging Jets," by R. J. Priem and M. F. Heidmann, both of NACA Lewis Flight Propulsion Laboratory, was presented by Mr. Priem. The paper described the four different spray shapes which were obtained using glycerol-water mixtures and hydrocarbon oils, and the conditions under which these sprays were formed, together with their apparent properties. A hypothesis was offered on the connection between spray fluctuations and combustion instability in rocket motors. Excellent high-speed photographs of the spray patterns accompanied the talk.

The second paper, "Earth Scanning Techniques for Orbital Rocket Vehicles," by Kurt R. Stehling of Bell Aircraft Corporation, examined two possible methods of utilizing an earth satellite vehicle to gather and transmit information about the earth's surface. One of these methods utilized an optical objective lens image-converter system; the other, a microwave scanner. Assumed were a vehicle flight altitude of 500 miles, orbital velocity of 5 miles per sec, a hypothetical target of 600-yd diam, and restricted design requirements of a minimum weight satellite vehicle payload.

It was shown that the net receiving power of the optical-video system is limited by the image converter and available transmission band width, and not by the optical train. Effects of the atmosphere, meteorological conditions, and albedo were also discussed. The approximate resolving power, weight, and power and space requirements of a microwave radar scanning unit were outlined, and the advantages and disadvantages of this system were weighed.

Mr. Stehling believed that, with the present state of radar scanning (which can be discussed on an unclassified status), the optical system has the weight and resolving power advantage, but its daylight dependence and atmospheric and cloud attenuation limitations are severe enough to indicate questionable feasility. Furthermore, the low resolving power of a radar unit, from the 500-mile altitude, and the attenuation losses tend to limit the system's usefulness.

The final paper, "Measurements in Rocket Engine Testing," was presented by Howland B. Jones, Jr., of the Potter Aeronautical Company. The paper covered the application of conventional and special instrumentation equipment to the static testing of liquid propellant rocket engines. In his introduction, Mr. Jones discussed peculiarities of this testing field, including accuracy limits and need for transient as well as static measurements. The conventional quantities of pressure, flow, force, temperature, linear and angular displacement, and vibrational acceleration were then treated. Modifications to conventional measuring equipment and specially designed instruments were then described. Of particular interest were the descriptions of a multichannel pressure recording unit operating into a single cathode-ray tube, a combination of a 4-gun cathode-ray oscillograph and tape recorder, and the use of a conventional sonic analyzer with associated equipment.

Washington-Baltimore Section Hears Rosen

MORE than 150 members and guests attended the Washington-Baltimore Section meeting on February 4, 1953, held at the Enoch Pratt Library, Baltimore, Md. Mr. Milton W. Rosen, Viking Project Chief, Naval Research Laboratory, was the guest speaker.

Mr. Rosen presented a talk on "High Altitude Sounding Rockets," which was highlighted by the showing of slides. Following his speech, he showed sound movies of the development and firing of the Viking rocket.

In the discussion after his speech, when asked his opinion of recent proposals to develop a satellite vehicle, Mr. Rosen's reply was to the effect that we should crawl before we walk; that there are too many unknown and uninvestigated factors to warrant immediately going overboard with large expenditures.

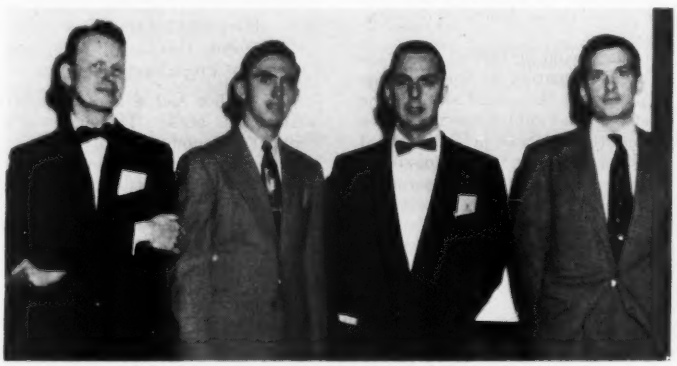

AT THE JOINT ARS-IAS ROCKET PROPULSION SESSION DURING THE IAS ANNUAL MEETING, JANUARY 26, 1953

Left to right: F. C. Durant, III, ARS president, with the three engineers whose papers were presented: R. J. Priem, NACA Lewis Flight Propulsion Laboratory; Kurt R. Stehling, Bell Aircraft Corporation; and Howland B. Jones, Jr., Potter Aeronautical Company.

Technical Literature Digest

H. S. SEIFERT, California Institute of Technology, *Associate Editor*

CONTRIBUTORS: D. Altman, D. I. Baker, R. B. Canright, F. C. Gunther, H. S. Seifert, F. H. Wright

Book Reviews

DEVELOPMENT OF THE GUIDED MISSILE, by K. W. Gatland, Philosophical Library, Inc., New York, N. Y., 1952, 133 pp. $3.75.

Reviewed by G. P. SUTTON
North American Aviation, Inc.

This book is a major revision of a series of articles published in the British magazine *Flight* in 1951. It contains separate chapters on antiaircraft (or antimissile) missiles, on air-to-air missiles, on supersonic rocket flight, on high-altitude research rockets, on satellite and space vehicles, and on interplanetary flight. The book gives a good discussion of many of the technical features necessary for these specialized applications of rocket power and as such is helpful to acquaint the reader with typical technical and developmental problems and in outline form also with existing or contemplated solutions. For this purpose this book is recommended.

Most of the examples used by the author to illustrate the various missile types and their technical features are taken from German World War II practice. Data and information on U. S. guided missiles are next most prominent, but there is relatively little additional mention of British missiles and other rocket devices.

The very fact that the author has not been able to secure much information on British rockets and missiles (a fact about which he seems to be unhappy) is a tribute to the British security system. In sharp contrast, it is amazing to this reviewer how much information the author has been able to obtain on American developments.

The reader should be careful not to interpret the information of this book as being a picture of the actual state of the art of rocketry and guided missiles in the various countries. Some of the detailed technical information on various missiles is not correct, and the emphasis given to specific missiles is not properly weighted. Some of the missiles which are treated in considerable detail in this book are relatively unimportant test missiles or merely missile studies, whereas others, which are mentioned only in passing, are important tactical weapons.

The last two chapters on space and satellite rockets and interplanetary flight differ in tenor from the rest of the book because they deal not with existing pieces of equipment but only with proposed plans and future thinking.

COMETS AND METEOR STREAMS, by J. G. Porter, John Wiley & Sons, Inc., New York, N. Y., 1952, 123 pp. $5.25.

Reviewed by S. B. NICHOLSON
California Institute of Technology

In this delightful little book, Dr. Porter tells about the celestial mechanics of bodies moving in the solar system subject to the gravitational pull of the sun and the planets. The problems of comets and meteor swarms are specifically discussed, but the general laws of motion are first developed. The presentation is simple and direct, technical enough to be rigidly correct but readable even for those who lack the mathematics to follow all the formulas. Although most of the developments follow the classical lines, some original departures and extensions are found.

Those who expect a book in the International Astrophysics Series to deal mainly with the spectra of comets may be surprised to find only one page of the 123 devoted to that subject. In addition to the orbital problems, the statistics of comets and meteors are discussed in detail. These statistics have direct application to the theories of the origin of comets and of their place in the solar system.

BALLISTICS IN THE SEVENTEENTH CENTURY, by A. R. Hall, Cambridge Univ. Press, N. Y., 1952, 186 pp. $4.

Reviewed by H. J. STEWART
California Institute of Technology
Jet Propulsion Laboratory

The author had a twofold purpose in writing this book. The first was to describe the foundations of the science of exterior ballistics, and the second was to relate the development of this science to the state of technological development, of practical military science, and of the governmental organization with respect to research and development existing during the 17th century. In particular he investigated the suggestion that exterior ballistics was the first applied science whose development was stimulated by military requirements and whose results were applied in increasing the effectiveness of artillery.

The author first presents the background of the relations between government and industry and of the techniques of manufacturing heavy ordnance. He then describes the practical aspects of the art of gunnery in the 17th century. The principal portions of the book trace the development of the science of mechanics with particular emphasis on ballistics from the Aristotleian period, through the "impetus" theories, through the Galilean period, and to the Newtonian period during which the theory of ballistics was placed on a basis very close to the currently accepted theory. The conclusions are reached that it is inappropriate to consider the classical development of ballistics as an example of applied science, that the scientific interest in ballistics was motivated primarily by the fact that the motion of a body through the air was one of the classical problems treated by Aristotle and was thus the most suitable test of any new theory, and that, even when the theory was placed on a firm foundation, the state of technological development was too primitive to permit effective applications. The idea that the theory should be useful was widespread but, in the 17th century, premature.

This book should be of general interest to any engineer or scientist and of particular interest to students of the history of science and to anyone concerned with the problems of military research and development.

ENGINEERING MATERIALS, THEIR MECHANICAL PROPERTIES AND APPLICATIONS, by J. Marin, Prentice-Hall, Inc., New York, N. Y., 1952, 491 pp. $8.70.

Reviewed by C. E. LEVOE
California Institute of Technology
Jet Propulsion Laboratory

The stated objective of the book is to provide the student with sufficient knowledge of the behavior of stressed engineering materials to permit their intelligent selection and use. The book is divided into three parts: Part one deals with mechanical properties, their definition, determination, and utilization. Part two is a brief treatment of certain important materials, emphasizing specific mechanical

EDITOR'S NOTE: This collection of references is not intended to be comprehensive, but is rather a selection of the most significant and stimulating papers which have come to the attention of the contributors. The readers will understand that a considerable body of literature is unavailable because of security restrictions. We invite contributions to this department of references which have not come to our attention, as well as comment on how the department may better serve its function of providing leads to the jet propulsion applications of many diverse fields of knowledge.

properties and the factors influencing these properties. Part three presents a description of materials-testing machines and strain gages.

The first part of the book, which is intended as an undergraduate text, deals with general mechanical properties and contains most of the basic information required for an understanding of the strength of materials. It treats several phases of the subject not ordinarily covered in a text of this type. For example, static properties under combined stress, fatigue properties, impact properties, and creep and temperature properties are thoroughly covered.

The section of the book covering specific properties of materials attempts to cover too broad a subject in a few short chapters to give really adequate information for selection and use of materials. It is probable that, by listing only typical or average mechanical properties of a few materials, certain misconceptions may arise. An example of a possible misconception may be cited. On page 47 of the book are listed strength-weight ratios of four materials: an aluminum alloy, a magnesium alloy, a steel alloy, and a glass laminated plastic. The strength-weight ratios for these materials as listed in the text show the aluminum alloy test (double that of the steel alloy), the magnesium alloy second, the laminated plastic third, and the steel a poor fourth. The design stresses selected for these materials are, however, inconsistent. Actually, if one inquires deeply enough into the strength of materials, it will be found that the strength-weight ratio is a function of the state of development of the group of materials. Compare, for example, a commonly used steel alloy SAE 4130 heat-treated to 200,000 ultimate tensile strength aluminum alloy 75S heat-treated to 77,000 UTS, and magnesium alloy AZ80A heat-treated to 47,000 UTS. The strength-weight ratio for each of the materials is $200{,}000/0.284 = 7.05 \times 10^5$, $77{,}000/0.101 = 7.62 \times 10^5$, and $47{,}000/0.065 = 7.24 \times 10^5$, respectively, in units of lb per in.^{2} divided by lb per in.^{3}. From this it is seen that the strength-weight ratio of most commonly used, high-strength materials is essentially the same. More often than not, other factors than strength-weight ratio govern selection of materials.

In general, it is considered that Part two of the book treats the subject in a manner not ideally suited for engineering design use. It would seem preferable to introduce the student to the need for certain information and then to supply tables of basic data rather than a few typical examples.

The bulk of Part one of the book can be recommended to rocket engineers. The remainder, although understandably written and containing much information, seems rather sketchy to be of use for design purposes.

Books

Proceedings of the London Conference on Heat Transfer, Institution of Mechanical Engineers and American Society of Mechanical Engineers, 1952, 496 pp. £2 5*s*.

Instrument Engineering, by C. S. Draper et al., McGraw-Hill Book Co., Inc., N. Y., 1952, 269 pp. $6.

The Design and Analysis of Experiments, by O. Kempthorne, John Wiley & Sons, Inc., N. Y., 1952, 631 pp. $8.50.

Numerical Mathematical Analysis, by J. B. Scarborough, Johns Hopkins Press, Baltimore, 1950, 511 pp. $6.

Rocket Engines

Tip-Pod Rockets for F-89D Confirmed, unsigned, *Western Aviation*, vol. 32, Sept. 1952, pp. 12–13.

Bell X-5; Variable Wing Sweep, unsigned, *Intervias*, vol. VII, no. 8, 1952, p. 446.

Rockets Push XF-91 Past Mach 1, unsigned, *Aviation Week*, vol. 57, Dec. 15, 1952, p. 17.

NACA's Rockets Gather Data for Missile Design, by J. A. Shortal, *SAE J.*, vol. 60, Nov. 1952, pp. 17–19.

Russians Push Rocket Fighter Program, unsigned, *Amer. Aviation*, vol. 15, Nov. 10, 1952, pp. 2–4.

Snarler Boosts the Jets, unsigned, *Aviation Age*, vol. 17, Nov. 1952, p. 44.

Jet Assisted Take-Off, by T. von Karman, *Interavia*, vol. VII, no. 7, 1952, pp. 376–379.

Jet Propulsion Engines

The Turbojet, Ram-Jet and Rocket Air Force of the Future, by N. Macmillan, *Aeronautics*, vol. 27, Aug. 1952, pp. 24–31.

Tests on a Working Model Ram Jet in a Supersonic Wind Tunnel, by J. R. Singham, F. W. Pruden, and R. C. Tomlinson, *Gt. Brit. Aero. Res. Counc.*, Reports and Memoranda 2568, 1951 (Nov. 1947); Brit. Info. Serv., N. Y., 16 pp., illus.

Ramjet Favored for Mach 2–4 Range, unsigned, *Aviation Week*, vol. 57, Dec. 15, 1952, pp. 21–28.

A Theoretical and Experimental Investigation of the Feasibility of the Intermittent Ram-Jet Engine, by A. Kahane et al., USN-Squid/TR-35, Princeton, Aug. 1, 1952.

Pulse-Jet Engine Has 200-Hour Operating Life, unsigned, *Mach. Design*, vol. 24, Oct. 1952, pp. 250–253.

Can Pulsejets Simplify Army Logistics, by W. Coughlin, *Aviation Week*, Oct. 13, 1952, pp. 21–28.

The Shock Ignition Engine, by F. F. Rand, Jr., *Aero. Engng. Rev.*, Oct. 1952, pp. 22–27, 62.

Afterburners and Variable Nozzles, by R. Kress, *Aeroplane*, vol. 82, Nov. 14, 1952, pp. 665–666.

Military Role for Ram-Jet Hiller, unsigned, *Flight*, vol. 37, Sept. 1952, p. 19.

Principles and Application of Jet Power to Aircraft, by I. B. Lakowitz, *Amer. Helicopter*, vol. 24, Oct. 1952, pp. 6–7.

Simulation and Linearized Dynamics of Gas Turbine Engines, by J. R. Ketchum and R. T. Craig, Nov. 1952, NACA TN 2826.

Protecting Aprons from Jet-Blast, unsigned, *Flight*, vol. 61, Oct. 3, 1952, p. 446.

Heat Transfer and Fluid Flow

A Comparative Study of Momentum Transfer, Heat Transfer, and Vapor Transfer. Part III. Free Convection, by C. S. Yih, Colorado A & M College, Report No. 3, Feb. 1951, 32 pp.

Heat-Transfer and Flow-Friction Characteristics of Some Compact Heat-Exchanger Surfaces. III, by A. L. London, W. M. Kays, and D. W. Johnson, *Trans. ASME*, vol. 74, Nov. 1952, pp. 1167–1178.

An Experimental Investigation of Convective Heat Transfer to Air from a Flat Plate with a Stepwise Discontinuous Surface Temperature, by S. Scesa and F. M. Sauer, *Trans. ASME*, vol. 74, Nov. 1952, pp. 1251–1255.

Convective Heat-Transfer and Flow-Friction Behavior of Small Cylindrical Tubes: Circular and Rectangular Cross Sections, by W. M. Kays and A. L. London, *Trans. ASME*, vol. 74, Nov. 1952, pp. 1179–1189.

Additional Measurements of Heat Conductivity of Nitrogen, Carbon Dioxide, and Mixtures, by F. G. Keys, *Trans. ASME*, vol. 74, Nov. 1952, pp. 1303–1306.

Design of Apparatus for Determining Heat Transfer and Frictional Pressure Drop of Nitric Acid Flowing Through a Heated Tube, by B. A. Reese and R. W. Graham, NACA RM 52D03, June 16, 1952, 18 refs., illus., 61 pp.

An Experiment on Nozzle Flow, by V. D. Naylor, *Aircraft Engng.*, vol. 24, Nov. 1952, pp. 344–347.

Convection Heat Transfer Coefficients in de Laval Nozzles, by S. J. Kline, Stanford Univ. ONR Contract N6-onr-251 T/O VI. TR HS-2, 1950.

Heat Transfer in a Nozzle at Supersonic Speeds, by O. A. Saunders, *Engineering*, vol. 173, Aug. 29, 1952, pp. 281–284.

On the Theory of the Ranque-Hilsch Cooling Effect, by J. J. van Deemter, *Appl. sci. Res.* (A), vol. 3, 1952, pp. 174–196.

On the Temperature Distribution Along a Semi-Infinite Sweat-Cooled Plate, by N. Ness, *J. Aero. Sci.*, vol. 19, 1952, pp. 760–768.

On Heat Transfer over a Sweat-Cooled Surface in Laminar Compressible Flow with a Pressure Gradient, by M. Morduchow, *J. Aero. Sci.*, vol. 19, Oct. 1952, pp. 705–712.

The Measurement of Skin Friction in a Turbulent Boundary Layer at a Mach Number of 2–5, Including the Effect of a Shock-Wave, by W. F. Cope, *Proc. Roy. Soc. Lond.* (A), vol. 215, Nov. 6, 1952, pp. 84–99.

A Free-Flight Investigation of the Possibility of High Reynolds Number Supersonic Laminar Boundary Layers, by J. Sternberg, *J. Aero. Sci.*, vol. 19, Nov. 1952, pp. 721–733.

Combustion

Activation Energies and Frequency Factors in the Thermal Decomposition of Paraffin Hydrocarbons, by M. G. Peard, *Proc. Roy. Soc. Lond.* (A), vol. 214, Oct. 9, 1952, p. 471.

Structural Influences in the Oxidation of Aliphatic Amines, by C. F. Cullis, *Trans. Faraday Soc.*, Nov. 1952, p. 1023.

The Oxidation, Decomposition, Ignition, and Detonation of Fuel Vapors and Gases, by R. O. King, *Canad. J. Technol.*, vol. 30, Sept. 1952, pp. 222–257.

The Water Gas Shift Reaction in Fuel Systems. I. The Water Gas Shift on Carbon, by D. G. Ingles, *Trans. Faraday Soc.*, vol. 48, Part 8, Aug. 1952, pp. 706–712.

Pressure Limits of Flame Propagation of Pure Hydrocarbon Air Mixtures at Reduced Pressure, by A. E. Spakowski, NACA RM E52H15, 1952, 35 pp.

Flame Stability of Liquid-Vapor Oxygen Mixture, by J. A. Browning and M. L. Thorpe, Project Squid TM DART-1, Feb. 11, 1952.

The Temperature of the Hydrogen-Fluorine Flame, by R. H. Wilson, Jr., J. B. Conway, A. Engelbrecht, and A. V. Grosse, *J. Amer. Chem. Soc.*, vol. 73, 1951, p. 5514.

On the Stability of Laminar Flame Fronts, by M. Lessen, *J. Aero. Sci.*, vol. 19, Dec. 1952, p. 852.

Combustion Tunnel Laboratory; Second Quarterly Report, by H. W. Emmons, Harvard University, Combustion Tunnel Lab. QR-2, May-Aug. 1952.

Investigation of Chemical Combustion Kinetics; Final Report, by R. A. Jermain, J. A. Pisani, and I. Rosen, Reaction Motors, Inc., Report RMI-442F, Nov. 17, 1952.

Spark Ignition; Effect of Molecular Structure, by H. F. Calcote, C. A. Gregory Jr., C. M. Barnett, and R. B. Gilmer, *Indust. Engng. Chem.*, vol. 44, no. 11, Nov. 1952.

Sur le passage par la vitesse du son au cours de la détente d'un gaz en combustion, by M. Serruys, *Comptes rendus des séances de l'académie des sciences*, vol. 235, no. 21, Nov. 24, 1952, pp. 1280–1281.

On the Solution of the Poisson-Boltzmann Equation with Application to the Theory of Thermal Explosions, by P. L. Chambré, *J. Chem. Phys.*, vol. 20, no. 11, Nov. 1952, pp. 1795–1797.

The Effect of High-Frequency Sound Waves on an Air-Propane Flame, by C. J. Kippenhan and H. O. Croft, *Trans. ASME*, vol. 74, Nov. 1952, pp. 1151–1155.

Study of Laws of Combustion of Colloidal Powders (in French), by H. Muraour and G. Aunis, *Mém. Artill. fr.*, vol. 25, no. 1, 1951, pp. 117–165.

Fuels, Propellants, and Materials

Solution to the Caking Problem of Ammonium Nitrate and Ammonium Nitrate Explosives, by J. Whetstone, *Indust. Engng. Chem.*, vol. 44, Nov. 1952, pp. 2663–2667.

Kinetics of the Transformations of the Polymorphous Modifications of Ammonium Nitrate. II. Effect of the Previous Treatment on the Rate of Transformation $NH_4NO_3IV \rightarrow NH_4NO_3III$, by B. V. Erofeev and N. I. Mitskevich, *Zhur. Fiz. Khim.*, vol. 26, 1952, pp. 848–861.

Behavior of Liquid Hydrocarbons with White Fuming Nitric Acid, by C. H. Trent and M. J. Zucrow, *Indust. Engng. Chem.*, vol. 44, Nov. 1952, pp. 2668–2673.

Determination of the Pore-Size Distribution in Porous Metal Bodies, by P. R. Marshall, *Nature*, vol. 170, Nov. 1952, p. 761.

The Metallurgy of Uranium, by E. W. Colbeck, *Metal Indus.*, vol. 81, Nov. 14, 1952, pp. 387–389.

A Half Century of Aluminum Developments, by J. D. Edwards, *J. Electrochem. Soc.*, vol. 99, Nov. 1952, pp. 298C–300.

New Titanium-Boron Alloy Steel Shows Promise for Jets and Rockets, by J. L. Everhart, *Materials and Methods*, vol. 36, Sept. 1952, pp. 97–98

Titanium; the New Light Metal, unsigned, *Light Metals*, vol. 15, Sept. 1952, pp. 292–293; Oct. 1952, pp. 318–319.

Physical-Chemical Topics

Calculation of Vibrational Relaxation Times in Gases, by R. N. Schwartz, Z. I. Slawsky, and K. F. Hersfeld, *J. Chem. Phys.*, vol. 20, Oct. 1952, pp. 1591–1599.

Ionization Produced in Metallic Salts in Flames. III. Ionic Equilibria in Hydrogen/Air Flames Containing Alkali Metal Salts, by H. Smith and T. M. Sugden, *Proc. Roy. Soc. Lond.* (*A*), vol. 211, 1952, pp. 31–58.

Integrated Absorption for Vibration-Rotation Bands of CO_2, by D. Weber, R. J. Holm, and S. S. Penner, *J. Chem. Phys.*, vol. 20, Nov. 1952, p. 1820.

Emissivity for CO_2 at Elevated Pressures, by R. J. Holm, D. Weber, and S. S. Penner, *J. Appl. Phys.*, vol. 23, Nov. 1952, p. 1283.

Infrared Emission and Absorption of Thermally Excited Carbon Dioxide, by R. H. Tourin, *J. Chem. Phys.*, vol. 20, 1952, p. 1651.

Vibration Spectrum of Nitric Acid in the Infrared, by C. Fréjacques, *Comptes rendus des séances de l'académie des sciences*, vol. 234, 1952, pp. 1769–1770.

Kinetics of Decomposition of Nitric Oxide at Elevated Temperatures. II. The Effect of Reaction Products and the Mechanism of Decomposition, by H. Wise and M. F. Frech, *J. Chem. Phys.*, vol. 20, Nov. 1952, pp. 1724–1727.

Flame Emission Spectrum of HBr, by B. W. Bullock et al., *J. Chem. Phys.*, vol. 20, Nov. 1952, pp. 1808–1809.

Separation of the Absorption Spectra of NO_2 and N_2O_4 in the Range of 2400–5000A, by T. C. Hall, Jr., and F. E. Blacet, *J. Chem. Phys.*, vol. 20, Nov. 1952, pp. 1745–1749.

Polytropic Exponent of Isentropic Expansions in the Co-existence Region, by S. G. Reed, Jr., *J. Chem. Phys.*, vol. 20, 1952, pp. 533–534.

An Equation of State Applicable to Gases at Densities Near That of the Solid and Temperatures Far Above the Critical, by T. L. Cottrell and S. Paterson, *Proc. Roy. Soc. Lond.* (*A*), vol. 213, 1952, pp. 214–225.

Thermodynamic Properties of Nitrogen as Function of Pressure and Temperature Between 0 and 6000 Atmospheres and -125 and $\pm 150°$, by R. J. Lunbeck, A. Michels, and G. J. Wolkers, *Appl. Sci. Res.*, vol. A3, 1952, pp. 197–210.

The Condensation of Nitrogen in a Hypersonic Nozzle, by W. W. Willmarth, *J. Appl. Phys.*, vol. 23, Oct. 1952, pp. 1089–1095.

Viscosity, Density, and Critical Constants of OF_2, by R. Anderson et al., *J. Phys. Chem.*, vol. 56, 1952, pp. 473–474.

Vapor Pressure of Tetranitromethane, by G. Edwards, *Trans. Faraday Soc.*, vol. 48, 1952, pp. 513–515.

Vapor Pressure-Composition Measurements on Aqueous Hydrazine Solutions, by J. G. Burtle, *Indust. Engng. Chem.*, vol. 44, 1952, pp. 1675–1686.

Vapor Pressures and Freezing Points of the System Nitrogen Tetroxide-Nitric Oxide, by A. G. Whittaker et al., *J. Amer. Chem. Soc.*, vol. 74, Oct. 5, 1952, pp. 4794–4797.

Instrumentation and Experimental Techniques

Rocket Test Aid Measures Pressures, unsigned, *Aviation Week*, vol. 57, Nov. 10, 1952, p. 83.

Calibration of Pressure Gages for Work in Ballistics, by S. Raynor, *J. Appl. Mech.*, vol. 19, Dec. 1952, pp. 517–520.

Short-Time Measurements (in French), by P. Fayolle, Actes Coll. inter. Mécan. II, Publ. sci. tech. min. air, Paris, no. 250, 1951, pp. 51–64.

A Chronophotographic Method of Recording Trajectories of Fast Devices from a Distance of Several Kilometers (in French), by A. Sestier, Actes Coll. inter. Mécan. II, Publ. sci. tech. min. air, Paris, no. 250, 1951, pp. 65–72.

Double-Flash Microsecond Silhouette Photography, by H. E. Edgerton, *Rev. Sci. Instrum.*, vol. 23, Oct. 1952, pp. 532–533.

The Development of a Multi-flash Camera and Its Application to the Study of Liquid Jets, by M. A. Mahrous, *Brit. J. Appl. Phys.*, vol. 3, Oct. 1952, pp. 329–331.

Radiofrequency Mass Spectrometer for Upper Air Research, by J. W. Townsend, Jr., *Rev. Sci. Instrum.*, vol. 23, Oct. 1952, pp. 538–541.

Mass Spectrometer; New Technique for Analysis of Metals, unsigned, *Metal Indus.*, vol 80, Aug. 22, 1952, pp. 149–150.

Six-Ton Parachutes, unsigned, *Interavia*, vol. VII, no. 8, 1952, pp. 444–445.

Instrument Servomechanisms, by W. J. Deerhake and A. C. Hall, USN ONR Project 24-DC-1, U. S. Department of Commerce, Office of Technical Services, Washington 25, D. C. 265 pp.

A Force-Reflecting Positional Servomechanism, by R. C. Goertz and F. Bevilacqua, *Nucleonics*, vol. 10, Nov. 1952, pp. 43–45.

Fundamental Aspects of a Hydraulic-Type-Powered Flight-Control System, by H. M. DeGroff, *Aero. Engng. Rev.*, vol. 71, Nov. 1952, pp. 42–55.

Fundamentals of General-Purpose Remote Manipulators, by R. C. Goertz, *Nucleonics*, vol. 10, Nov. 1952, pp. 36–42.

Bearings for Gyroscope Rotors, unsigned, *Engineer*, vol. 194, Nov. 14, 1952, p. 651.

Proc. Inst. Radio Engrs., Transistor Issue (50 papers), vol. 40, Nov. 1952.

High Frequency Heating, by A. E. Williams, *Engineer*, vol. 194, Aug. 15, 1952, pp. 215–219.

Terrestrial Flight, Ballistics, and Vehicle Design

Windtunnel is a Firing Range, unsigned, *Aviation Week*, vol. 56, Oct. 20, 1952, p. 35.

Ballistics for Engineers (in Swedish), by S. Rydberg, *Tekn. Tidskr.*, vol. 81, Dec. 1951, pp. 1073–1083.

Pilotless Aircraft, by R. Goldin, *Aero. Engng. Rev.*, vol. 11, Nov. 1952, pp. 22–28.

The First Guided Missile Was a British Invention, by A. M. Low, *Flight*, vol. 61, Oct. 3, 1952, pp. 436–438.

British Guided Missiles, unsigned, *Engineering*, vol. 173, Aug. 1, 1952, p. 137.

Guided Missiles Blast Off New Oerlikon Arms Program, by Swiss correspondent, *Aviation Age*, vol. 17, Dec. 1952, pp. 25–27.

Missile Guidance System Outlined, unsigned, *Aviation Week*, vol. 57, Nov. 24, 1952, pp. 60–61.

Shipping Unit Saves Missile from Shock, unsigned, *Aviation Week*, vol. 57, Nov. 24, 1952, p. 28.

Space Flight

The Practical Approach to Astronautics, by J. Humphries, *Flight*, vol. 61, Oct. 24, 1952, pp. 528–532.

Escape from Earth, by J. G. Vaeth, *Flying*, vol. 52, Dec. 1952, pp. 27–44.

Ascent from Earth, by L. Grant, *J. Space Flight*, vol. 4, Sept. 1952, pp. 1–4.

A Possible Method of Generating Power in Space, unsigned, *J. Space Flight*, vol. 4, Sept. 1952, p. 7.

A Preliminary Survey of the Constructional Features of Space Station, by H. B. Ketchum, *J. Space Flight*, vol. 4, Oct. 1952, pp. 1–4.

Von Braun Offers Plan for Station in Space, by Von Braun, *Aviation Age*, vol. 17 Dec. 1952, pp. 61–63.

Interorbital Transport Techniques (with Special Reference to Solar Derived Power), by H. Preston-Thomas, *J. Brit. Interplan. Soc.*, vol. 11, July 1952, pp. 173–193.

Flights to the Major Planetary Systems, by H. B. Ketchum, *J. Space Flight*, vol. 4, Nov. 1952, pp. 1–3.

Astrophysics, Aerophysics, and Atomic Physics

Pressures, Densities, and Temperatures in the Upper Atmosphere, by The Rocket Panel, Harvard College Observatory, *Phys. Rev.*, vol. 88, Dec. 1952, pp. 1027–1032.

Radiation Hazards in High-Altitude Aviation, by A. Tobias and E. R. Smith, *Tech. Data Digest*, vol. 17, Nov. 1952, pp. 3–14.

Deflection and Diffusion of a Light Ray Passing Through a Boundary Layer, by H. W. Liepman, Douglas Aircraft Report SM 14397, May 16, 1952, p. 12.

The Increase or Decrease of Mean-Flow Energy in Large-Scale Horizontal Flow in the Atmosphere, by G. W. Platzman, *J. Meteor.*, vol. 9, Oct. 1952, pp. 347–358.

High-Altitude Research, by E. Burgess, *Engineer*, vol. 194, Sept. 19, 1952, pp. 370–373.

High-Altitude Research, by E. Burgess, *Engineer*, vol. 194, Sept. 12, 1952, pp. 338–340.

Meteorites and Cosmic Rays, by S. F. Singer, *Nature*, vol. 170, Nov. 1, 1952, pp. 728–729.

Reactor That Even Looks Safe, unsigned, *Business Week*, Nov. 8, 1952, p. 76.

General Topics

Reliability Analysis of Modern Weapons by M. M. Munk, *Aero. Digest*, vol. 63, Nov. 1952, pp. 101–102, 104, 106–108.

Probabilitistic Logics and the Synthesis of Reliable Organisms from Unreliable Components, delivered by J. von Neumann, noted by R. S. Pierce, Calif. Inst. of Technology Lectures, Jan. 1952, 51 pp.

From Newton's Note Book to Mammoth Research Organizations, by T. von Kármán, *Interavia*, vol. VII, 1952, pp. 431–432.

The University and Government Sponsored Research, by V. L. Parsegian, *Chem. and Engng. News*, vol. 30, Oct. 27, 1952, pp. 4470–4472.

Records of Research, by J. G. Jackson, *J. Franklin Inst.*, vol. 254, Nov. 1952, pp. 355–368.

Through the Curtain to Woomera, by L. C. Shepherd, *Aeroplane*, vol. 82, Nov. 7, 1952, pp. 630–633.

Specializing in

PRECISION INSTRUMENT

Screws

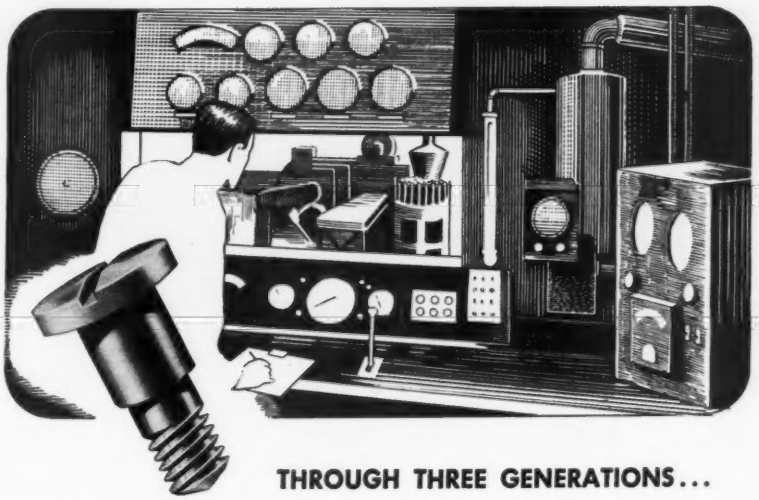

THROUGH THREE GENERATIONS...

Recognized as outstanding producers of small parts and close tolerance work . . . with plenty of Yankee ingenuity plus a wide open mind for the best ideas of others.

In our modern plant we also have the automatic screw machines for producing quality parts up to 1⅛" diameter by 8½" long.

Through constant research and development work in the interest of our customers we have maintained our leadership as specialists in fine instrument screws for over sixty years . . . with a variety of products which cover *every department* of the screw machine products field.

MEMBER OF NATIONAL SCREW MACHINE PRODUCTS ASSOCIATION

Specialists in Screw Machine Products Since 1893

WALTHAM

SCREW COMPANY

76 Rumford Avenue, Waltham, Massachusetts

CURRAN ENGINEERING CO.

Manufacturer of

MECHANICAL COMPONENTS
from
METALS, CERAMICS, AND PHENOLICS

Consultants and Specialists of
ROCKET IGNITER ASSEMBLIES
and
LONGITUDINAL SHAPED CHARGE CUTTERS

"CENGO" Process for
HIGH TEMPERATURE-HIGH DIELECTRIC INSULATING OF METALLIC ASSEMBLIES

4423 W. Jefferson Blvd.
Los Angeles 16 California.

Serving the rocket industry since 1946

"O" RINGS
MANUFACTURED OF POLYETHYLENE, TEFLON, AND KELL-F TO A.N. SPECIFICATIONS

HOSES
FLEXIBLE HIGH PRESSURE – BRAIDED STAINLESS STEEL POLYETHYLENE LINED WITH A. N. END CONNECTIONS

POLYETHYLENE SHEET, RODS, AND TUBES
LARGE STOCK AVAILABLE FOR GASKETING AND CHEMICAL CARRIAGE

VALVES
STAINLESS STEEL CHECK VALVES – HIGH PRESSURE – POLYETHYLENE OR TEFLON POPPET

Jet SPECIALTIES COMPANY
3348 East 14th Street, Los Angeles, California

G. M. GIANNINI & CO., INC., Pasadena 1, California

INDUSTRIAL SOUND CONTROL • INDUSTRIAL SOUND CONTROL • INDUSTRIAL SOUND CONTROL • INDUSTRIAL SOUND CONTROL

rocket ROAR silenced by ISC mufflers

● In the laboratory, in the test cell, on the airfield, hundreds of INDUSTRIAL SOUND CONTROL installations are subduing the noise, heat and gas velocities generated during testing of the big jets.
Whatever *your* noise problem, ISC's skilled engineering, design, and installation "know how" — gained through years of practical experience — can help you, and is at your instant service.
We welcome the challenge of the unusual problem. For full information

WRITE ISC TODAY

Foreign Licensees:
Cementation (Muffelite) Limited, London
Les Travaux Souterrains, Paris

Industrial Sound Control, Inc.

45 Granby Street, Hartford, Conn.
2119 So. Sepulveda Blvd., Los Angeles, Calif.

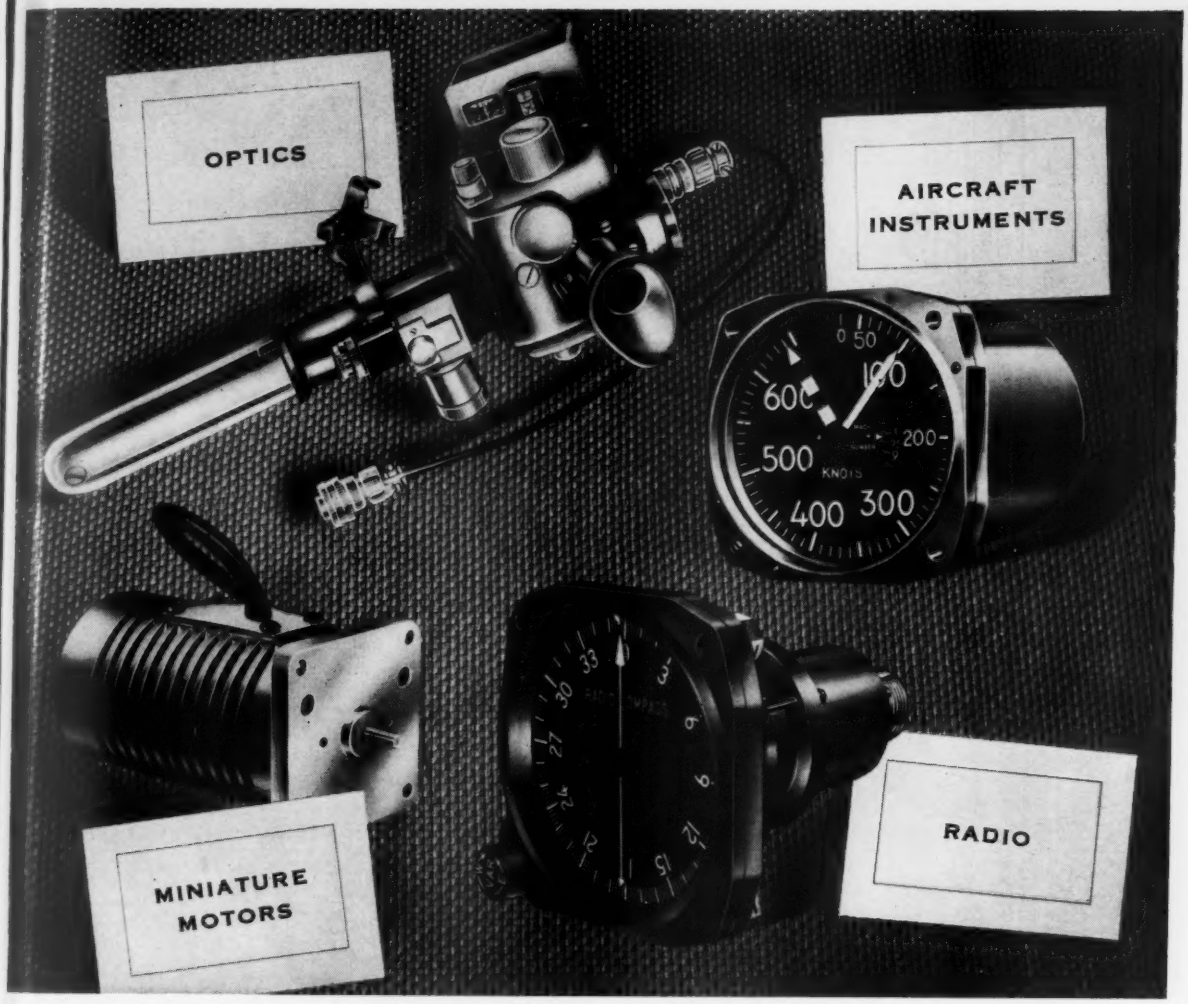

At KOLLSMAN— *Versatility*

Twenty-three years back, the Kollsman Instrument Corporation took its first forward steps by devising a sensitive altimeter *twenty times* more responsive than preceding models. This instrument actually made possible the first completely blind flight in the history of aviation.

Today, this venturesome spirit continues to spark the design, development and manufacture of products of precision and dependability in the four distinct yet allied fields of:

Aircraft Instruments and Controls • • Miniature AC Motors for Indicating and Remote Control Applications • • Optical Parts and Optical Devices • • Radio Communications and Navigation Equipment

While current production is largely devoted to National Defense, the research facilities of the Kollsman Instrument Corporation remain available to scientists working toward the solution of instrumentation and control problems.

KOLLSMAN INSTRUMENT CORPORATION
ELMHURST, NEW YORK — GLENDALE, CALIFORNIA
SUBSIDIARY OF
Standard COIL PRODUCTS CO. INC.

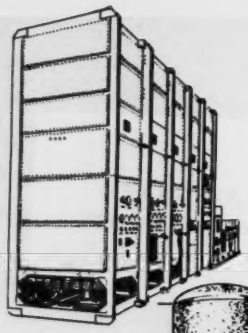

LIQUID OXYGEN GENERATORS

An air-transportable plant for the separation of high-purity oxygen from the air.

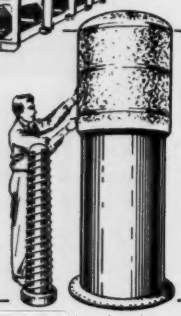

LIQUEFIED-GAS STORAGE CONTAINERS

Containers for the storage or transport of liquefied gases such as liquid hydrogen or oxygen.

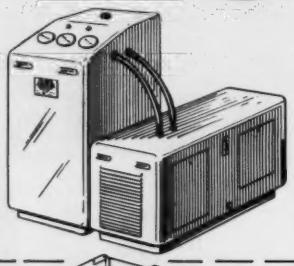

LIQUID OXYGEN PUMPS

A compact, noncontaminating unit for supplying high-pressure oxygen gas from low-pressure liquid oxygen storage containers.

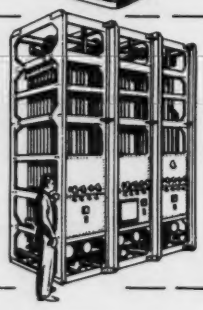

HEAT EXCHANGERS

A gas-to-gas heat exchanger with exceptional characteristics.

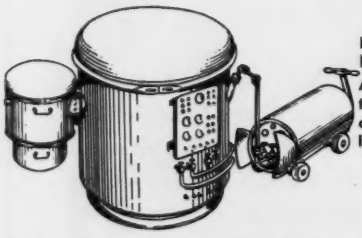

HELIUM REFRIGERATORS

A practical system for the prevention of evaporation loss in stored liquefied gases.

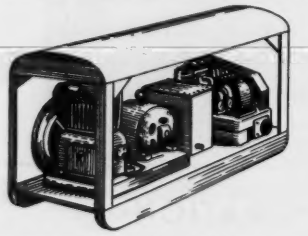

AIR COOLERS

A unit which provides cooled, compressed air which is free of dirt, oil, or entrained water.

THERMODYNAMICS • HEAT TRANSFER • REFRIGERATION TO MINUS 456°F • GAS LIQUEFACTION • VACUUM ENGINEERING • ELECTROMAGNETISM • MECHANICAL DESIGN • VIBRATION

UNIQUE PROTOTYPE DEVELOPMENT

Arthur D. Little, Inc. has blended its scientific and engineering skills in the Mechanical Division to provide industry with a unique service . . .

Scientists in the fields of chemistry, physics, metallurgy, mathematics, biology, electronics and technical economics regularly engaged in diversified research and development projects join with our engineers in prototype development of equipment requiring a high level of engineering skills.

Our staff is experienced in interpreting the ideas of industry and following through with the perfection of specialized equipment.

ADL Mechanical Division

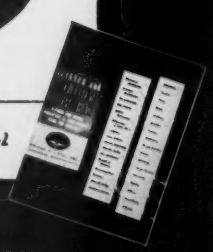

WRITE FOR BROCHURE RJ28-2

MECHANICAL DIVISION

Arthur D. Little, Inc.

30 MEMORIAL DRIVE — CAMBRIDGE 42, MASS.

Offices in New York, St. Louis, and Mexico City

CREATIVE TECHNOLOGY SINCE 1886